CATALYST SCREENING FOR COMPLETE OXIDATION OF
NITROGEN CONTAINING COMPOUNDS

A THESIS SUBMITTED TO
THE GRADUATE SCHOOL OF NATURAL AND APPLIED
SCIENCES OF
MIDDLE EAST TECHNICAL UNIVERSITY

BY
ALPER SEVİNÇ

IN PARTIAL FULFILLMENT OF THE REQUIREMENTS FOR
THE DEGREE OF MASTER OF SCIENCE
IN
CHEMICAL ENGINEERING

SEPTEMBER 2017

Approval of the thesis:

CATALYST SCREENING FOR COMPLETE OXIDATION OF NITROGEN CONTAINING COMPOUNDS

submitted by **ALPER SEVİNÇ** in partial fulfillment of the requirements for the degree of **Master of Science in Chemical Engineering Department, Middle East Technical University** by,

Prof. Dr. Gülbin Dural Ünver
Dean, Graduate School of **Natural and Applied Sciences**　————————————

Prof. Dr. Halil Kalıpçılar
Head of Department, **Chemical Engineering**　————————————

Prof. Dr. Gürkan Karakaş
Supervisor, **Chemical Engineering Dept., METU**　————————————

Examining Committee Members:

Prof. Dr. Deniz Üner
Chemical Engineering Dept., METU　————————————

Prof. Dr. Gürkan Karakaş
Chemical Engineering Dept., METU　————————————

Assoc. Prof. Dr. Burcu Akata Kurç
Micro and Nano technology Dept., METU　————————————

Prof. Dr. Sena Yaşyerli
Chemical Engineering Dept., Gazi University　————————————

Prof. Dr. Ayşen Yılmaz
Chemistry Dept., METU　————————————

Date: _08.09.2017_

I hereby declare that all information in this document has been obtained and presented in accordance with academic rules and ethical conduct. I also declare that, as required by these rules and conduct, I have fully cited and referenced all material and results that are not original to this work.

Name, Last name   : ALPER SEVİNÇ

Signature   :

ABSTRACT

CATALYST SCREENING FOR COMPLETE OXIDATION OF NITROGEN CONTAINING COMPOUNDS

Sevinç, Alper

M.S., Department of Chemical Engineering

Supervisor: Prof. Dr. Gürkan Karakaş

September 2017, 121 pages

High temperature catalytic oxidation (HTCO) of nitrogen containing compounds has great importance with regard to determination of the nitrogen in the environmental and industrial samples. The complete oxidation of bound nitrogen in different functional groups, ammonia, nitrates and organic nitrogen to nitric oxide is a crucial step for the determination of nitrogen in samples. The main goal of this work is catalyst screening for the complete oxidation of total bound nitrogen in the nitrogen containing compounds to nitric oxide. Four different catalyst samples, 10 % wt Cu/Al_2O_3, 3% wt Cu- 7 % wt Ce/Al_2O_3, 5 % wt Fe/Al_2O_3 and 1 % wt Pt/Al_2O_3, were synthesized by impregnation method. Characterization of the catalyst samples was performed by X-ray diffraction (XRD) and BET. High temperature catalytic oxidation (HTCO) experiments were conducted with compounds containing different nitrogen functional groups to observe the catalytic activities of the catalyst samples. Temperature

programmed oxidation (TPO) studies were carried out to observe reaction mechanism of bound nitrogen at different temperatures.

HTCO experiments showed that, water is as important oxidizing agent as oxygen for the oxidation of organic nitrogen to NO. According to conversion results of HTCO experiments, 5 % wt Fe/Al_2O_3 catalyst showed the best catalytic activity for conversion of bound nitrogen in tested model compounds to NO. 1 % wt Pt/Al_2O_3 catalyst also showed good catalytic activity for the model compounds oxidation except pyridine. 10 % wt Cu/Al_2O_3 catalyst performed bad catalytic activity for conversions of bound nitrogen to NO for EDTA, glutamic acid and ammonium sulfate. 3% wt Cu- 7 % wt Ce/Al_2O_3 catalyst showed poor conversions of bound nitrogen to NO for compounds, EDTA, pyridine, ammonium nitrate and glutamic acid.

TPO studies showed that complete conversion of bound nitrogen of acetonitrile to NO occurs at temperatures between 700-800 ^oC for the 5 % wt Fe/Al_2O_3 and 1 % wt Pt/Al_2O_3 catalysts. The results of TPO experiment over 10 % wt Cu/Al_2O_3 catalyst showed that N_2 formation is seen up at temperatures to 900 ^oC. According to TPO experiment results over 3% wt Cu- 7 % wt Ce/Al_2O_3, it can be stated that N_2 and N_2O are the main nitrogen containing products at temperatures up to 900 ^oC.

In this study, 5 % wt Fe/Al_2O_3 catalyst showed the best catalytic activity for high temperature oxidation of bound nitrogen to NO in the selected model compounds. Therefore; it can be stated for the future works that, alumina supported iron catalysts will be one of the first alternative to platinum containing catalysts in the nitrogen determination by using HTCO technique.

Keywords: Nitrogen determination, HTCO, Pt, CuO, CeO_2, Fe_2O_3, TPO

ÖZ

AZOT İÇEREN MADDELERİN TAM OKSİDAYONU İÇİN KATALİZÖR TARAMASI

Sevinç, Alper

Yüksek Lisans, Kimya Mühendisliği Bölümü

Tez Yöneticisi: Prof. Dr. Gürkan Karakaş

Eylül 2017, 121 sayfa

Azot içeren maddelerin yüksek sıcaklıkta katalitik oksidasyonu (YSKO), çevresel ve endüstriyel numunelerde azotun tayininde için büyük önem taşımaktadır. Amonyak, nitratlar ve organik azotlar gibi farklı fonksiyonel gruplarda bağlı azotun azot oksite tam oksidasyonu örneklerdeki azotu belirlemek için çok önemli bir adımdır. Bu çalışmanın temel amacı azot içeren bileşiklerdeki toplam bağlı azotun azot okside tam oksidasyonu için katalizör taramasıdır. 4 farklı katalizör örneği, ağırlıkça % 10 Cu/ Al_2O_3, ağırlıkça % 3 Cu- % 7 Ce / Al_2O_3, ağırlıkça % 5 Fe/ Al_2O_3 ve ağırlıkça % 1 Pt/ Al_2O_3, emdirme metodu ile sentezlenmiştir. Katalizör numunelerinin karakterizasyonu, X-ışını difraksiyonu (XRD) ve BET ile gerçekleştirilmiştir. Katalizör numunelerinin katalitik aktivitelerini gözlemlemek için farklı azot fonksiyonel grupları içeren maddeler ile yüksek sıcaklıkta katalitik oksidasyon (YSKO)

deneyleri gerçekleştirilmiştir. Numune yapısında bağlı olan azotun yanma reaksiyonu mekanizmasını farklı sıcaklıklara göre incelemek için sıcaklık programlı oksidayon (SPO) çalışmaları yapılmıştır.

YSKO deneyleri organik yapılı azot içeren maddelerdeki azotun NO gazına oksidayonu için suyun oksijen kadar önemli bir oksidant olduğunu göstermiştir. YSKO deneyleri sonuçlarına göre, ağırlıkça % 5 Fe/ Al_2O_3 katalizörü test edilen model bileşiklerdeki bağlı azotun NO gazına dönüştürülmesinde en iyi katalitik aktiviteyi göstermiştir. Ayrıca ağırlıkça % 1 Pt/ Al_2O_3 katalizörü de pyridine oksidasyonu dışında iyi bir katalitik aktivite göstermiştir. Ağırlıkça %10 Cu/ Al_2O_3 ve ağırlıkça % 3 Cu- % 7 Ce/Al_2O_3 katalizörleri seçilen bir çok model azot içeren maddelerdeki azotun NO' ya oksidasyonu için kötü performans sergilemişlerdir.

Ağırlıkça % 1 Pt/ Al_2O_3 ve ağırlıkça % 5 Fe/ Al_2O_3 katalizörleri ile yapılan SPO çalışmaları asetonitril yapısında bulunan bağlı azotun 700 ^{o}C üzerindeki sıcaklıklarda tamamen NO gazına dönüştüğünü göstermektedir. Ağırlıkça % 10 Cu / Al_2O_3 katalizörü üzerinde gerçekleşen SPO deneylerinin sonuçları, N_2 oluşumunun 900 ^{o}C'ye kadar olan sıcaklıklarda görüldüğünü göstermiştir. Ağırlıkça % 3 Cu- %7 Ce/Al_2O_3 katalizörü ile yapılan SPO deneyleri sonuçlarına göre; N_2 ve N_2O'nun 900 ^{o}C'ye kadar olan sıcaklıklarda temel azot içeren ürünler olduğu belirtilebilir.

Bu çalışmada, ağırlıkça% 1 Pt / Al_2O_3, ağırlıkça% 5 Fe / Al_2O_3 katalizörleri seçilen model bileşiklerinde bağlı azotun NO'ya yüksek sıcaklıkta oksidasyonu için en iyi katalitik aktiviteyi göstermiştir. Bu nedenle; gelecekteki çalışmalarda, alümina destekli demir katalizörlerinin, HTCO tekniği kullanılarak azot tayininde platin içerikli katalizörlere ilk alternatiflerden biri olacağı belirtilebilir.

Anahtar Kelimeler: Azot tayini, YSKO, Pt, CuO, CeO_2, Fe_2O_3, SPO

To My Dad

ACKNOWLEDGEMENTS

TABLE OF CONTENTS

LIST OF TABLES

LIST OF FIGURES

FIGURES

LIST OF ABBREVIATIONS

HTCO	High Temperature Catalytic Oxidation
CLD	Chemiluminescence
TPO	Temperature Programmed Oxidation
MS	Mass Spectrometer
IR	Infrared
FTIR	Fourier-transform Infrared Spectroscopy
XRD	X-ray Diffraction
BET	Bruauer – Emmett – Teller
BJH	Barrett – Joyner - Halenda
$Cu(NO_3)_2 . 3H_2O$	Copper (II) nitrate trihydrate
$Fe(NO_3)_3 \cdot 9H_2O$	Iron (III) nitrate nona hydrate
$H_2PtCl_6 \cdot 6H_2O$	Chloroplatinic acid hexahydrate
$Ce(NO_3)_3 .6H_2O$	Cerium nitrate hexahydrate
$C_{10}H_{16}N_2O_8$	Ethylenediaminetetraacetic acid disodium salt dihydrate
$C_5H_9NO_4$	Glutamic Acid
$(NH_4)(NO_3)$	Ammonium nitrate
C_5H_5N	Pyridine
CH_4N_2O	Urea
$(NH_4)_2SO_4$	Ammonium sulfate
C_2H_3N	Acetonitrile
NO	Nitric Oxide
NO_2	Nitrogen Dioxide
N_2O	Nitrous Oxide
N_2	Nitrogen molecule
Sccm	Standard Cubic Centimeters per Minute
TCD	Thermal Conductivity Detector
RSD	Relative Standard Deviation

CHAPTER 1

INTRODUCTION

Total bound nitrogen refers to nitrogen containing compounds such as amines, nitrates, nitrites, ammonia, ammonium salts and organic nitrogen forms. Total bound nitrogen is an utmost important parameter for environmental concerns related with consumer and industrial compounds (including soils, sediments, sludge, fertilizers, bio wastes, composts, foods, oils, fuels, industrial and municipal wastes, drinking water, waste water, fuels and many human-made compounds) [5,6,7].The measurement of total nitrogen (TN) content of various compounds and environmental samples are important element of the environmental remediation and ecological studies.

Kjeldahl, Dumas combustion and high temperature catalytic oxidation (HTCO) methods are the commonly used analytic techniques for the determination of the nitrogen content of the samples. Kjeldahl method is based on the digestion of the sample with concentrated acid to convert bound nitrogen to ammonium sulfate. Formed ammonium sulfate reacts with sodium hydroxide, then ammonium ion forms ammonia and ammonia is trapped in an acid solution. Finally, remained acid content of the solution is back titrated with a known concentration of base solution to calculate the nitrogen content of the sample. Sum of organic N and ammonia in the sample can only be measured by using Kjeldahl method. Although nitrate/nitrite nitrogen in the samples cannot be determined [54] by Kjeldahl method, it is still employed for the nitrogen analysis since it provides precise, accurate and reliable results in both low and high level nitrogen analysis. It is also time consuming, toilsome, and requires hazardous chemicals such as acids, bases and heavy-metal catalysts [16]. Dumas combustion method consists of high temperature oxidation of the sample in the presence of pure

oxygen to convert all nitrogen content of the sample to NO_x and N_2. NO_x gases are reduced in the following steps to N_2, which is further detected by TCD detector to calculate the nitrogen content of the samples. Dumas combustion method provides fast accurate, reliable analysis of nitrogen content of the samples without the use of hazardous chemicals. High initial investment of the instrument and the small sample size which cause low precision are the main disadvantages of the Dumas combustion method [16, 24, 53]. HTCO technique is another common nitrogen determination method especially for liquid samples and it is based on the selective catalytic oxidation of the bound nitrogen in the sample to NO and detection of produced NO as nitrogen content. It provides fast, precise and reproducible analysis of nitrogen in the samples. In addition, HTCO technique is more economic than Dumas method due to long-life of catalyst, use of air or oxygen as oxidation and carrying gas. However, most of these studies for nitrogen determination by using HTCO technique have focused on analysis of liquid samples [10], there are few studies concerned with TN determination of solid samples [11]. Moreover, the presence of different nitrogen containing functional groups in the same sample may result with inconsistent measurement results at different temperatures over the same catalyst due to complex oxidation kinetics. Therefore, the poor catalyst selectivity for the oxidation products of different nitrogen groups is the main restriction of HTCO method. Therefore, choice of the catalyst and the optimum temperature is utmost important for complete conversion of nitrogen compounds to NO.

It is known that; the required catalytic functions for conversion of bound nitrogen to NO are carried out by the transition metals (including Fe, Cu, Co, Pd, Pt, Ag, Au, Mn, Cr). In several nitrogen analyzers, which use HTCO principle, alumina supported Pt, Pd and different metallic catalyst such as CoO, CoCr, CuO, MnO_2 are used for the oxidation of bound nitrogen to nitric oxide [68]. Noble metals, Pt and Pd, provide great advantage due to high excellent oxidation activity, higher resistance to sulfur poisoning and sintering. They can be synthesized easily over various oxide supports such as alumina, silica,

2

zirconia and high dispersion can be achieved easily at lower loadings $(0.1 – 1 \%$ wt). In spite of these advantages of the noble metals, the high cost of these metals is the major shortcoming. Therefore, there is a great interest to develop new catalysts for the selective oxidation of bound nitrogen to NO. Copper is an interesting transition metal as an oxidation catalyst due to its high reducibility and low price [74, 64]. Furthermore, the catalytic activity of catalyst containing copper ion could be improved by impregnation of copper with ceria due to interaction of ceria with Cu ions, and ceria species could block copper sintering and increase the thermal stability due to these interactions [75]. Even if iron containing catalysts have never been used before for nitrogen determination by using HTCO technique, they are also widely used combustion catalyst due to low price and high oxidation capacity [76].

In this study, catalyst samples of 10 % wt Cu/Al_2O_3, 3 % wt Cu-7 % wt Ce/Al_2O_3, 1 % wt Pt/Al_2O_3 and 5 % wt Fe/Al_2O_3 were synthesized by incipient wetness impregnation method to investigate their oxidation activity for complete conversion of bound nitrogen in nitrogen containing samples to NO.

CHAPTER 2

LITERATURE SURVEY

2.1 Nitrogen for the Environment

Nitrogen is the most common element in the atmosphere as making up about %80 of the Earth's atmosphere. It is found in soils, sediments, sludge, fertilizers, animal and plant wastes, industrial products and essential for all living creatures [1]. It is required as main nutrients for all plants and animals to survive and important component of the organic molecules such as nucleic acids, amino acids and proteins. Nitrogen is also found in the water sources such as lake, sea, and river. In brief, nitrogen is the key element found in the ecosystem and the environment.

While nitrogen is found in atmosphere as dinitrogen (N_2), which is predominant form, relatively unreactive and cannot be digested by most of the organisms, there are many reactive nitrogen forms such as nitrates, nitrites, ammonia, and organic nitrogen [2,3]. Furthermore, it is also found in the atmosphere as pollutant (NO_x) which is emitted by agricultural, industrial and combustion facilities. Figure 2.1 shows the transformation of the nitrogenous compounds in the environment including formation of NO_x gases, transformation of organic nitrogen to ammonia, nitrates and nitrites.
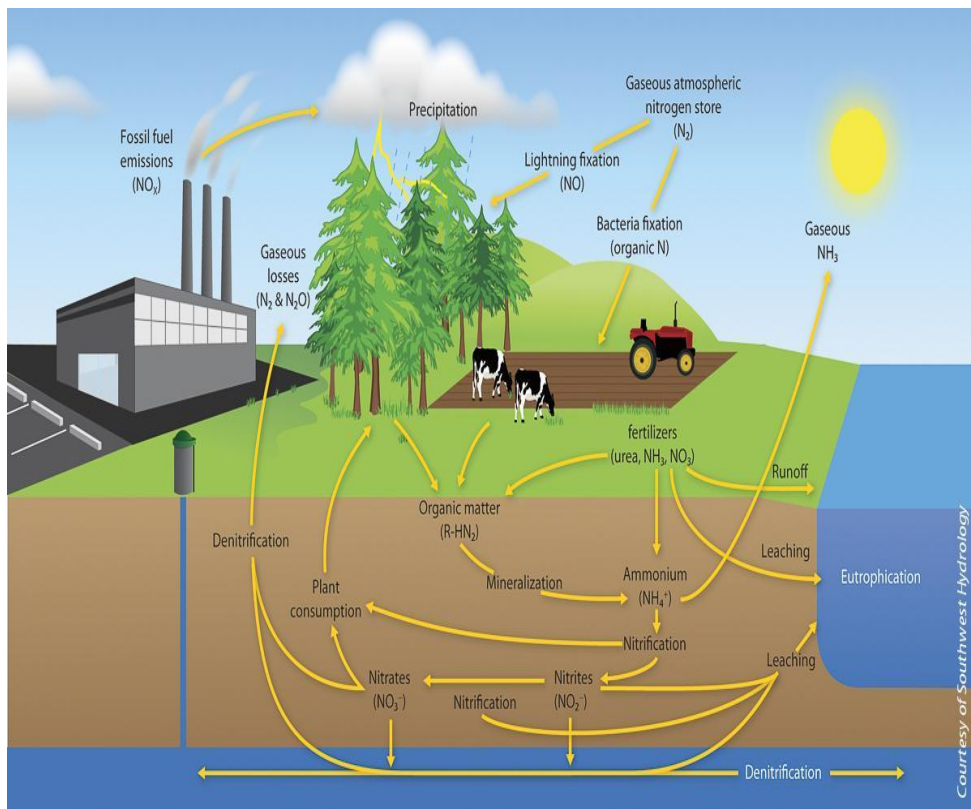
Figure 2. 1: Nitrogen forms and cycle in the environment [4]

Common forms of the nitrogen in the environment are as the follows;

- *Gaseous dinitrogen (N_2)*: Mostly unreactive inorganic compound composing about % 78 by volume of the Earth's atmosphere.

- *Ammonia (NH_3)*: reactive inorganic compound that is mostly occurs in the environment naturally. Generally, it is produced by bacterias in the water sources and soil as the final product of decomposition of the animal and plant wastes. It goes through some biochemical transformations, which is part of the nitrogen cycle, in the soil and water. Moreover, it is also produced industrially, used for the production of fertilizers, plastics, fibers etc.

- *Nitric oxide (NO)*: Reactive inorganic compound that is found in the nature generally as a result of the catalytic reaction of N_2 and O_2 molecules above temperature 1300 ^{o}C, and combustion of bound nitrogen in a sample. It also react with oxygen or ozone to produce NO_2.

- *Nitrous oxide (N_2O)*: Reactive inorganic compound which is found in the environment in low amounts around 0.30 ppb. Microorganisms in soil and water sources produce most of the nitrous oxide in the environment.

- *Nitrogen dioxide (NO_2)*: Reactive inorganic nitrogen form that is mainly found in the environment as a result of combustion facilities such as combustion of fossil fuels, waste incineration facilities.

- *Cyanides (-CN)*: Reactive inorganic or organic nitrogen containing compound that mainly occurs in the nature as product of bacteria, fungi, algae and they are also found in the structure of the plants.

- *Nitrite (NO_2^-) and Nitrate (NO_3^-)*: Reactive inorganic forms of the nitrogen presenting in the environment. They are found in the soil and water sources due to nitrification processes, which is decomposition of organic nitrogen to ammonia, oxidation of ammonia to nitrite and oxidation of nitrite to nitrate by microorganisms. In addition, they are emitted in the environment by synthetically prepared fertilizers. Nitrate ions also found naturally in the body of some vegetables.

- *Urea (CH_4N_2O):* Reactive organic nitrogen containing compound that is found in nature as waste product of many living organisms. It is also used in the nature as fertilizer since nitrogen content of the urea is higher than all solid nitrogen containing fertilizers [88].

- *Other organic nitrogen forms such as amino acids, amines, amides ($H_2NCHRCOOH$, $R–CO–NR'R''$, $R_nE(O)_xNR'_2$ where R, R'and R'' refers*

to organic groups): Reactive other organic forms of the nitrogen found in the environment. They mainly occur as decomposition of plant and animal residues in the environment. Moreover, they occur in the environment as a result of the industrial processes wastes.

2.1.1 Total Bound Nitrogen (TNb)

Total bound nitrogen defines the total mass of nitrogen in the sample containing both organic and inorganic compounds such as nitrates, nitrites, ammonia, ammonium salts, amines and other organic-inorganic nitrogen-containing compounds. Total bound nitrogen (TNb) content is very important parameter for many environmental and industrial studies such as soils, sediments, sludge, fertilizers, bio wastes, composts, foods, oils, industrial and municipal wastes, drinking water, waste water, fuels and many human-made compounds [5,6,7]. The characterization of these different matrices and determination of total nitrogen (TN) content of these different matrices is an important element of the environmental remediation and ecological study.

a)   *Organically Bound Nitrogen*

Organic nitrogen can be defined as nitrogen bound to carbon, hydrogen and oxygen in the compounds. Organic nitrogen is found in proteins, amino acids, water, living or dead organisms, plants, human-made compounds and petrochemicals, etc. as dissolved or particulate forms [35]. In nature, biological transformation of organic nitrogen generates ammonia, nitrate, nitrites which are dominant inorganic forms of the nitrogen in the environment. Organic nitrogen containing compounds are also the source for nitrogen oxides (NO, NO_2, and N_2O) formation, as a result of waste incineration facilities and fossil fuel combustion for transportation, electric utilities and other industrial purposes [42, 43]. Nitrogen oxide gases are detrimental for the environment due to several reasons such as; acid deposition, greenhouse effect and ozone layer destruction [42, 43].

b)   *Inorganically Bound Nitrogen*

Nitrates, nitrites, cyanides, ammonia and ammonium salts can be defined as the common forms of inorganically bound nitrogen in the environment. The main sources of these nitrogen forms are fertilizers, soil, human and animal wastes and the nitrogen cycle. In nitrogen cycle, organic materials decompose in soil and ammonia is released. Soil living bacteria carry out the ammonia oxidation and forms nitrates and nitrates [31]. Moreover, ammonia and the ammonium salts, which are found in the fertilizer and living wastes, can be thought as a source of inorganic nitrogen forms of the environment [32].

2.1.1.1 Total Nitrogen in Soil and Sediments

Decomposition of animals, plants, fertilizers, manures, chemical contaminants and organic waste mainly derives nitrogen contents of soil and sediments [5, 8]. As seen in the figure 2.1, nitrogen can be found in soils and sediments in several forms such as organic, nitrate, nitrite, ammonia.

Total nitrogen (TN) in soil has long been identified because of the importance in soil fertility for both managed and natural ecosystems [9]. Total nitrogen in soil is accepted as the macronutrient for the growth of the plants on soil [10, 11, 12]. Although the nitrogen content of the soil is important for soil fertility, it is also very important for the pollution of ground water sources due to nitrate and ammonium ions mobility. Therefore, it is critical to determine, evaluate and control the nitrogen content of soil from the point of agricultural and environmental remediation. Just as it is in the soil, total nitrogen content in sediments has much importance in terms biogeochemical and contaminant partitioning studies such as growth of the algeas and other plants and pollution of the ecosystem [13].

2.1.1.2 Total Nitrogen in Fertilizers, Composts and Biomass

Carbon and nitrogen are the most important elements for the health of the soil, especially ratio of their masses to each other which is defined as Carbon Nitrogen ratio (C:N).While carbon is necessary for the energy requirements of plants, nitrogen is required for the growth of the plants. The carbon and nitrogen ratio (C:N) specifies the decomposition rate of organic matter in the soil resulting immobilization or mineralization of nitrogen in the soil and the optimum C:N ratio for the soil is generally between $15:1 - 30:1$ [88]. When high carbon content compound (high C:N ratio) such as sawdust is added to soil, microorganisms need additional nitrogen to break down the carbon source [89]. Therefore, they take additional nitrogen content from the soil and this phenomena brings about nitrogen deficiency in the soil. If compounds that have low carbon to nitrogen ratio (C:N) are added to soil, microorganisms break down to carbon easily due to high content of the nitrogen and leads to carbon deficiency in the soil. Fertilizers and composts are added to soil to adjust C:N ratio to create healthy soil, and biomass is naturally effective on establishing the appropriate ratio. The organic matter of fertilizer, biomass and compost are broken down by bacteria and fungi, which causes the change in carbon nitrogen ratio [33]. Therefore, total nitrogen content of fertilizer, biomass, compost and other soil additives are very important parameter for the environmental and agricultural issues.

2.1.1.3 Total Nitrogen in Water

Several forms of organic and inorganic nitrogen exist in water; however, the dominant forms of nitrogen in water are ammonia (NH_3), nitrate (NO_3^-) and nitrite (NO_2^-) [35]. Microorganisms in the soil convert organic nitrogen forms to ammonia and further oxidize the ammonia to nitrate and nitrite. Moreover, atmospheric nitrogen (N_2) is converted to ammonia by the living organisms. Also, ammonia is found in water sources in consequence of animal waste products. Mobility of nitrate (NO_3^-) and ammonium ions (NH_4^+) from fertilizers, soil, human and animal wastes, sewage disposal systems, livestock facilities, is

the major sources of nitrates and ammonia in water.

Total nitrogen (TN) is one of the main pollution parameter for water sources [34]. In addition, excess amount of total nitrogen content in water can decrease dissolved oxygen (DO) so it can negatively affect the life of the plants and organisms [36]. Hence, total nitrogen is a crucial control parameter to determine pollution level of water sources.

2.1.1.4 Total Nitrogen in Other Compounds

While total nitrogen is critical in soils, sediments, fertilizers and water sources, it is also a significant parameter for many different compounds such as; milk, foods, fuels, explosives, wastes and many other human-made compounds. The total nitrogen content of the milk and other dairy products is critical for the calculation of protein content for nutritional quality control and research purposes. For the food and animal feed industries, the protein content attract significant social and economic attention due to legal issues, nutritional, health and economic implications [38]. To determine protein content of the foods, total nitrogen content of the food is multiplied by a factor. Some common factors which are called as specific (Jones) factors for the determination of protein content of food by using nitrogen content are shown in the table 2.1.

Table 2. 1: Some factors for the determination of the protein contents by total nitrogen content [37]

Food	Factor	Food	Factor
Animal Origin		Rye	5.83
Eggs	6.25	Sorghums	6.25
Meat	6.25	Wheat: Whole kernel	5.83
Milk	6.38	Bran	6.31
Vegetable Origin		Endosperm	5.70
Barley		Beans: Castor	5.30
Corn (Maize)	6.25	Jack, lima, navy, mung	6.25
Millets	6.25	Soybean	5.71
Oats	5.83	Velvet beans	6.25
Rice	5.95	Peanuts	5.46

Total bound nitrogen is an important parameter for the wastes, fossil fuels, petroleum products and processes [39, 40]. Analysis of total nitrogen in petroleum products is crucial since nitrogen containing petroleum products have negative effects on refinery catalyst life and reactions such as hydrogenation. [41].

Moreover, total nitrogen determination in wastes, biomass and fuels is crucial quality control parameter for NO_x emissions. NO_x defined as nitrogen oxides, mainly includes nitric oxide (NO), nitrogen dioxide (NO_2) and the NO_x emission term is directly relevant for the pollution of air. NO_x gases are formed mainly in three ways; thermal NO_x, prompt NO_x, and fuel NO_x. Thermal NO_x is formed as a result of the reactions between nitrogen molecule (N_2) and oxygen molecule (O_2) at high temperatures mostly higher than 1300 ^{o}C. Prompt NO_x, which is formed mainly in the high fuel-air ratios, defined as the reaction between atmospheric nitrogen (N_2) and hydrocarbon radicals to produce HCN which can be further oxidized to NO_x. Fuel NO_x is formed by the oxidation of chemically bound nitrogen in the compounds such as coal, natural gas, fuel oil, wastes and biomass.

NO$_x$ gases give rise to acid deposition, greenhouse effect, photochemical smog and ozone layer destruction in the environment [42, 43] and they also cause health problems such as decreasing lung function, increasing respiratory conditions risks and response to allergy [44]. According to European Union emission inventory report, the greatest source of the NO$_x$ emissions is road transport and energy production in EU during 2011 [44]. NOx emissions can be controlled by utilizing low nitrogen containing fuels, combustion control, and catalytic/noncatalytic selective reduction of NO$_x$ in the flue gases [70].

2.2 Total Nitrogen Determination

The importance of total nitrogen content of many compounds such as soils, sediments, fertilizers, fuels is described in section 2.1 in detail. Therefore, the analysis of total nitrogen content of the samples is an important element for the environmental remediation and ecological study. As mentioned in the introduction part, there are three commonly used analytic methods for nitrogen determination in the compounds;

1) Kjeldahl Method
2) Dumas Combustion Method,
3) High Temperature Catalytic Oxidation Method (HTCO).

2.2.1 Kjeldahl Method

This method was developed by Johan Kjeldahl (1849–1900) for the determination of nitrogen in organic substances and originally used to measure the protein content in beer (Kjeldahl, 1883; Editor of The Analyst, 1885). Because of the constant ratio of nitrogen to protein ratio in food materials, Kjeldahl method provides indirect determination of protein content of the foods. Today, this is a widely used as an analytical method for the determination in nitrogen in several compounds such as; soil, fertilizer, waste water, food, and fossil fuels. This method consists of three steps: digestion, distillation, and titration [14].

The first step is the digestion in which the sample is subjected to oxidative decomposition with boiling concentrated sulfuric acid (H_2SO_4) around 390 ^oC in the presence of catalyst to convert bound nitrogen to ammonium sulfate ((NH_4)$_2SO_4$).

$$C_xH_yN_zO_t + H_2SO_{4(l)} \rightarrow CO_{2(g)} + H_2O_{(g)} + (NH_4)_2SO_{4(aq)} \qquad [25]$$
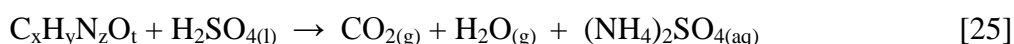
Some amount of potassium sulfate (K_2SO_4) is added to elevate the boiling point of sulfuric acid (H_2SO_4) from 337 ^oC to 390 ^oC to increase decomposition rate [45]. Moreover, several catalysts have been studied in digestion step to increase decomposition rate such as Mercury (II) oxide (HgO), Copper (II) sulfate ($CuSO_4$), selenium (Se), titanium oxide (TiO_2) [16, 45, 46, 47]. Mercury (II) oxide (HgO) catalyst has the highest effectiveness and commonly used; however, it has some problems from the point of safety and environmental concerns such as emission of mercury vapour to the atmosphere, difficulty in handling and disposal of mercury [48]. Selenium catalyst is another widely used catalyst but it is also toxic substance [49]. Titanium oxide and copper (II) sulfate are the metal oxides that are used as alternatives to mercury (II) oxide and selenium catalyst and their combination which gives better catalytic performance [47].

The following step after digestion is distillation. In distillation step, ammonium sulfate reacts with excess sodium hydroxide (NaOH), ammonium ion is then liberated in the form of ammonia (NH_3).

$$(NH_4)_2SO_4 + 2NaOH \rightarrow 2NH_{3(g)} + Na_2SO_4 + 2H_2O \qquad [15]$$

The formed ammonia gas is trapped by using acid solution such as boric acid (H_3BO_3), hydrochloric acid (HCl) or sulfuric acid (H_2SO_4) [50]. When the ammonia dissolves in the acid solution, some of the acid is neutralized by ammonia [50].

The last step of the Kjeldahl Method for nitrogen determination is titration. In this step, the remained acid content of the solution is back titrated with a known concentration base solution (usually NaOH), then distilled ammonia amount is determined so the nitrogen content is determined [45].

The Kjeldahl method has been applied for analysis of micro and macro sized samples by choosing appropriate size of digestion and distillation apparatus. Generally, micro Kjeldahl method is used to analyze of homogenous and high nitrogen containing samples and small sample size less than 250 mg [16]. Macro-sized apparatus was used in the original procedure to analyze large amount of sample from 0.5 to 5 grams [16]. Even though Macro Kjeldahl method provides higher accuracy of low level nitrogen analysis and greater amounts of sample sizes to increase representation of real samples by enhance the homogeneity, it leads to usage of the large amount of acid, base and catalyst and also increase the analysis time [16]. Therefore, high cost of this macro analysis and usage of large amount of chemicals have led scientist to scale down these procedure [17]. Although the Kjeldahl method for nitrogen determination gives precise, reliable and accurate analytical results, it is time consuming and analysis requires the use of chemicals and heavy-metal catalysts [8, 19]. Moreover, the Kjeldahl method determines the nitrogen content of only organic substances such as proteins, amino acids nucleic acids [52]. The other nitrogen forms such as nitrate and nitrite cannot be analyzed by using this method [52]. Therefore, alternative methods have been developed to obtain precise, reliable, low-cost analysis of all nitrogen forms in short analysis time.

2.2.2 Dumas Combustion Method

Dumas combustion method was developed by Jean-Baptiste Dumas (1880-1884) for the determination of nitrogen in the samples in 1826. Nowadays, this method is widely used as an alternative method to overcome some of the limitations in Kjeldahl Method such as long-time analysis and high cost per analysis. The nitrogen content of a sample can be determined as precise as the Kjeldahl method

at least [20, 21].

In this method, nitrogen containing samples is subjected to high temperature between 900 ^{o}C and 1300 ^{o}C in the presence of excess oxygen and metallic catalysts such as tungstic oxide, zirconium oxide, vanadium pentoxide, chromium oxide, to convert all of the bound nitrogen to molecular nitrogen and nitrogen oxides [20, 51].

$$\text{Sample} + O_{2(g)} \xrightarrow{\textit{Catalyst}} CO_{2(g)} + NO_{x(g)} + N_{2(g)} + H_2O_{(g)} + O_{2(g)} + \text{other oxides}$$
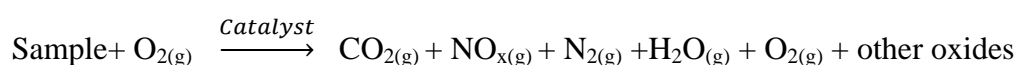
The combustion gases (NO_x, SO_x N_2, H_2O, CO_2, O_2) are passed through a second reactor at 600 ^{o}C in order to reduce all NO_x to N_2 over copper catalyst to detect N_2 by TCD detector.

$$CO_{2(g)} + NO_{x(g)} + N_{2(g)} + H_2O_{(g)} + \text{ other oxides} \xrightarrow[@\ 600\ o_C]{\textit{Cu reducer}} N_{2(g)} + CO_{2(g)}$$
$$+ H_2O_{(g)} + \text{ other oxides}$$
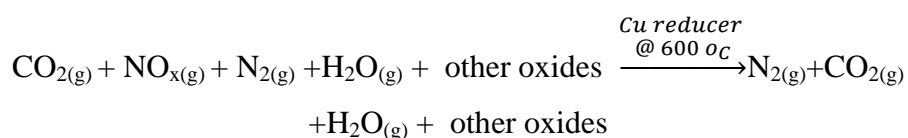
Then, gases goes through some gas conditioning units such as cooler, water to prevent damage of the water vapor and condensate to the detector. CO_2 and other oxides such as SO_2 gases are collected via some absorbers to prevent any interference in the N_2 thermal conductivity detector (TCD).

$$N_{2(g)} + CO_{2(g)} + H_2O_{(g)} + \text{ other oxides} \xrightarrow[\textit{and Absorbers}]{\textit{Traps}} N_{2(g)}$$
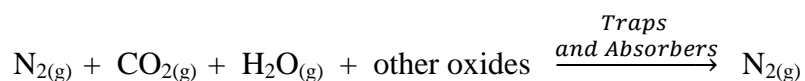
After the reaction and conditioning steps, remaining N_2 gas, which is carried by helium gas, is detected by thermal conductivity detector (TCD) of which electronic signal changes proportional to N_2 gas concentration in the cell [22, 23]. The nitrogen content of the sample is determined from the calibration curve that is obtained for TCD [22]. Basic flow diagram of the Dumas combustion method is shown in figure 2.5.
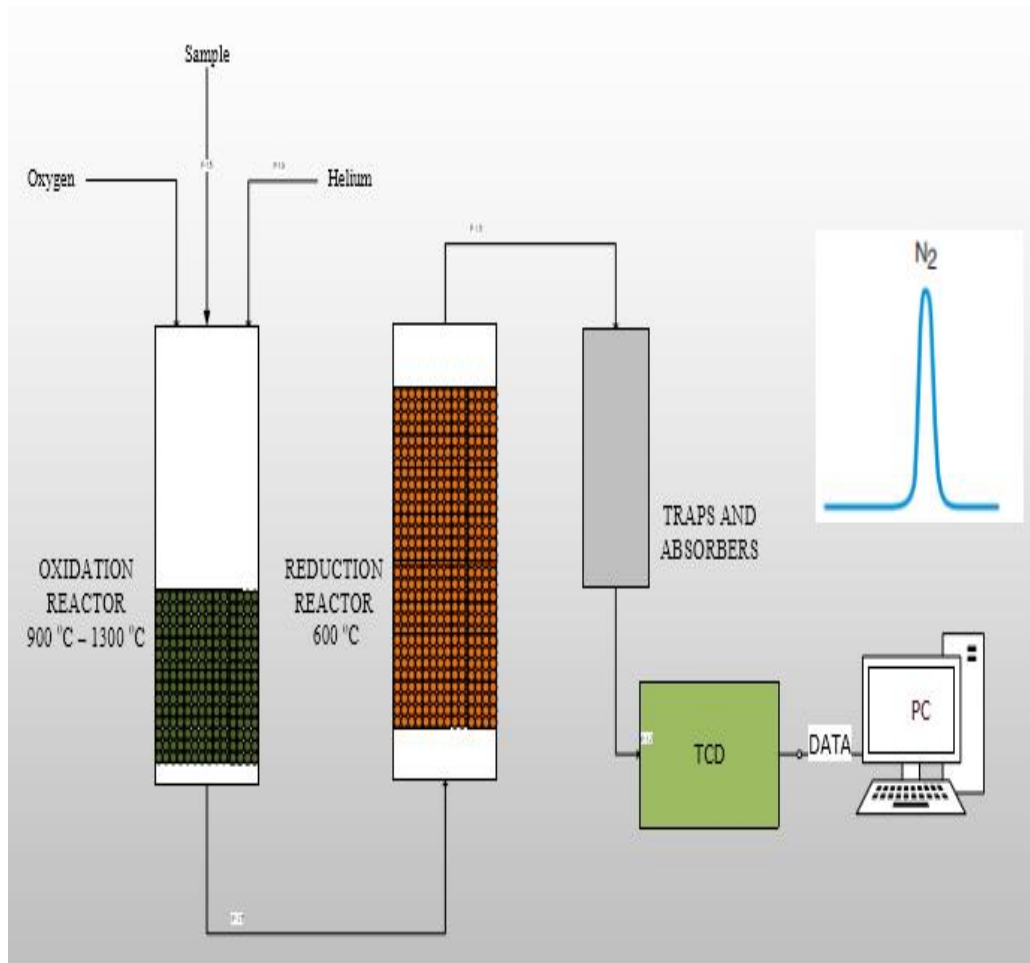
Figure 2. 2: Basic schematic of Dumas combustion principle for nitrogen determination

Dumas combustion method offers accurate, reliable nitrogen determination in a short analysis time without the use of hazardous chemicals. However, the equipment requires high initial investment and skilled and experienced operator for use and maintenance [16]. The capability for analysis of small sample size is another critical shortcoming of the Dumas combustion method [24, 53]. When the heterogeneity of the samples increases, sample size is very crucial [16]. Small sample size leads to a failure of reproducibility and accuracy of the real samples due to sampling technique, weighting errors and heterogeneity issues [24]. The greater amounts of sample improve the representability of real samples by enhancing the homogeneity, as well as accuracy of low level nitrogen analysis [16, 24]. Although Dumas combustion method provides fast, reliable and accurate nitrogen determination, the developments of alternative methods have

been studied due to restrictions mentioned above.

2.2.3 High Temperature Catalytic Oxidation Method (HTCO)

In 1980's, HTCO method has been developed for the measurement of the nitrogen in liquid samples [26, 27, 28]. After Seattle workshop on the development of HTCO in 1991, HTCO was approved as the most precise and effective method for the determination of organic bound nitrogen in the aqueous samples [54]. This method is based on the catalytic combustion of the sample at high temperatures between 680 ^{o}C and 1100 ^{o}C in the presence of oxygen and catalysts [54, 55, 56]. The bound nitrogen in the sample oxidized selectively to nitric oxide (NO) as a result of catalytic combustion process.

$$\text{Sample}+ O_{2(g)} \xrightarrow{Catalyst} CO_{2(g)} + NO_{(g)} + H_2O_{(g)} + O_{2(g)} + \text{other oxides}$$

Then, gases pass through, water vapor trap and the CO_2 and SO_2 gases are collected over some absorbers due to prevent any interference in the NO detector.

$$NO_{(g)} + CO_{2(g)} + H_2O_{(g)} + \text{other oxides} \xrightarrow{Traps \ and \ Absorbers} NO_{(g)}$$
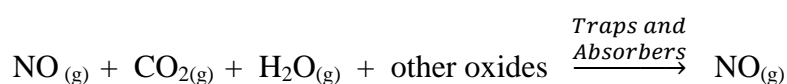
The nitric oxide can be measured by spectrophotometer, electrochemical sensor (EC), or chemiluminescence (CLD) detector [27, 15, 55, 56].

EC detection principle is based on reaction of NO electrolyte in the electrochemical NO detector that creates a voltage difference on the measuring electrode relative to reference electrode. This voltage difference, which is directly proportional with the NO concentration, provides to achieve quantitative analysis of nitric oxide (NO) (ASTM International, Designation: WK50658) [55].

The chemiluminescence principle is based on the principle that combustion

18

nitrogen gas product, nitric oxide (NO), reacts with ozone (O_3) in the reaction chamber to form nitrogen dioxide in excited state (NO_2^*).

$$NO + O_3 \rightarrow NO_2^* + O_2$$
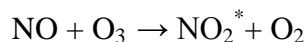
Excited state (NO_2^*) generates light when it reverts to a lower energy state.

$$NO_2^* \rightarrow NO_2 + h\nu$$
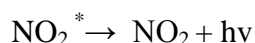
The emitted light intensity (chemiluminescence) is directly proportional to nitric oxide (NO) concentration in the reaction chamber and is measured with a photomultiplier tube lead to achieve quantitative analysis of nitric oxide (NO).

CLD detectors are usually preferred in commercial HTCO nitrogen analyzers because of the wide measurement range which enables the determination of both high and trace level concentration of NO.

HTCO technique was used for nitrogen determination and compared with the other methods in several studies in which HTCO method provided fast, precise and reproducible analysis of nitrogen [5, 57, 58, 54, 59]. Moreover, HTCO technique offers more economic analysis for nitrogen determination because only air/oxygen is necessary for the oxidation and flow; there is no need for the second reactor for any additional reaction step and long catalyst life relative to Dumas method.

Although, there are many successful studies about nitrogen determination by using HTCO technique in the literature, there are also some restrictions. Total nitrogen refers to a composition parameter that can include different nitrogen compounds as organic and inorganic in a sample [54]. Conversion of all bound nitrogen in the sample to single product, NO is necessary for the nitrogen determination. However, the oxidation products of the samples containing different nitrogen functional groups may result with the formation of different

oxidation products at different temperatures over the same catalyst due to complex reaction kinetics. Especially the environmental samples (including natural water, soil, sediment, sludge, etc.) have more complex chemical composition including several nitrogen functional groups compared to more homogeneous industrial samples such as explosives, fertilizers. Therefore the NO selectivity and the conversion performance of the catalysts are very critical for the accuracy and sensitivity of the HTCO units. Similar to Dumas method, HTCO equipment also requires high initial investment, skilled and experienced operator for the use and maintenance.

Moreover, most of the available HTCO analyzers are designed and sold for liquid sample analysis, very few papers focused on the HTCO technique for analysis of solid samples [5]. Therefore, HTCO technique still requires improvements for the analysis of the solid samples.

2.3 Catalysts for Determination of Nitrogen with HTCO Method

As mentioned section 2.2.3, total nitrogen may consist of several nitrogen functional groups. Combustion products of the sample are highly depend on operating parameters mainly temperature, oxygen concentration and flowrate, nitrogen functional groups in sample and catalyst. This case is the main difficulty of HTCO method. Nitrogen determination by using HTCO method includes NO formation by oxidation of organic nitrogen and ammonium, nitrate and nitrite nitrogen [64].

The major paths of oxidation of organic nitrogen to nitrogen oxides and nitrogen molecule via HCN and NH_i intermediates are shown in figure 2.8. Oxidation of the nitrogen in the compounds occurs via formation of HCN and CN molecules. While it is known that oxygen is the most important oxidizing molecule, water (H_2O) is another important oxidizing molecule for the oxidation of organic nitrogen forms [64].

20
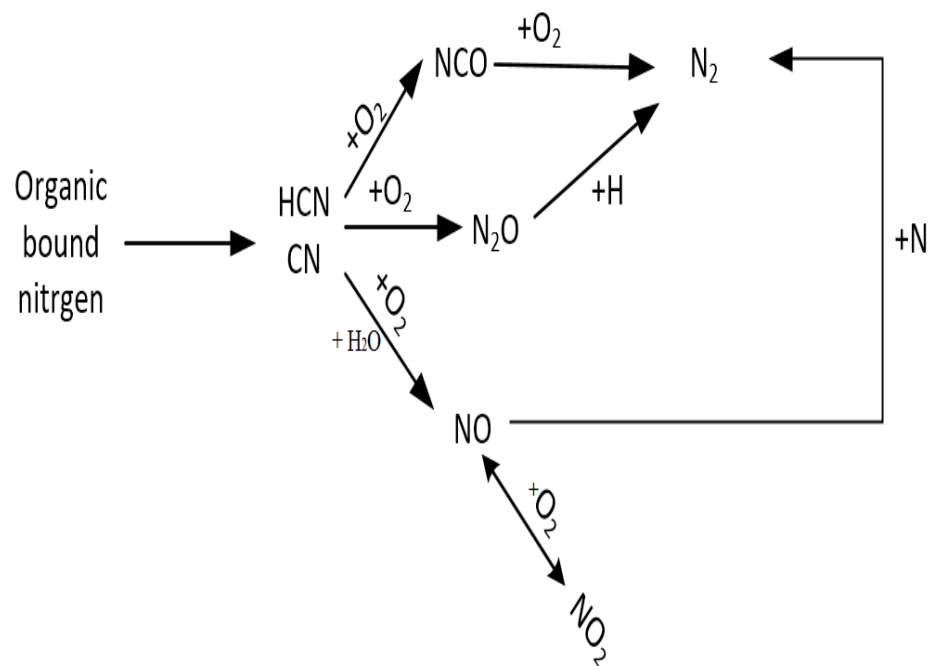
Figure 2. 3: Major paths for combustion of organic nitrogen [62]

Elementary reaction steps of combustion of organic nitrogen containing samples are shown in the table 2.3 [62, 90]. First intermediate in the reaction steps is HCN which formed rapidly during the reaction [62]. HCN reacts with O, OH, H free radicals and produce CN (reactions 2.2, 2.3, 2.4) [63]. Reaction of HCN and OH can also form HNCO radical (reaction 2.6) [62]. The NCO intermediate is formed as a result of reaction between CN radicals and OH (reaction 2.5 [63]).The intermediates, NCO and HNCO, are unstable at high temperatures so rapid reaction occurs between these radicals and H atoms and NH_i species are formed (reaction 2.7, 2.8) [62]. The chain carrier radicals (OH, O, H) can react with NH_2 and NH radicals to form NH radicals (reactions 2.9, 2.10, 2.20) and N atoms (reactions 2.12, 2.13, 2.14). The reaction between NH radicals and O or OH forms the NO (reactions 2.15 and 2.16). Nitrogen molecule can be formed as a product according to reactions 2.17-2.20. Further oxidation of nitric oxide (NO) with O or OH_2 forms the nitrogen dioxide at high temperatures (reactions 2.21-2.22). Nitrous oxide molecule can be formed as product of the reactions of NO

with NCO radical or N atom (reactions 2.23-2.24)

Table 2. 2: Reactions of nitrogen during the combustion [62,90]

Bound N $\rightarrow$ HCN	(2.1)
HCN + OH $\rightarrow$ CN + H$_2$O	(2.2)
HCN + H $\rightarrow$ CN + H$_2$	(2.3)
HCN + O $\rightarrow$ CN + OH	(2.4)
CN + OH $\rightarrow$ NCO + H	(2.5)
HCN + OH $\rightarrow$ HNCO + H	(2.6)
NCO + H $\rightarrow$ NH + CO	(2.7)
HNCO + H $\rightarrow$ NH$_2$ + CO	(2.8)
NH$_2$ + H $\rightarrow$ NH + H$_2$	(2.9)
NH$_2$ + O $\rightarrow$ NH + OH	(2.10)
NH$_2$ + OH $\rightarrow$ NH + H$_2$O	(2.11)
NH + OH $\rightarrow$ N + H$_2$O	(2.12)
NH + O $\rightarrow$ N + OH	(2.13)
NH + H $\rightarrow$ N + H$_2$	(2.14)
NH + O $\rightarrow$ NO + H	(2.15)
NH + OH $\rightarrow$ NO + H$_2$	(2.16)
NH + NO $\rightarrow$ N$_2$ + OH	(2.17)
NO + N $\rightarrow$ N$_2$ + O	(2.18)
NH + NH $\rightarrow$ N$_2$ + H$_2$	(2.19)
NH + N $\rightarrow$ N$_2$ + H	(2.20)
NO + O $\rightarrow$ NO$_2$	(2.21)
2NO + O$_2$ $\rightarrow$ 2NO$_2$	(2.22)
NO + NCO $\rightarrow$ N$_2$O	(2.23)
NO + N $\rightarrow$ N$_2$O	(2.24)

While organic and ammonium nitrogen compounds must be oxidized from the oxidation state of -3 to +2, nitrate and nitrite must be oxidized to +2 from +5 and +3, respectively [64]. It is known that; metals in d-electron groups such as Ag, Au, Co, Fe, Ir, Ni, Pd, Pt, Re, Rh, Ru and Os, have capability of facilitating

oxidation reactions [65]. Noble metal Pt and Pd is known as high specific activity catalysts that convert the bound nitrogen to NO at temperatures around 700 ^{o}C [65]. Alumina supported Pt, Pd and different metallic catalyst such as CoO, CoCr, CuO, MnO$_2$ are already used in several commercial HTCO-CLD nitrogen analyzers [68]. Alumina is generally used as a catalyst support for Pt and Pd catalysts due to its low cost, thermal resistance, high surface area. In addition, the interaction of alumina with Pt and Pd catalyst improve thermal stability in the oxidizing atmospheres [62].

The catalyst selection for an optimum temperature is crucial for selective oxidation of nitrogen in complex compounds to NO. Therefore, many studies have been still carried out to select optimum reaction conditions and catalyst for nitrogen determination by using HTCO-CLD technique.   The HTCO method for nitrogen determination was first proposed by Suzuki *et. al.* in 1985 [27]. In this study, Al$_2$O$_3$ supported Pt catalyst was used at 680 ^{o}C for selective oxidation of bound nitrogen in several compounds to nitric oxide. Then, the generated gas products were passed from acid permanganate solution to oxidize nitric oxide to nitrogen dioxide. The nitrogen dioxide was detected by spectrometrically at 545 nm. Several nitrogen containing compounds (thiourea, antipyrine, caffeine, 8-hydroxyquinoline, bovine serum albumin, sulfathiazole) were tested in this study and nitrogen conversion to nitric oxide were found almost % 100 for all components except sulfathiazole. The reason of low conversion of nitrogen to nitric oxide in sulfathiazole was mentioned a problem for the further studies.

Bekiari *et. al.* also used Pt/Al$_2$O$_3$ catalyst to measure nitrogen content of water samples [34]. The catalyst temperature was set to 720 ^{o}C and pure oxygen was used as oxidation gas at a flow rate 130 mL/min. Samples analyzed by direct injection into the vertically oriented reactor at 720 ^{o}C. In this work, HTCO-CLD system provided reliable results with lower detection limits.

Rogora *et. al.*studied the determination of nitrogen in fresh water samples (lakes, rivers) with HTCO method [54]. In this work, they used two different catalyst samples of CoCr - Pt and CoCr – CeO$_2$ at 850 ^{o}C under the pure oxygen flow rate

of 250 ml/min. CoCr- Pt catalyst gave low recoveries of ammonium nitrogen to nitric oxide; therefore, this catalyst was not found efficient for the samples that contain high amount of ammonium. Another catalyst, CoCr-CeO$_2$ performed better conversion of organic and ammonium nitrogen to nitric oxide in the range of 0.1 – 7 mg/L N content.

Ammann *et. al.* made an interesting research for nitrogen determination in surface and waste water by using HTCO method [58]. For the simulation of surface and waste water, synthetic solutions of different nitrogen model components (urea, 4-NH$_2$Antipyrine, 4-OH-Bezonitril, Picolinic acid, EDTA, Cystein, Ammonium, Hydrazine sulfate) were tested over Pt/Al$_2$O$_3$ catalyst at 690 ^{o}C under air flow of 150 ml/min. In this work, nitrogen recoveries were tested by two different sampling methods, which are: direct injection of solution over the catalyst surface and injection of solution on quartz wool on top of a catalyst. Nitrogen recoveries to nitric oxide were determined between 50-80% when the samples were directly injected over the catalyst surface. When the samples were injected over quartz wool layer on top of catalyst bed, the results increased up to 90-100 % conversion. The reason of low recoveries on the direct injection on the catalyst surface was reported as insufficient conditions that prevent the further oxidation of N to NO. The quartz wool layer on the top of the catalyst dramatically increased the nitrogen recoveries to NO by converting sample to the gas phase before the contact with catalyst surface.

Watanabe *et. al.* made an catalyst screening study for the liquid samples [64]and tested four different catalysts (Shimadzu and Johnson 0.5% Pt–alumina, 13% Cu(II)O–alumina, 0.5% Pd–alumina) and quartz beads for oxidation of bound nitrogen to NO at 680 ^{o}C in the presence of 150 ml/min oxygen flowrate. They tested the solutions of caffeine, thiourea, urea, ethylenediaminetetraacetic acid (EDTA), ammonium pyrrolidine dithiocarbamate (APDC) as organic, and ammonium chloride, sodium nitrate, sodium nitrite representing inorganic nitrogen components. The converison of nitrogen to nitric oxide in all organic nitrogen containing solutions over quartz beads were reported as above 90%

except urea and APDC solution. The recoveries of nitrogen in $NaNO_2$ structure were found < 92% for all catalyst samples. Recoveries for NH_4Cl were also smaller than 80 % over the 13% CuO–alumina, 0.5% Pd–alumina, and quartz beads. They reported the low recoveries for the nitrite samples as the conversion of NO_2^- on metallic catalyst to N_2, N_2O, NO_2 as well as NO. These oxidation products (N_2, N_2O, NO_2) can not be detected by CLD technique. The Shimadzu 0.5 % Pt/Al_2O_3 catalyst showed best recovery for nitrite sample. The low recovery of NH_4Cl over the 13% CuO/Al_2O_3 catalyst was explained as the catalytic oxidation of ammonia to N_2O as well as NO.. Similarly, the low recovery of NH_4Cl over quartz beads and 0.5% Pd/Al_2O_3 catalyst was also explained by same mechanisms. As a result of this study, 0.5 % Pt/Al_2O_3 catalyst was found the most effective for the conversion of the bound nitrogen to nitric oxide and the low recoveries in NH_4Cl and nitrite samples were attributed to different oxidation pathways over the catalyst.

Alavoine *et. al.* also tested HTCO technique for the nitrogen determination in K_2SO_4 soil extracts [19]. They used quartz reactor placed in a double temperature zone furnace which are maintained at 900 ^{o}C. The first zone of the reactor was to decomposition and vaporization of the samples and the second zone is for the catalyst (0.5 % Pt/Al_2O_3) packing under the flow of oxygen-argon mixture. The samples packed with quartz wool were loaded into the sample boat and layer of alumina powder were applied to prevent the rapid flush of sample into the furnace and catalyst bed. The samples in the quartz boats were rapidly inserted into the reactor by an automatic mechanism and the gas stream was analyzed. Several nitrogen functional groups were tested as model compounds (including ammonium sulfate, potassium nitrate, urea, sodium nitrate, humic acid, yeast extract, atropine, acetanile, DL-Serine, DL-metionine). As a result of three replicate analyses of each sample, all N recoveries to NO were found almost as % 100. It is reported that, the indirect injection system provided to prevent the destruction quartz reactor and catalyst, as well as rapid and reliable nitrogen measurement at 900 ^{o}C.

HTCO technique was used by Avramidis *et al.* for nitrogen determination in soil certified materials (CRM) and sediment samples [5]. They used also double-zone temperature controlled reactor and the second zone of the reactor was packed with Pt/Al_2O_3 catalyst at 720 ^{o}C. Samples were introduced to the pyrolysis part of the reactor in the presence of pure air; then, oxidation pyrolysis gas treated over the catalyst bed for the further oxidation of bound nitrogen to nitric oxide which was measured by CLD. They reported that, TN measurements in these solid samples gave fast, accurate, precise, and reproducible result with this method.

Similar studies performed by using Pt/Al_2O_3 catalyst were also reported in literature at 720 ^{o}C by HTCO-CLD technique. These researches reported that reliable and repeatable results obtained with low detection limits in liquid samples [8, 66, 67]. However, there are few studies interested in TN determination of solid samples by using HTCO-CLD technique [5, 11]. Therefore, there is still requirement for improving catalyst and reaction parameters for HTCO technique to convert the bound nitrogen in the solid samples to nitric oxide (NO).

CHAPTER 3

EXPERIMENTAL

In this study, Al_2O_3 supported Cu, Pt, Fe and Cu-Ce catalysts were synthesized by incipient wetness impregnation method. X-ray diffraction (XRD) and Bruauer–Emmett–Teller (BET) methods were used for catalyst characterization. The high temperature catalytic oxidation (HTCO) tests of model nitrogen containing compounds were performed over different catalyst samples and temperature programmed oxidation (TPO)-mass spectrometry experiments were conducted to identify the oxidation mechanisms of nitrogen containing model compounds.

3.1 Catalyst Synthesis and Materials

The following materials were used in this study for synthesis of catalyst samples, high temperature catalytic oxidation (HTCO) tests and temperature programmed oxidation (TPO) experiments.

- Alumina support (γ- Al_2O_3, Damla Kimya)
- $Cu(NO_3)_2 . 3H_2O$ (Copper (II) nitrate trihydrate,Merck)
- $Fe(NO_3)_3 \cdot 9H_2O$ (Iron (III) nitrate nona hydrate, Merck)
- $H_2PtCl_6 \cdot 6H_2O$ (Chloroplatinic acid hexahydrate, Johnson–Matthey)
- $Ce(NO_3)_3 .6H_2O$ (Cerium nitrate hexahydrate Sigma-aldrich)
- $C_{10}H_{16}N_2O_8$ (Ethylenediaminetetraacetic acid disodium salt dihydrate, Sigma-aldrich),
- $C_5H_9NO_4$ (Glutamic Acid, Merck)
- $(NH_4)(NO_3)$ (Ammonium nitrate, Merck)
- C_5H_5N (Pyridine, Sigma-aldrich)
- CH_4N_2O (Urea, Sigma-aldrich)

- $(NH_4)_2SO_4$ (Ammonium sulfate, Merck)
- C_2H_3N (Acetonitrile, Sigma-aldrich)

3.2 Catalyst Preparation

3.2.1 Synthesis of 10 % wt Cu/Al_2O_3, 5 % wt Fe/Al_2O_3 and 1 % wt Pt/Al_2O_3 Catalyst with Incipient Wetness Impregnation Method

10 wt % Cu/Al_2O_3, 5 wt % Fe/Al_2O_3, 1 wt % Pt/Al_2O_3, catalysts were prepared by incipient wetness impregnation method. For the high temperature catalytic oxidation (HTCO) tests, commercial Al_2O_3 support beads were first washed with ultra-pure water and dried at 110 ^{0}C over the night. Appropriate amounts of $Cu(NO_3)_2 . 3H_2O$, $Fe(NO_3)_3 \cdot 9H_2O$ and $H_2PtCl_6 \cdot 6H_2O$ were used for preparation of copper, iron and platinum solutions, respectively. Prepared solutions were impregnated into the Al_2O_3 supports by using incipient wetness method. The catalyst samples were first dried at room temperature overnight and at 110°C for 5 h. Finally, the catalyst samples were calcined at 700 ^{o}C for 4 h. The incipient wetness impregnation method is is schematized in figure 3.1 and the synthesis details are summarized in Table 3.1

Table 3. 1: Amounts of support and catalyst precursors for the preparation of catalyst samples

Catalyst Precursors and Support	10 wt % Cu/Al_2O_3	5 wt % Fe/Al_2O_3	1 wt % Pt/Al_2O_3
Al_2O_3 added (g)	18.0	19.0	19.8
$Cu(NO_3)_2 . 3H_2O$ added (g)	7.6	0.0	0.0
$Fe(NO_3)_3 \cdot 9H_2O$ added (g)	0.0	7.2	0.0
$H_2PtCl_6 \cdot 6H_2O$ Added (g)	0.0	0.0	0.53
Ultra-pure water volume for precursor solution (mL)	12	12	12

28

3.2.2 Synthesis of 3 % wt Cu – 7 % wt Ce/Al$_2$O$_3$ Catalyst with Incipient Wetness Coimpregnation Method

3 wt % Cu - 7 wt % Ce on Al$_2$O$_3$ support catalyst samples were prepared by incipient wetness co-impregnation method. Commercial Al$_2$O$_3$ beads firstly were washed with deionized water and dried at 110 ^{0}C over the night. Appropriate amounts of Cu(NO$_3$)$_2$. 3H$_2$O and Ce(NO$_3$)$_3$ .6H$_2$O, which are shown in table 3.2, were dissolved in ultra-pure water together to prepare the copper-cerium metal solution. This solution was impregnated over the Al$_2$O$_3$ supports. The catalyst samples were dried at room temperature overnight and at 110°C for 5 h. Finally, the catalyst samples were calcined at 700 ^{o}C for 4 h.

Table 3. 2: Amounts of support and catalyst precursors for the preparation of catalyst samples

Catalyst Precursors and Support	3 wt % Cu and 7 wt % Ce/Al$_2$O$_3$
Al$_2$O$_3$ added (g)	18.0
Cu(NO$_3$)$_2$. 3H$_2$O added (g)	2.3
Ce(NO$_3$)$_3$ .6H$_2$O)	4.32
Ultra-pure water volume for precursor solution (mL)	12.0
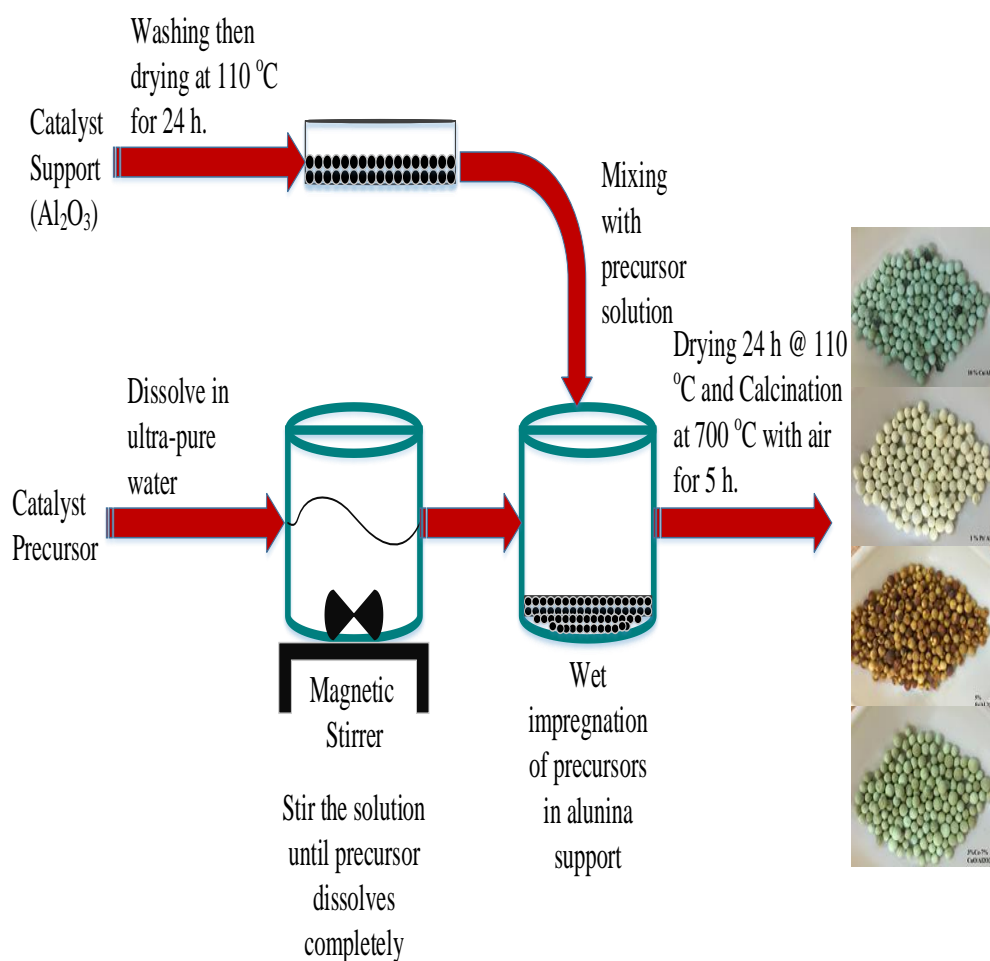
Figure 3. 1: Catalyst preparation by wet impregnation method

3.3 Catalyst Characterization

3.3.1 X-Ray Diffraction (XRD) Analysis

The crystallographic structures of the catalyst samples were investigated by X-Ray diffraction (XRD) analysis (Rigaku Ultima IV diffractometer) in METU Central Laboratory. The properties and parameters of XRD instrument (Rigaku Ultima IV diffractometer) are shown in table 3.1.

Table 3. 3: Properties and parameters of XRD instrument (Rigaku Ultima IV diffractometer)

Parameter	Value
Radiation	Cu Kα (X= 1.5418Å)
Voltage (kV)	40
Anode Current (mA)	40
Filter	NA
Sampling Width (degree)	0.02
Scan Speed (degree/min)	2
Scan Range (2θ, degree)	20 - 100
Grazing angle (degree)	0.5

3.3.2 Surface Area, Pore Volume and Pore Size Distribution

The rule of physical adsorption of gas molecules on a solid surface was used for the analysis of specific surface area, pore volume and pore size distribution of catalyst samples. Specific surface areas of the catalyst samples were determined by using multipoint BET method based on N_2 adsorption at 77 K. Barrett - Joyner – Halenda (BJH) technique was used to determine pore volume and pore size distribution of the catalyst samples.
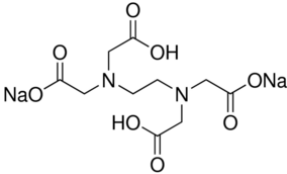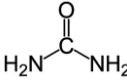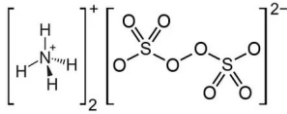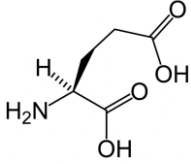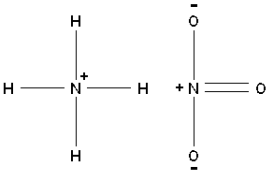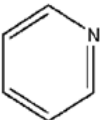
3.4 Experimental Setup

Two different experimental setups were used for catalyst screening and catalytic activity tests of the synthesized catalyst samples respectively. The first setup is to examine performance of the synthesized catalyst samples for oxidation of different samples representing various nitrogen functional groups. The second setup, which is Temperature Programmed Oxidation (TPO), is to investigate reaction mechanisms and catalytic activity of the catalyst samples at different temperatures.

3.4.1 High Temperature Catalytic Oxidation (HTCO) Tests of Model Nitrogen Containing Compounds

For this experimental setup, EDTA disodium salt dihydrate (Sigma-aldrich), urea (Sigma-aldrich), ammonium sulfate, glutamic acid (Merck), ammonium nitrate, pyridine were selected as nitrogen containing model components representing various nitrogen containing functional groups for high temperature catalytic oxidation experiments. Model components, their functional groups and chemical structures are shown in table 3.4.

Table 3. 4: Functional groups and chemical structures of selected Model Components

Sample	Chemical Structure	Functional Group
EDTA		Amino polycarboxylic acid
Urea		Urea
Ammonium Sulfate		Ammonium salts
Glutamic Acid		Amino acids
Ammonium Nitrate		Ammonium salts
Pyridine		Heterocyclic (N)

The experimental setup (Figure 3.5) for the catalytic activity test composes of the following five units:

- *Gas feed unit:* This unit is used to adjust desired dry air (%99.999, Elite gas) flow rate for the oxidation of samples. There are one inlet gas pressure regulator and one mass flow controller (MFC, Alicat scientific) in this system.

- *Sample feed unit:* Quartz sample boats (Figure 3.2) and a stainless steel wire was used to feed model components to the reactor as a pulse input. Samples were prepared as in figure 3.3 before feeding to the reactor. After weighing and loading the sample to the quartz combustion boats, the sample is covered by a thin layer of quartz wool to prevent the flush and spill out from the boat during combustion. Before the HTCO experiments a number of test were done and it was seen that water addition is required for the oxidation of bound nitrogen in the organic components to NO and nitrogen dioxide. Therefore, 200 µl of water was added on the sample for better pyrolysis and oxidation of the compounds.
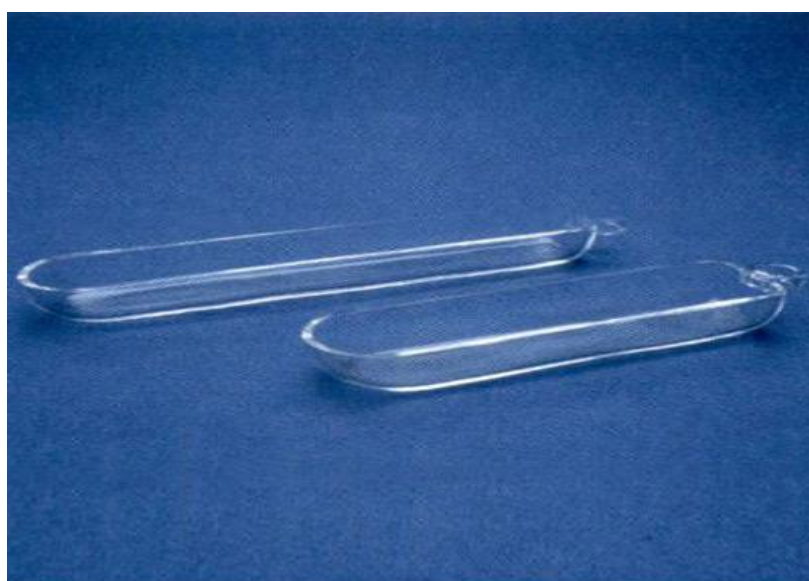
Figure 3. 2: Quartz combustion boats
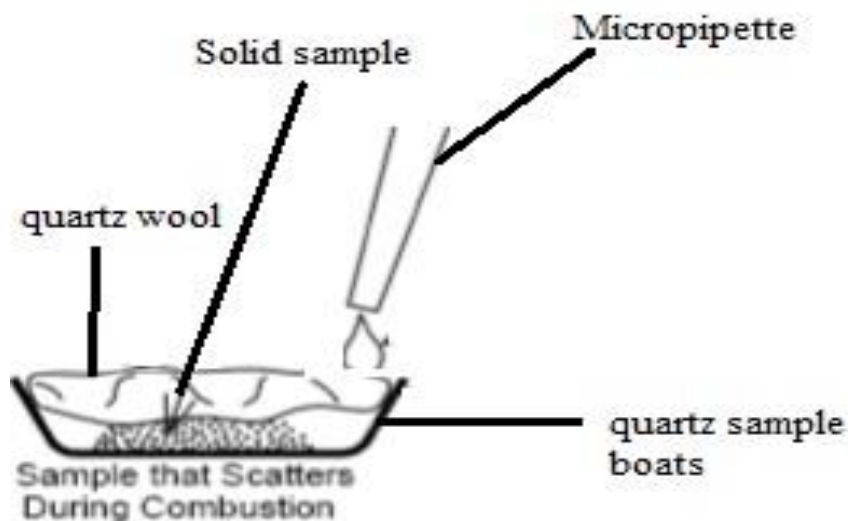
Figure 3. 3: Loading sample to the combustion boats

- Reactor unit: This unit comprises quartz tubular reactor (Figure 3.4) with inner diameter (ID) of 2.8 cm. This reactor has two zones which are designated as pyrolysis and catalyst bed respectively. Pre-weighed catalyst was packed inside of reactor by the aid of quartz wool plugs. Inlet part of the reactor was connected to gas inlet with PTFE fitting, and the outlet of the reactor was connected to gas line with stainless steel nuts (Swagelok Company, USA). A two zone tubular furnace with two temperature controllers and two thermocouples was used for the temperature control of the pyrolysis and catalyst bed zones. Before determining the reactor temperatures a number of preliminary tests were done to determine the appropriate reactor temperatures. For catalyst bed temperatures between 500-800 ^{o}C and for pyrolysis part temperatures between 700-900 ^{o}C were tested. According to the m/z=30 signal, the best conversion to nitric oxide was observed at 700 ^{o}C for pyrolysis and catalyst part of the reactor. Therefore, 700 ^{o}C were selected as optimum temperature for both reactor zones due to low conversion efficiency of bound nitrogen to nitric oxide at the other temperatures.

Figure 3. 4: Double-zone quartz reactor

- Gas conditioning unit: This unit consists of cooler fan, liquid-vapour separator and mist trap. Cooler fan, after reactor, is the first step for the cooling the combustion gases and condensing of the water vapor. The condensate water vapor is trapped in the liquid vapor separator and only the gas stream goes through analyzers. The final gas conditioning unit member is the mist trap to prevent the entry of any condensate granule or any mist to capillary inlet of mass spectrometer.

- Gas analysis / Data acquisition unit: The gas analysis/data acquisition unit contains a quadruple mass spectrometer (HPR 20, Hiden Analytical Inc., UK). The mass spectrum data were collected during the combustion experiments.
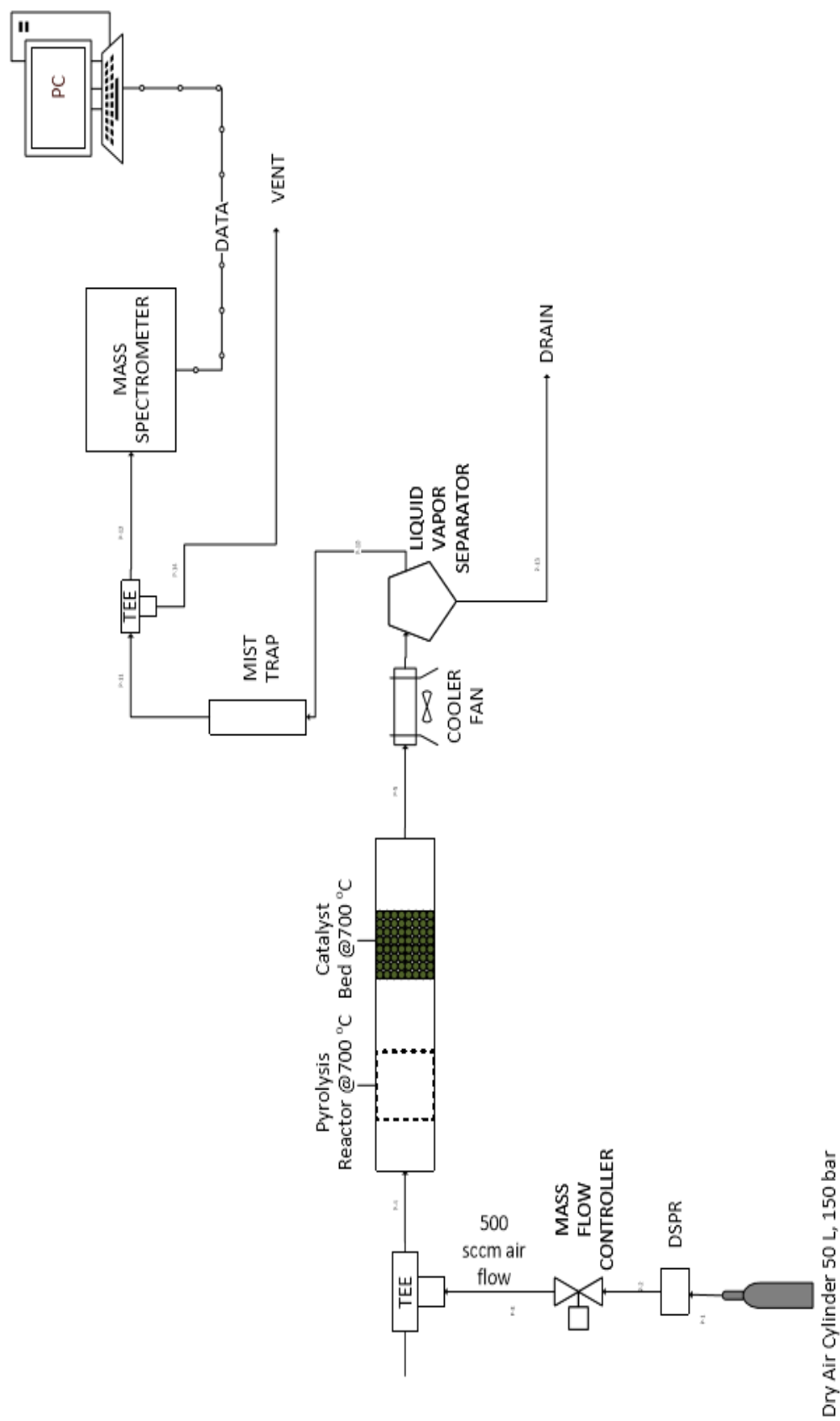
Figure 3. 5: Piping and instrumentation diagram of HTCO experiments setup

3.4.2 Temperature Programmed Oxidation (TPO) Experiments

This experimental setup was used to examine the catalyst activities and reaction mechanism of oxidation of the bound nitrogen at different temperatures. The experimental setup (Figure 3.6) for the catalytic activity test composes of the following four units.

- *Gas and sample feed unit:* This unit is used to provide sample and desired amount of gases flow to the reaction system. There are two inlet gas pressure regulator and two mass flow controllers (Alicat Scientific and Aalborg) in this system. Two check valve also are used at the outlet of the mass flow controllers for backflow in case of any pressure change. When three way valve is at purge position, the O_2/He gas mixture is directly fed into the reactor. When the valve position is switched to analysis position, the O_2/He gas mixture is passed from acetonitrile filled gas washer and then acetonitrile containing gas mixture is fed into the reactor.

- *Reactor unit:* This unit consists of quartz tubular reactor with inner diameter (ID) 4 mm. Pre-weighed amount of catalyst was packed inside of reactor by the aid of quartz wool plugs for each run. Inlet part of the reactor was connected to gas inlet with connected to gas line with stainless steel nuts (Swagelok Company,USA) . An auto-tune PID temperature controller with programmable ramp and level feature (Love Controls, USA) was used to control of the temperature of the reactor. A K-type sheathed thermocouple (Ordel Company, Turkey) which was embedded in the quartz wool packing over the catalyst sample was used for temperature control.

- *Gas conditioning unit:* This unit is same in section 3.4.1.

- *Gas analysis / Data acquisition unit:* The gas analysis/data acquisition unit contains a quadruple mass spectrometer (HPR 20, Hiden Analytical Inc., UK) and a Fourier transform infrared spectrometer (FTIR, Bruker equinox 55, USA) equipped with DEGS detector. The FTIR gas transmission cell has a path length of 19.5 cm and radius 3 cm. The gas cell was equipped with CaF_2 windows suitable for transmission between 150 and 8000 nm. The mass signal of selected ions and FTIR spectrum data were collected during the oxidation experiments with respect to temperature.
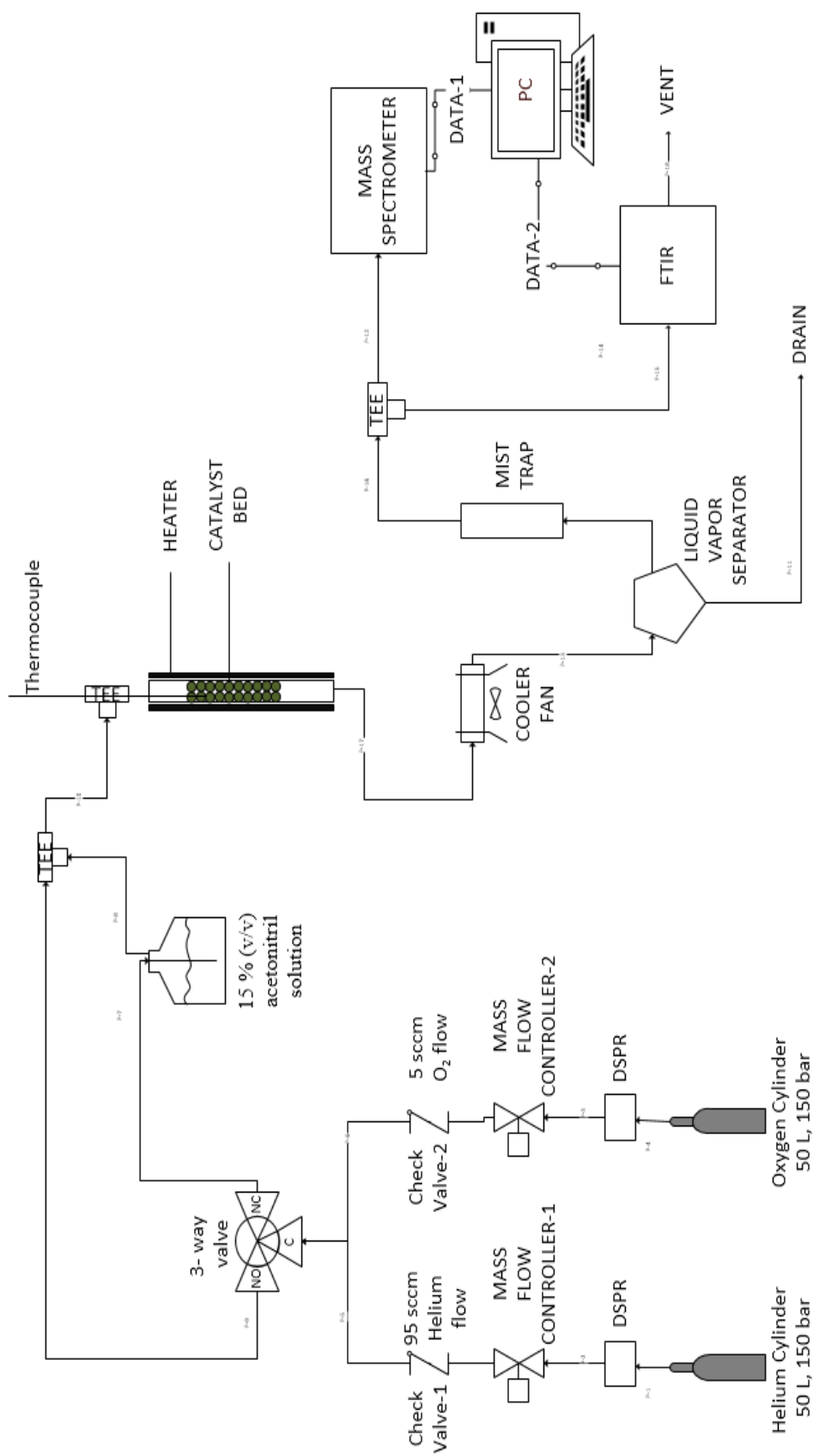
Figure 3. 6: Piping and instrumentation diagram of TPO experiments setup

3.5 Experimental Procedures

In this study, high temperature catalytic oxidation (HTCO) tests of selected model nitrogen components over the catalyst samples and temperature programmed oxidation of acetonitrile over the catalyst samples were performed.

3.5.1 High Temperature Catalytic Oxidation (HTCO) Test

High temperature oxidation tests for catalyst screening with this experiment were conducted in double-zone furnace with MS set-up described in section 3.3.1. For the experiments, predetermined amount of model compound is suddenly inserted into a preheated pyrolysis part of the double-zone reactor and the time course of reaction products were analyzed by mass spectrometry of selected ions. The detailed procedure for these experiments as follow;

a) Before starting the experiment 15 g of %1 wt Pt / Al_2O_3 catalyst sample was carefully weighed and placed in a quartz reactor which has 2.5 cm inner diameter. Both temperature zones of the furnace were set to $700\,^{\circ}C$.

b) Ammonium sulfate ($(NH_4)_2SO_4$) is generally used as a calibration agent for the nitrogen analyzers and it is completely oxidized into NO over the Pt/Al_2O_3catalysts**.** Therefore, 5 different amounts of ammonium sulfate ($(NH_4)_2SO_4$) was used to create a calibration curve for the HTCO experiments over 4 different catalysts. 5, 10, 20, 40, 60 mg of samples which contain 1.06, 2.12, 4.24, 8.48 and 12.72 mg nitrogen, respectively, were carefully weighed and loaded in different quartz sample boats. The samples were covered by a thin layer of quartz wool (0.1 gr) to prevent the spill out of samples during flash combustion. Finally, 200 μl of ultra-pure water was also injected on the samples. Each sample in quartz boats was suddenly inserted into the pyrolysis part of the reactor as a pulse input by aid of stainless steel rod in the presence of 500 sccm air flow rate, respectively. Each experiment was repeated three times to examine the repeatability of the analysis.

c) For ammonium sulfate oxidation experiments over the Pt/Al_2O_3 catalyst sample, mass signal of m/z 28, 30, 32, 44, 46 ions were monitored by mass spectrometer as a function of time and area under the curve of m/z=30 curve representing nitric oxide (NO) was calculated with the software Originlab™. Integrated areas of m/z=30 peaks and nitrogen content in the original sample was compared and drawn as a calibration curve for the further HTCO experiments.

d) 20 mg EDTA disodium salt dihydrate (Sigma-aldrich), 15 mg urea (Sigma-aldrich), 20 mg glutamic acid (Merck), 20 mg ammonium nitrate (Merck) and 400 µl of 2.5 % volume Pyridine (Merck) solution were studied for the high temperature catalytic oxidation experiments over the Pt/Al_2O_3 catalyst sample at 700 ^{o}C. The each model was tested three times in order to ensure reproducibility and the integrated area of m/z = 30 ions from mass spectrometer were determined and compared with calibration curve. The area under the peak of mass spectrometer was calculated by using Originlab™ software and the amount of NO formed and the percentage conversion of bound nitrogen to NO was determined by comparing the area and calibration curve.

e) 15 grams of 10 wt % Cu / Al_2O_3 catalyst sample was carefully weighed and placed in a quartz reactor. Reactor temperatures were set to 700 ^{o}C.

f) 20 mg EDTA disodium salt dihydrate (Sigma-aldrich), 15 mg urea (Sigma-aldrich), 20 mg glutamic acid (Merck), 20 mg ammonium sulfate, 20 mg ammonium nitrate (Merck) and 400 µl of 2.5 % volume Pyridine (Merck) solution were prepared in the quartz sample boat as in the part a.

g) Each sample in the quartz sample boats was suddenly inserted into the pyrolysis part of the reactor as a pulse input in the presence of 500 sccm air flow rate, respectively. The each model was tested two times in order to assure reproducibility.

h) The m/z=30 signal was collected with mass spectrometer (MS) and areas under the m/z=30 signal were integrated by means of the software Originlab™.

i) Relative standard deviation (RSD) of the repeats of same sample calculated according to integrated area results to examine the reproducibility of the repeats.

j) Percentage conversion of bound nitrogen to NO was calculated according to created calibration curve according to HTCO experiments of ammonium sulfate over %1 wt Pt / Al_2O_3 catalyst sample.

k) Steps e-j were repeated for 15 g of the catalyst samples 5 wt % Fe / Al_2O_3 3 wt % Cu - 7 wt % Ce / Al_2O_3.

3.5.2 Temperature Programmed Oxidation Experiments

Temperature programmed oxidation (TPO) experiments over different catalyst samples were conducted to observe the relationship between the reaction temperature and the reaction mechanism. The other goal of this part of study is to determine the temperature range for best performance of the catalyst samples. TPO experiments were carried out by using set-up described in section 3.3.2. Acetonitrile, which is a simple volatile organic nitrogen compound, was selected as a model compound for the temperature programmed oxidation (TPO) studies. The detailed procedure for these experiments as follow;

a) 0.2 g of Al_2O_3 support was carefully weighed and placed in a quartz reactor which has 4 mm inner diameter.

b) System was purged under the flow of 100 sccm of %5 O_2 in He gas mixture at 150 ^{o}C for 1 hour to remove the nitrogen gas (N_2) and water vapor in the system.

c) Reactor temperature was set to 50 ^{o}C under gas flow.

d) Three-way valve was changed to analysis position after temperature of the reactor decreased to 50 ^{o}C which swithes the gas flow into acetonitrile filled gas washing bottle.

e) Steady-state condition was waited by observing m/z = 41 (acetonitrile), m/z = 28 (nitrogen), m/z = 32 (oxygen), m/z = 4 (helium) signals on the mass spectrometer.

f)   The reactor temperature was raised from 50 ^{o}C to 900 ^{o}C with a ramp rate 20 ^{o}C/min

g)   Oxidation gases were passed over gas conditioning unit and analyzed with mass spectrometer and FTIR spectrometer which are connected to each other in parallel as shown in the figure 3.6. The signals m/z = 41 (acetonitrile), m/z = 28 (nitrogen and carbon monoxide), m/z = 32 (oxygen), m/z = 30 (nitric oxide) , m/z = 44 (carbon dioxide and nitrous oxide) were investigated on the mass spectrum to understand the reaction mechanisms at different temperatures.

h)   Steps a-g were repeated for 0.2 g of the catalyst samples 10 wt % Cu / Al_2O_3, 5 wt % Fe / Al_2O_3 1 wt % Pt / Al_2O_3 3 wt % Cu - 7 wt % Ce / Al_2O_3.

CHAPTER 4

RESULT AND DISCUSSION

4.1 Catalyst Characterization

The catalyst samples of $CuO-CeO_2/Al_2O_3$, CuO/Al_2O_3, Fe_2O_3/Al_2O_3 Pt/Al_2O_3 were characterized by high temperature catalytic oxidation (HTCO) of nitrogen containing model compounds, temperature programmed oxidation (TPO) of a model compound, XRD and N_2-BET methods.

4.1 Catalyst Characterization

The catalyst samples synthesized for the oxidation of nitrogen containing samples were characterized by XRD analysis and BET method.

4.1.1 X-Ray Diffraction Analysis

X-ray powder diffraction (XRD) technique was used to identify crystal structure of the catalyst samples. The synthesis method of catalyst samples are explained in section 3.1 in detail.

XRD patterns of the catalyst samples are presented in figure 4.1. As it can be seen unambiguously, all XRD patterns include small and broad diffraction peaks at 2θ value at 37.5^o and 67.3^o, which indicates γ-Al_2O_3 structure (ICSD PDF Card No: 01-088-1609, See in Appendix C). The γ-Al_2O_3 structure has also peaks around 46.7^o which can be easily seen in the XRD patterns of catalyst samples except 3%Cu- 7%Ce / Al_2O_3. The reason for not observing of 46.7^o Al_2O_3 peaks in the XRD patterns of ceria containing catalyst can be the interference of ceria peak at 46.5^o. Moreover, this phenomenon can be the reason of the strong interaction between Cu, Ce and Al oxides which is

mentioned in the study of *Guo et al* [83].

In the XRD pattern of 10% Cu / Al_2O_3 catalyst sample, CuO diffraction peaks can be seen around 35.6^o, 38.7^o (ICSD PDF Card No: 01-089-5897, See in Appendix C).

XRD peaks of 3 % wt Cu – 7 % wt Ce / Al_2O_3 catalyst was indexed according to ICDS PDF Card No: 01-073-7747 (See in Appendix C) and observed the cubic $Fm\overline{3}m$ structure of CeO_2. XRD pattern of the 3 % wt Cu – 7 % wt Ce / Al_2O_3 catalyst sample shows that diffraction peaks of crystalline CeO_2 can be seen at 28.6^o, 33.1^o, 47.7^o and 56.5^o which are in agreement with literature [82]. The CuO diffraction lines, which can be seen in the XRD patterns of 10% Cu / Al_2O_3 catalyst sample, cannot be seen in the pattern of the 3 % wt Cu – 7 % wt Ce / Al_2O_3 catalyst sample. This phenomenon is the result of the decreasing of copper loading from 10 to 3 %. Broad diffraction lines and the low band intensities of the CeO_2 were also attributed to good dispersion of CeO_2 over the support in the literature [83].

XRD patterns of alumina supported platinum containing catalysts have small diffraction lines at 39.2°, 46.2° (ICSD PDF Card No: 01-087-06412, See in Appendix C)

Small diffraction lines at 33.1° and 36.2° in the XRD pattern of 5% Fe / Al_2O_3 catalyst can be assigned for α-Fe_2O_3 phase (ICSD PDF Card No: 01-084-0311 ,See in Appendix C).
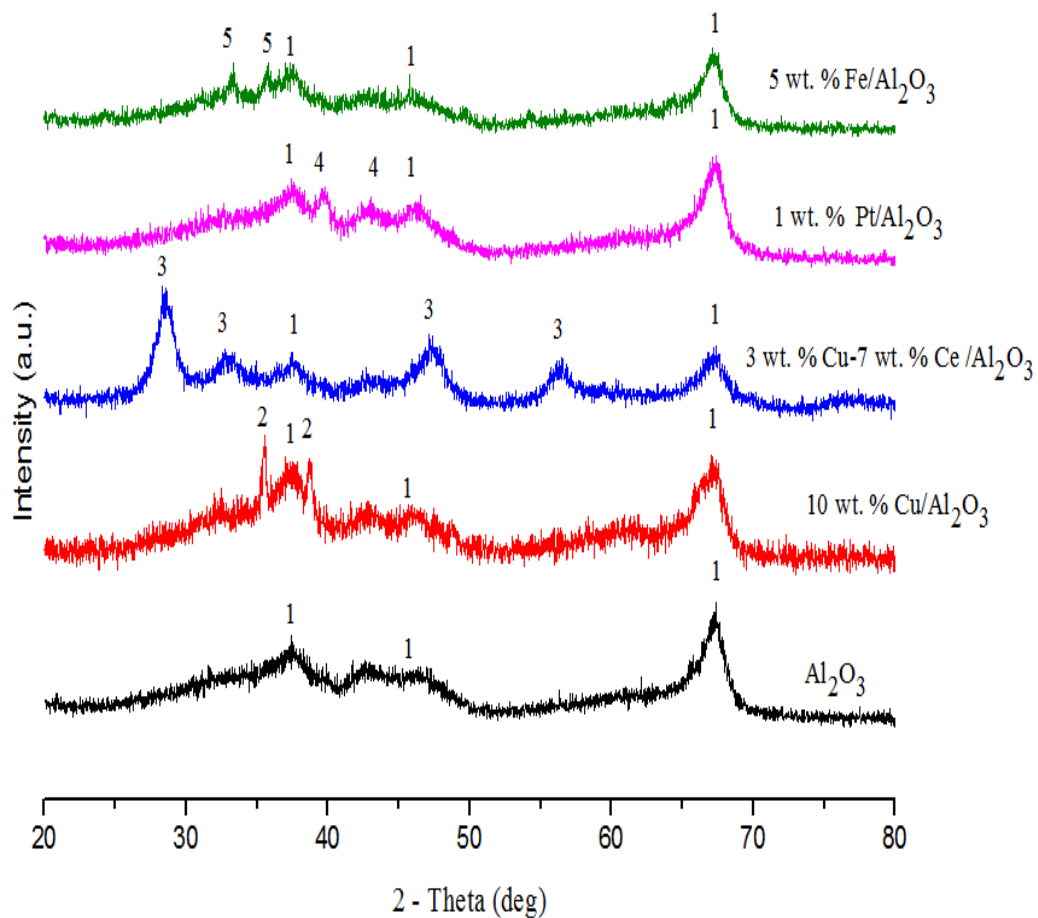
Figure 4. 1: XRD patterns of Al_2O_3 support and catalyst samples that are calcined at 700 ^{o}C under air flow (lines (1) attributed to γ- Al_2O_3, lines (2) attributed to CuO, lines (3) attributed to CeO_2, lines (4) attributed to Pt, lines (5) attributed to α-Fe_2O_3)

4.1.2 BET Surface Area, BJH Pore Size Distribution and Pore Volume

Nitrogen sorption method was used to investigate the textural properties of the catalyst samples. BET and BJH techniques were used to determine the surface area and pore size distribution of the catalyst samples. Surface area of Al_2O_3 support and catalyst samples are shown in table 4.1.

According to table 4.1, it can be clearly seen that, the surface area decreases as the metal loading increases. While loading of 1 % wt. platinum metal does not change the surface area, 5 % wt. iron, 10 % wt. copper and 3 % wt. copper- 7%

47

wt. ceria metal loadings over alumina support decrease the surface area of the support from 192 m^2/g to162 m^2/g, 147 m^2/g and 153 m^2/g, respectively. However, the change in the surface area of the Al_2O_3 is not significant after the impregnation with the cerium, copper, iron oxides and platinum. Therefore, it can be said that there is no significant blockage in the pores of the Al_2O_3 support by the impregnation of the metals.

Table 4. 1: BET surface areas of the catalyst samples

Sample	BET Surface Area (m^2/g)
Al_2O_3	192
10% Cu / Al_2O_3	147
3%Cu- 7%Ce / Al_2O_3	153
5% Fe_2O_3 / Al_2O_3	162
1%Pt / Al_2O_3	194

N_2 adsorption isotherms of Al_2O_3 support and catalyst samples were analyzed by BJH method to investigate pore size distribution of the samples. The N_2 adsorption isotherms of the alumina support and the catalyst samples are presented in figure 4.2. According to adsorption/desorption isotherms, it can be clearly seen that when the amount of loading increases, total nitrogen uptake decreased on the catalyst surface, which indicates decreasing surface area due to increasing metal loading. However, the increasing amount of catalyst loading did not form significant blockage in the pores in the support since there is no a huge difference in the amount of adsorbed nitrogen. The Al_2O_3 support and catalyst samples showed type IV adsorption isotherm and had H3 hysteresis loop according to the International Union of Pure and Applied Chemistry (IUPAC) classification. H3 hysteresis loop represents the nitrogen capillary condensation within the mesoporous structure of the support and catalyst samples [86].
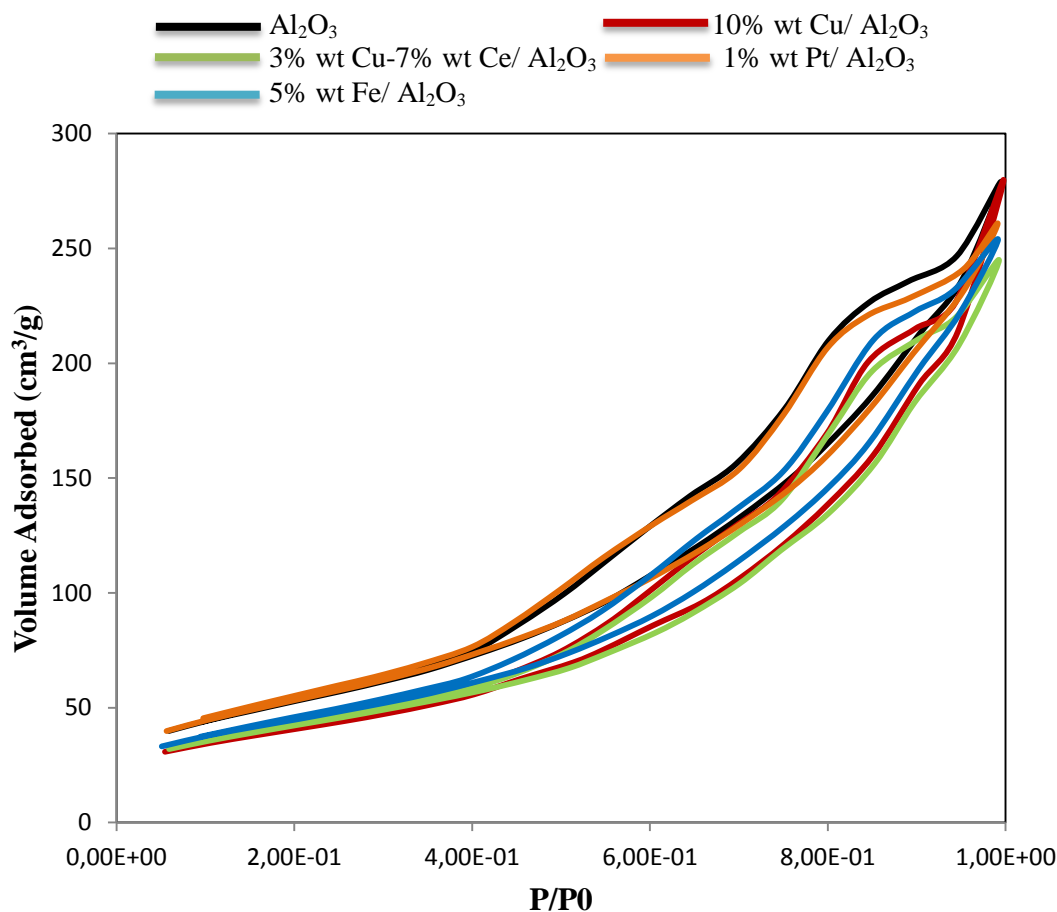
Figure 4. 2: Nitrogen adsorption/desorption isotherms of Al_2O_3 support and catalyst samples

The pore size distributions of the alumina support and the catalyst samples are presented in figure 4.3. The pore volume data of the alumina support and catalyst samples are listed in table 4.2. According to pore volume data, the increasing amount of catalyst loading to the support decrease the pore volume of the support. Pore size distributions shows that the support and the catalyst samples exhibit bimodal pore size distribution. The first domain is comprised of smaller mesopores having 4-5 nm pore diameter and the second domain with 10-12 nm pores.
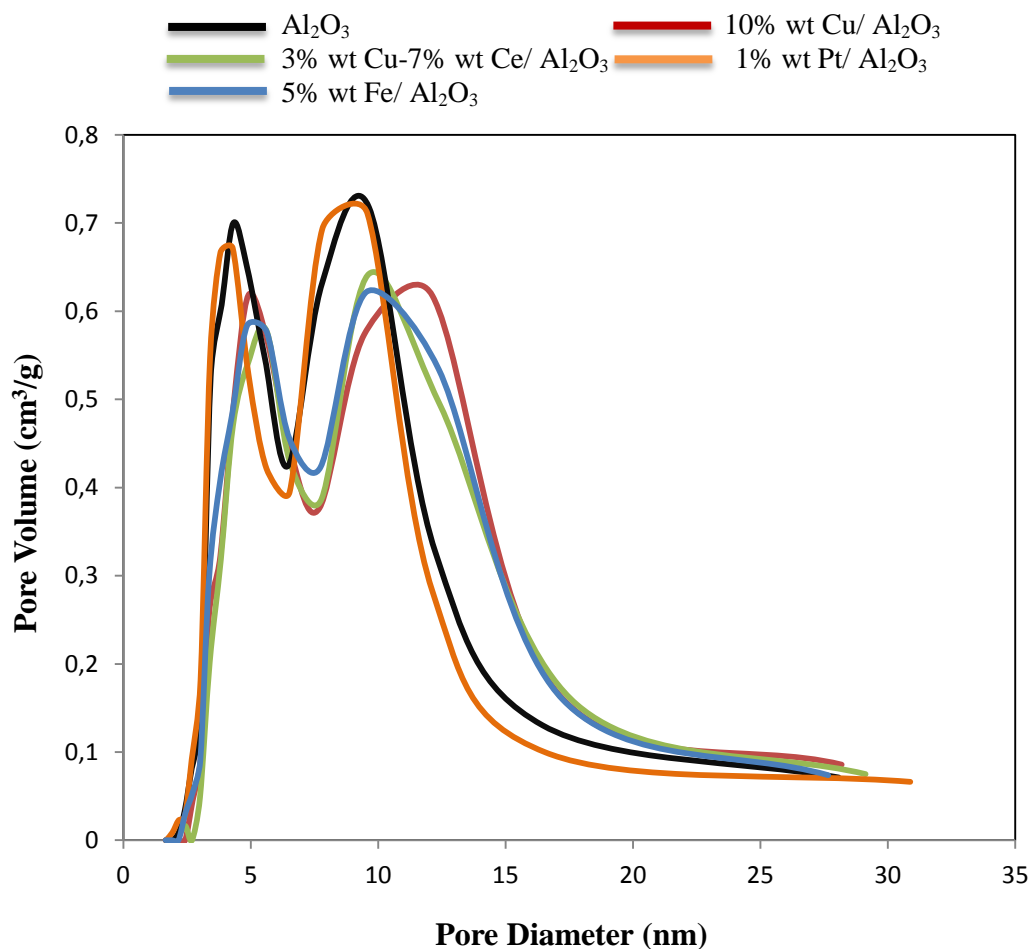
Figure 4. 3: Pore size distribution of Al_2O_3 support and catalyst samples

Table 4.2: Average pore volumes and pore diameters of the catalyst samples and Al_2O_3 support

Sample	Pore Volume ($cm^3 \, g^{-1}$)
Al_2O_3	0.438
10 % Cu / Al_2O_3	0.440
3 % Cu- 7 % Ce / Al_2O_3	0.383
5 % Fe / Al_2O_3	0.398
1 % Pt / Al_2O_3	0.409

4.2 Catalytic Activity Tests

4.2.1 High Temperature Catalytic Oxidation (HTCO) Tests

High Temperature Catalytic Oxidation (HTCO) tests were carried out for the screening of 1 % Pt / Al_2O_3, 10 % Cu / Al_2O_3, 3 % Cu -7 % Ce / Al_2O_3, 5 % Fe / Al_2O_3 catalyst samples for the oxidation of bound nitrogen in the selected model compounds (EDTA di sodium salt hydrate ($C_{10}H_{14}N_2Na_2O_8 \cdot 2H_2O$), glutamic acid ($C_5H_9NO_4$), ammonium sulfate (($NH_4)_2SO_4$), ammonium nitrate (($NH_4)(NO_3)$), pyridine ($C_5H_5N$) and urea ($CH_4N_2O$)) to NO. The reaction products were analyzed by using mass spectrometer. The possible reaction products and the assigned parent m/z ratios of the product molecules are shown in the table 4.3. The m/z=30 signal was examined to observe the conversion of bound nitrogen to nitric oxide (NO). By analyzing parent m/z signals, it is not possible to distinguish nitrous oxide (N_2O, m/z=44) from carbon dioxide (CO_2, m/z=44), carbon monoxide (CO, m/z=28), nitrogen in air and produced nitrogen molecule as a result of the reaction (m/z=28).

Table 4. 3: Parent m/z signals of the combustion gas products

Molecule	Parent m/z signals
CO_2	44
CO	28
NO_2	46
NO	30
N_2O	44
N_2	28
O_2	32

The response of mass spectrometer to nitric oxide was determined by calibration study. In HTCO technique, ammonium sulfate is generally used as calibration compound in many study and commercial nitrogen analyzers which used Pt/Al_2O_3 catalyst at temperatures over 700 ^{o}C [67, 91, 19]. In this study, 5, 10,

51

20, 40, 60 mg of ammonium sulfate was used to create a calibration curve at 700 ^{o}C over 1 % Pt / Al$_2$O$_3$ catalyst by assuming the complete oxidation of bound nitrogen of ammonium sulfate to NO. Moreover, it controlled by calculating percentage relative standard deviation (%RSD) of three repetitive analyzes of each amount and R-squared value of the calibration curve indicating how close the data are to the fitted regression line. For this purpose, the complete oxidation of five different charges of ammonium sulfate (NH$_4$)$_2$SO$_4$) (5, 10, 20, 40, 60 mg) which contain 1.06, 2.12, 4.24, 8.48 and 12.72 mg of nitrogen were performed and m/z=30 signal in combustion gases were monitored. The details of calibration study are described in section 3.5.1 in detail. Integrated area of the m/z=30 signal was calculated by using Originlab™ and the area results was drawn to create a calibration curve as a function of nitrogen content of the sample.

In figure 4.4, m/z = 30 signal change was shown as a function of time which represents the three repetitive HTCO analysis of 5 mg of ammonium sulfate over 1 % Pt/Al$_2$O$_3$ catalyst sample at 700 ^{o}C under 500 sccm air flow. Calculated integrated areas of the three peaks of 5 mg ammonium sulfate HTCO experiments over 1 % Pt / Al$_2$O$_3$ are shown in the figure 4.5. (See Appendix A for, m/z = 30 signal change was shown as a function of time and integrated areas of m/z=30 signal of 10, 20, 40 and 60 mg of ammonium sulfate over 1 % 1 wt Pt/ Al$_2$O$_3$ catalyst.)
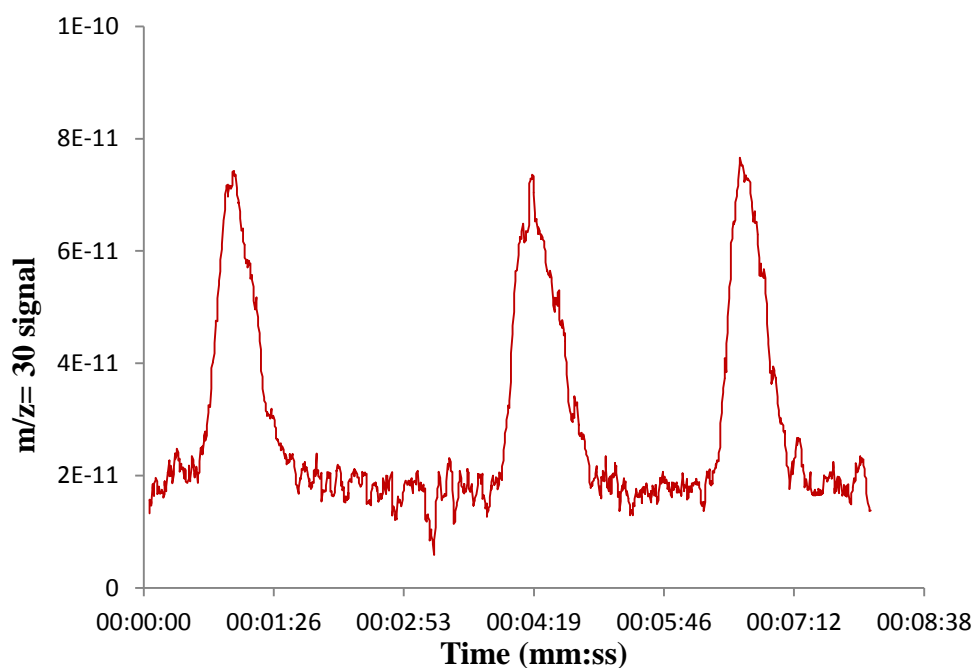
Figure 4. 4: m/z = 30 signal trend of three repetitive high temperature catalytic oxidation tests of 5 mg $(NH_4)_2SO_4$ over 1 % Pt/Al_2O_3 catalyst sample at 700 ^{o}C in the presence of 500 sccm air flow
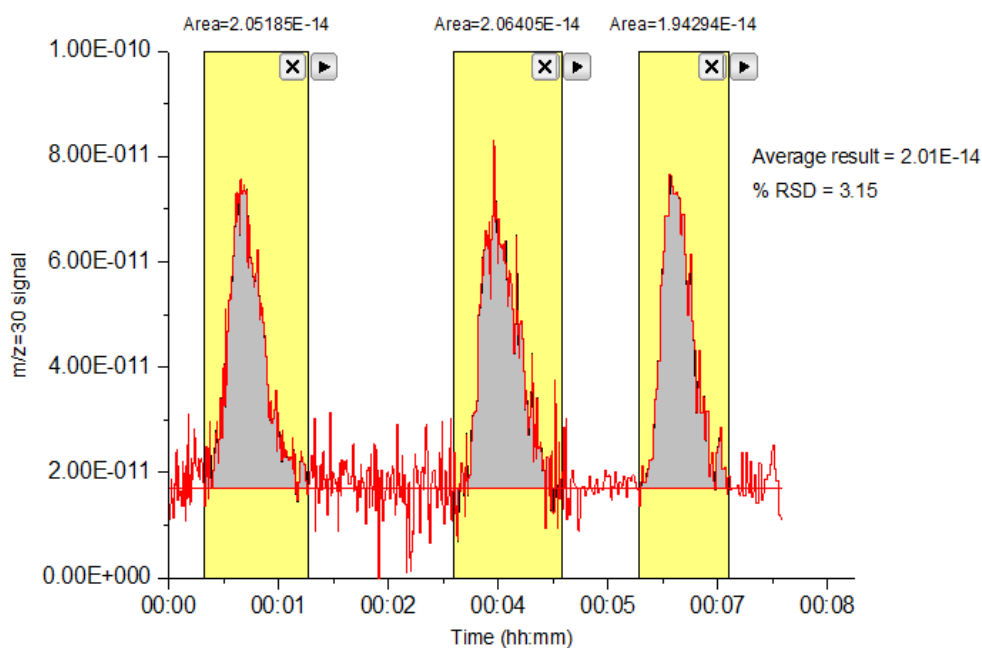
Figure 4. 5: Integrated area of the m/z = 30 signal curve of three repetitive high temperature catalytic oxidation tests of 5 mg $(NH_4)_2SO_4$ over 1 % Pt / Al_2O_3 catalyst sample at 700 ^{o}C in the presence of 500 sccm air flow

The integrated area of the m/z=30 signal are presented in table 4.4, and the calibration curve is shown in the figure 4.6. It can be said that bound nitrogen content of ammonium sulfate was completely oxidized to nitric oxide (NO) according to reproducible analysis results, which refers to smaller % RSD values, shown in table 4.3 and linearity of calibration curve in the figure 4.6

Table 4. 4: Average integrated areas of the m/z = 30 signal curve of three repetitive HTCO tests of 5 different amounts of ammonium sulfate over 1 % Pt / Al_2O_3 catalyst sample at 700 ^{o}C in the presence of 500 sccm air flow and the % relative standard deviation (RSD) values of the repetitive analyzes

Sample	Nitrogen Content (mg)	Repeat Number	Average Integrated area of m/z=30 signal	% RSD of repetitive HTCO analyses
5 mg $(NH_4)_2SO_4$	1.06	3	2.01E-14	3.15
10 mg $(NH_4)_2SO_4$	2.12	3	3.11E-14	2.11
20 mg $(NH_4)_2SO_4$	4.24	3	5.08E-14	3.31
40 mg $(NH_4)_2SO_4$	8.48	3	9.43E-14	1.99
60 mg $(NH_4)_2SO_4$	12.72	3	1.34E-13	2.61
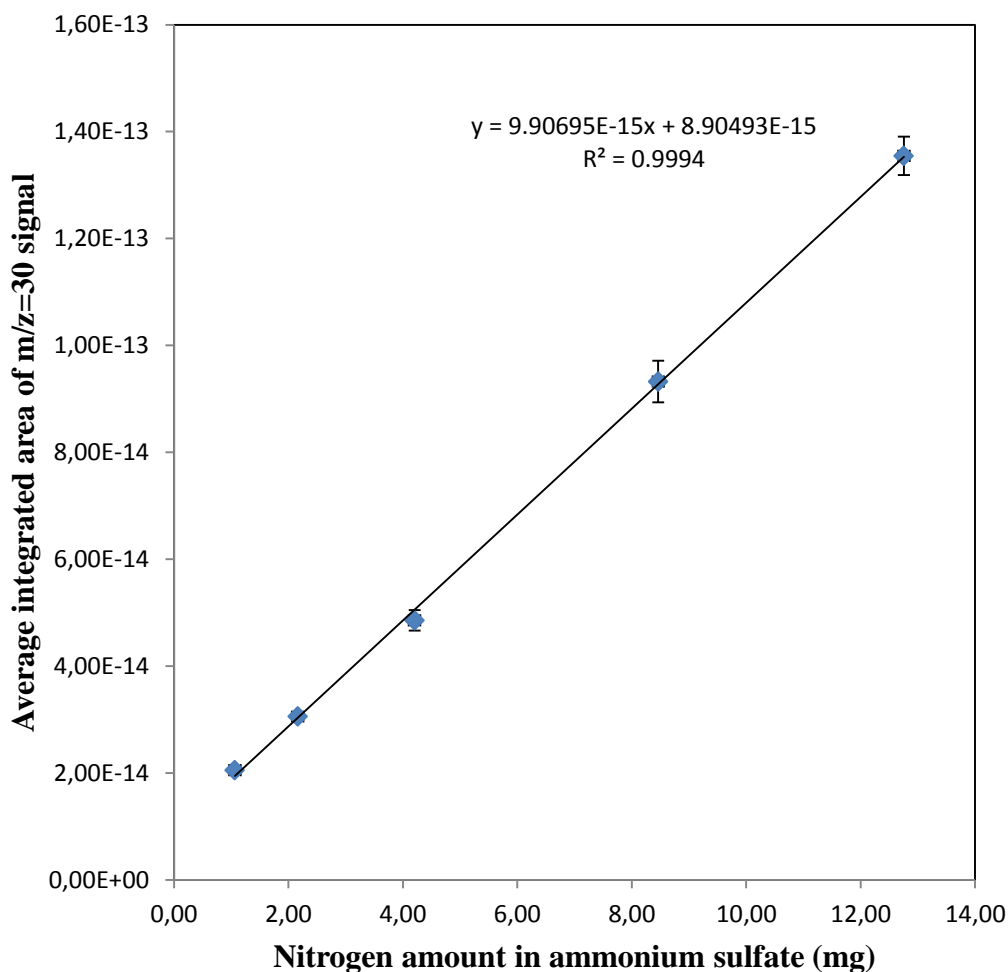
Figure 4. 6: Calibration curve obtained according to oxidation of 5 different amount of ammonium sulfate on 1 % wt Pt/Al_2O_3 catalyst at 700 ^{o}C in the presence of 500 sccm air flow

Similarly, 20 mg EDTA di sodium salt hydrate ($C_{10}H_{14}N_2Na_2O_8 \cdot 2H_2O$), , 20 mg glutamic acid ($C_5H_9NO_4$), 20 mg ammonium sulfate (($NH_4)_2SO_4$), 20 mg ammonium nitrate (($NH_4)(NO_3)$), 400 μl of 2.5 % volume Pyridine (C_5H_5N) solution and 15 mg urea (CH_4N_2O) were analyzed over 1 % Pt / Al_2O_3, 10 % Cu / Al_2O_3, 3 % Cu -7 % Ce / Al_2O_3, 5 % Fe / Al_2O_3 catalyst samples. Pyrolysis and catalyst zones of the reactor were set at 700 ^{o}C and the air flow rate was set 500 sccm. After the reaction gases pass through gas conditioning unit, which provides separation of condensed water vapor and preventing formation of any condensate or mist in capillary of the mass spectrometer, the reaction product gases were investigated with mass spectrometry. The m/z =

30 signal, representing nitric oxide, were collected and peak areas were integrated with Originlab™ software. The amount of nitrogen converted to nitric oxide was calculated by using the calibration curve in figure 4.6 as in the Appendix B.2.2. Then, percentage conversions of bound nitrogen in the compounds to nitric oxide were calculated by using known nitrogen amount that fed to the reactor and calculated nitrogen amount according to calibration curve. The integrated area calculations and percentage conversion results are shown in Appendix A and B, respectively. The reason of the difference between fed nitrogen amount and calculated nitrogen amount according to calibration curve (figure 4.6) can be incomplete combustion or the conversion of the fed bound nitrogen to nitrous oxide (N_2O) or molecular nitrogen (N_2). The interference of parent MS signals of carbon dioxide and nitrous oxide at $m/z=44$ hinders distinguish these combustion products. Moreover, if the nitrogen molecule forms as a result of combustion reaction, it is impossible to distinguish due to nitrogen feed in the carrier gas air.

High temperature oxidation tests of model compounds to nitric oxide are shown in the figure 4.7. As it is seen from the figure 4.7, alumina supported iron catalyst performed best and more than 95 % conversion was observed for all tested model compounds. The bound nitrogen in different model compounds were chiefly oxidized to nitric oxide over the 5 % wt Fe/Al_2O_3 catalyst at 700 °C.

Alumina supported platinum catalysts are the commercial catalyst, which are used in the commercial nitrogen analyzers that work according to HTCO-CLD technique. Moreover, it is used in many studies for conversion of bound nitrogen to nitric oxide, which are mentioned in the section 2.3, and it is proven that alumina supported platinum catalyst is very successful for the oxidation of bound nitrogen to nitric oxide. According to figure 4.7, 1 % wt Pt/Al_2O_3 catalyst sample performed a good catalytic activity to conversion of bound nitrogen to nitric oxide for all model compounds except pyridine. Therefore, it can be clearly stated that 5 % wt Fe / Al_2O_3 catalyst performed good catalytic activity

relative to 1% wt Pt / Al_2O_3 catalysts for conversion bound nitrogen in pyridine to NO. Some of the experiment results over 5 % wt Fe / Al_2O_3 and 1% wt Pt / Al_2O_3 catalysts showed conversion values greater than % 100, which can be seen in the tables B.4 and B.5. These conversion values could be the results of the weighing errors and error margin in the created calibration line. This might be also explained as better oxidation or conversion of bound nitrogen to nitric oxide (NO) in these compounds than with the ammonium sulfate used to create a calibration curve.

The lowest activity was observed over 10 % wt. Cu / Al_2O_3 and 3 % wt. Cu – 7 % wt. Ce / Al_2O_3 catalyst samples for the conversion of the bound nitrogen to nitric oxide. It can be seen that; bound nitrogen conversions of edta, glutamic acid, and ammonium sulfate samples over 10 % wt. Cu / Al_2O_3 catalyst sample are 36 %, 36% and 69 % , respectively,. The reason of the low conversion of ammonium sulfate over 10 % wt. Cu / Al_2O_3 catalyst sample can be explained by significant conversion of bound nitrogen to N_2O as well as NO which is agreement with literature [64]. The low recoveries of nitrogen in edta and glutamic acid can be explained by conversion of the bound nitrogen to N_2O and N_2 as well as NO. 3 % wt. Cu – 7 % wt. Ce / Al_2O_3 catalyst samples also performed poor catalytic activity except urea and ammonium sulfate. The same reaction mechanism over the 10 % wt. Cu / Al_2O_3 catalyst may explain the reason of lower conversions. Therefore, it can be clearly stated that 5 % wt Fe / Al_2O_3 catalyst is more selective than 10 % wt Cu / Al_2O_3 and 3 % wt. Cu – 7 % wt. Ce / Al_2O_3 catalysts for bound nitrogen to NO.

Alternative reaction pathways of nitrogen in edta, glutamic acid, and ammonium sulfate over the 10 % wt. Cu / $Al_2O_3,$ 3 % wt. Cu – 7 % wt. Ce / Al_2O_3 catalysts samples can be attributed to pyrolysis reactor temperature, catalyst temperature and the molecular structures. However, it is difficult to exactly distinguish the alternative reaction pathways to nitrous oxide or nitrogen molecule due to interferences of carbon dioxide, carbon monoxide and nitrogen in the air that mentioned above.
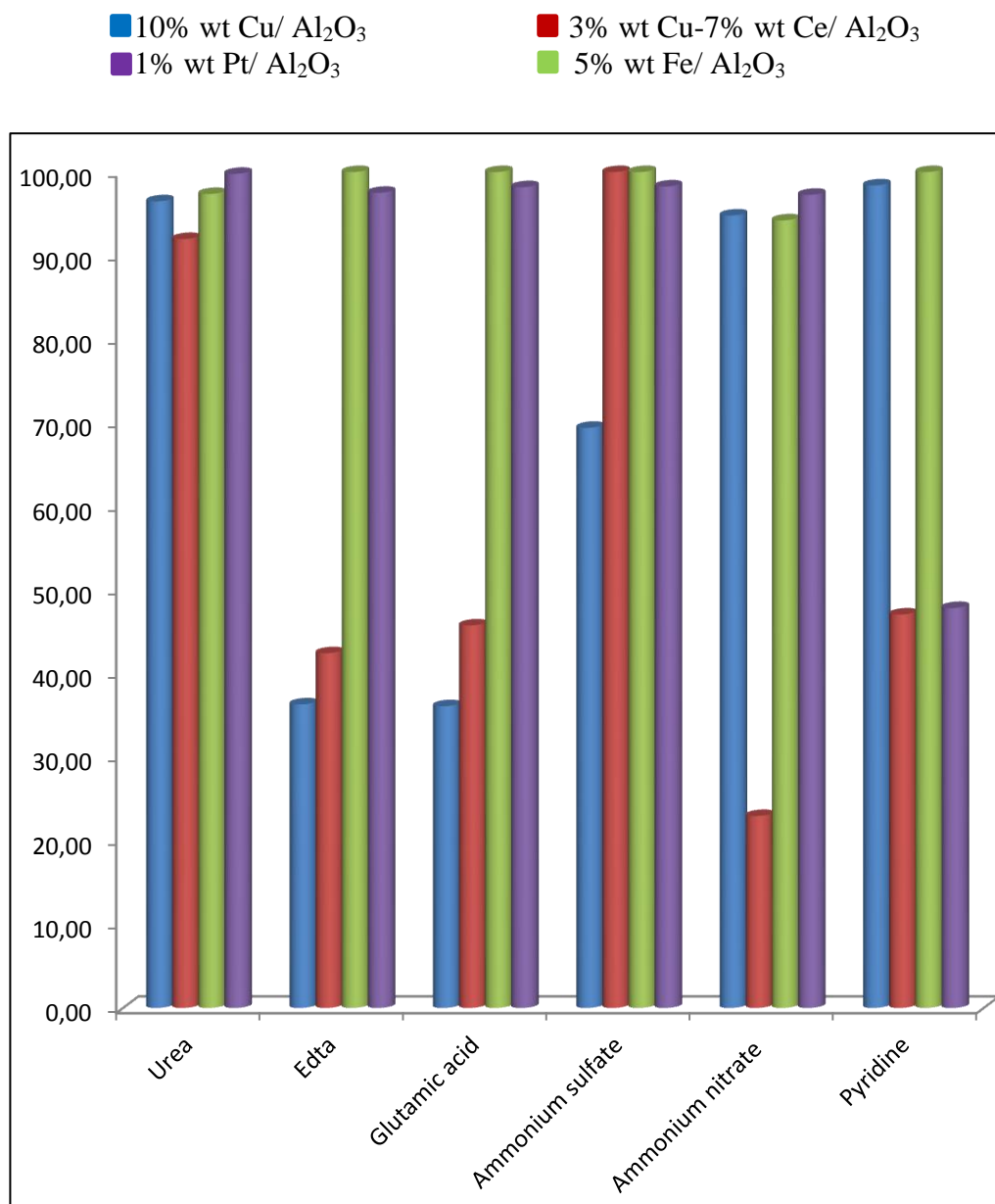
Figure 4. 7: Percentage conversion of bound nitrogen to nitric oxide results of selected model compounds over 5 % wt Fe / Al_2O_3, 1% wt Pt / Al_2O_3, 10 % wt Cu / Al_2O_3 and 3 % wt. Cu – 7 % wt. Ce / Al_2O_3 catalyst samples at 700 °C, in the presence of 500 sccm air flow

As a result of the HTCO experiment results, 5 % wt Fe / Al_2O_3 catalyst performed the best catalytic activity for the complete oxidation of the bound

nitrogen in the model components to NO. 1% wt Pt / Al_2O_3 also performed very good catalytic activity, except oxidation of bound nitrogen in pyridine to NO. 10 % wt. Cu / Al_2O_3 and 3 % wt. Cu − 7 % wt. Ce / Al_2O_3 catalyst showed poor catalytic activity. According to preliminary tests, which were done before HTCO experiments, conversion of organic nitrogen in EDTA and glutamic acid to NO is very low. Therefore, samples were fed to the reactor after 200 μl of water was added to sample boat to enhance oxidation of organically bound nitrogen. After water addition, complete organic nitrogen conversions to NO were achieved over 1% wt Pt / Al_2O_3 catalyst. According to HTCO experiments, it is understood that water plays an important role as an oxidizing agent for the conversion of organically bound nitrogen to NO which is agreement with the literature [64].

In section 4.4.2, the low conversion values in HTCO experiments are investigated by conducting temperature-programmed oxidation (TPO) studies which show the oxidation mechanisms of a nitrogen containing sample at different temperatures over the catalyst samples and support.

4.2.2 Temperature Programmed Oxidation (TPO) Studies

Temperature programmed oxidation (TPO) experiments over Al_2O_3 support, 1 % wt. Pt / Al_2O_3, 10 % wt. Cu / Al_2O_3, 3 % wt. Cu − 7 % wt. Ce / Al_2O_3, 5 % wt. Fe / Al_2O_3 catalyst samples were utilized to explore temperature effects on oxidation mechanisms of nitrogen containing compounds and catalytic activities of the catalyst samples. Moreover, these experiments were conducted to understand the low conversion values of model compounds over 10 % wt. Cu / Al_2O_3 and 3 % wt. Cu − 7 % wt. Ce / Al_2O_3 catalysts in HTCO tests. Acetonitrile (C_2H_3N), which is a simple volatile organic compound, was selected as a model compound for the temperature programmed oxidation (TPO) studies. Before the TPO studies, the system was purged under the flow of 100 sccm of %5 O_2 in He gas mixture at 150 ^oC for 1 hour to remove the nitrogen gas (N_2) coming from atmosphere and water vapor in the system. Therefore, the

change in the m/z= 28 signal can only be the reason of nitrogen molecule and carbon monoxide which are formed as a result of the combustion reaction. The TPO experiments were carried out in fixed bed reactor in which gas mixture (%5 O_2 and %95 He by volume), comes from bubbling 15 % volume acetonitrile solution in water passed over 0.2 g catalyst bed in the presence of 100 sccm gas flow rate (%5 O_2 and %95 He by volume). The reactor was fixed in a furnace of which temperature was raised from 50 ^{o}C to 900 ^{o}C with a ramp rate of 20 ^{o}C/min. Oxidation gases were passed over gas conditioning unit, which provides condensation and removal of the water and also trapping of any mist vapor in the gas stream, and analyzed with mass spectrometer and FTIR spectrometer which are connected to each other in parallel. The details of the temperature programmed oxidation (TPO) experiments were explained in section 3.5.2.

Acetonitrile oxidation mechanisms, which are schematized in the figure 4.8 as two main reaction paths, have been already found in the literature [85]. The first path is decomposition of acetonitrile to HCN, CN and NCO intermediates and further oxidation of bound nitrogen in the intermediates to NO, N_2, N_2O and NO_2. The second reaction mechanism for combustion of acetonitrile is NO, N_2, N_2O and NO_2 formation via CH_3CONH_2 and NH_3 intermediates. In this study, the results of the TPO studies were evaluated according to these reaction paths.
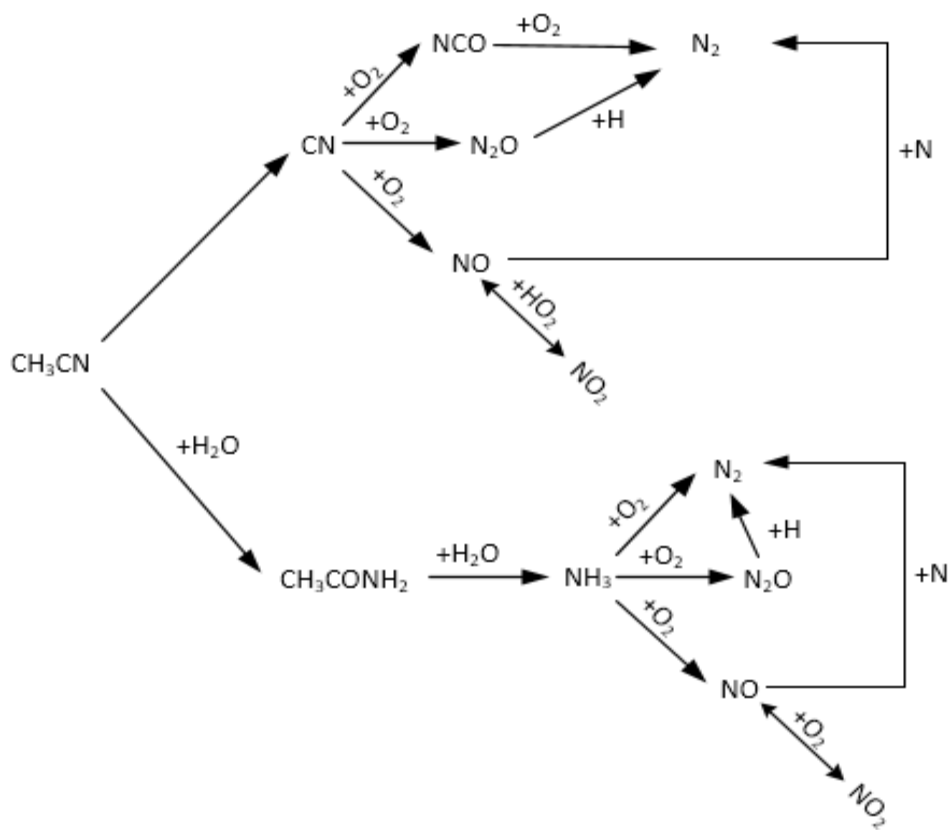
Figure 4. 8: Oxidation mechanisms of acetonitrile (C_2H_3N)

Table 4.3 and 4.5 show the parent m/z signal and IR absorption range of combustion products of the acetonitrile, respectively, during the TPO studies. The gas mixture (%5 O_2 and %95 He by volume) was used as carrier/oxidation gas in the TPO studies, therefore; N_2 formation can be easily seen in the m/z=28 signal of the MS due to lack of air nitrogen in the product gases. Moreover, N_2O could not be distinguished in the HTCO experiments because of interference of CO_2 at the m/z=44 signal, it can be distinguished in the TPO experiments by using FTIR spectrometer.

Table 4. 5: IR absorption range of the combustion gas products

Molecule	IR Absorption range (cm^{-1})
CO_2	2025 – 2225, 3500 – 3900
CO	2250 – 2400
NO_2	1550 – 1650, 2800 – 2950
NO	1800 – 1950
N_2O	2150 – 2300, 1200 – 1400, 3400 – 3600
NH_3	800 – 1200, 1800 – 1500, 3200 – 3400
-$CONH_2$	1650 – 1750
H_2O	3400 – 4000, 1400 – 2000
-NCO	1250 – 1300

TPO mass spectrometer profiles obtained during the time course of temperature programmed oxidation (TPO) over Al_2O_3 support is shown in figure 4.8. The increase in the m/z=44 signal starts around 380 ^{o}C which refers to oxidation of acetonitrile. The m/z=41 signal, representing acetonitrile, steadily decreases up to 900 ^{o}C. When the temperature exceeds 430 ^{o}C, it is observed in the figure 4.9 that m/z=44 and m/z=28 signals starts to increase which indicates the generation of CO_2 and N_2. The signal m/z=28 might also be attributed to the production of CO by incomplete combustion. The m/z=30 signal, which represents major mass spectrum peak of nitric oxide (NO), slightly increase at 800 ^{o}C, that is; bound nitrogen in the acetonitrile starts to convert into nitric oxide. Moreover, the decrease in the m/z=28 signal, which represents major mass spectrum peak of carbon monoxide (CO) and nitrogen molecule (N_2) above 800 ^{o}C can be explained by the oxidation of carbon monoxide to carbon dioxide and/or bound nitrogen to nitrogen oxides. It is very difficult to understand the reaction mechanism clearly according to the MS results due to the interferences mentioned in the results of HTCO experiments. To overcome the interferences in the MS, IR spectra of the TPO results over Al_2O_3 support, which is shown in figure 4.10, are used to explain the reaction mechanism. According to figure 4.10, the increase in the carbon monoxide (CO) intensity (2025-2225 cm^{-1}) and

carbon dioxide (2250-2400 cm^{-1}) can be easily observed after 400 ^{o}C. The carbon monoxide (CO) intensity (2025-2225 cm^{-1}) shows increase up to 800 ^{o}C, then it slightly decrease at 900 ^{o}C. The nitrogen dioxide intensity (1550-1650 cm^{-1}) starts to increase after 800 ^{o}C. Hence, the decrease in the m/z=28 signal can be interpreted as partial oxidation of carbon monoxide to carbon dioxide due to decrease in the carbon monoxide IR intensity. The decrease in the m/z=28 signal can also be understood as shifting reaction mechanism to nitric oxide and nitrogen dioxide path via ammonia (NH$_3$) formation mechanism since NH$_3$ intensity in the IR spectrum (800-1200 cm^{-1}) increases after 600 ^{o}C up to 900 ^{o}C. After 800 ^{o}C, the increase in the m/z=30 signal of MS and NO intensity in the IR Spectra (1800 – 1950 cm^{-1}) shows the conversion of bound nitrogen molecule to nitric oxide (NO). Also, nitrogen dioxide (NO$_2$) intensity (1550-1650cm^{-1}) starts to increase after this temperature, but there is not any change in the parent signal of nitrogen dioxide (m/z=46) in the MS. This might be explained by greater IR activity of the NO$_2$ than NO. In other words, the peak intensities of the molecules can change according to their IR activities, they does not proportional to concentration of the molecules. Although NO$_2$ intensity is greater than NO intensity in the IR spectrum, only parent signal of the NO can be seen in the MS signal. In other words, the main nitrogen product of the combustion reaction is the nitric oxide after 700 ^{o}C, the concentration of nitrogen dioxide is very small compared to nitric oxide. As a result, incomplete combustion occurs over Al$_2$O$_3$ support and it can be interpreted for the conversion of the bound nitrogen; the reaction mechanism follows NO, N$_2$ formation mechanism via NH$_3$.
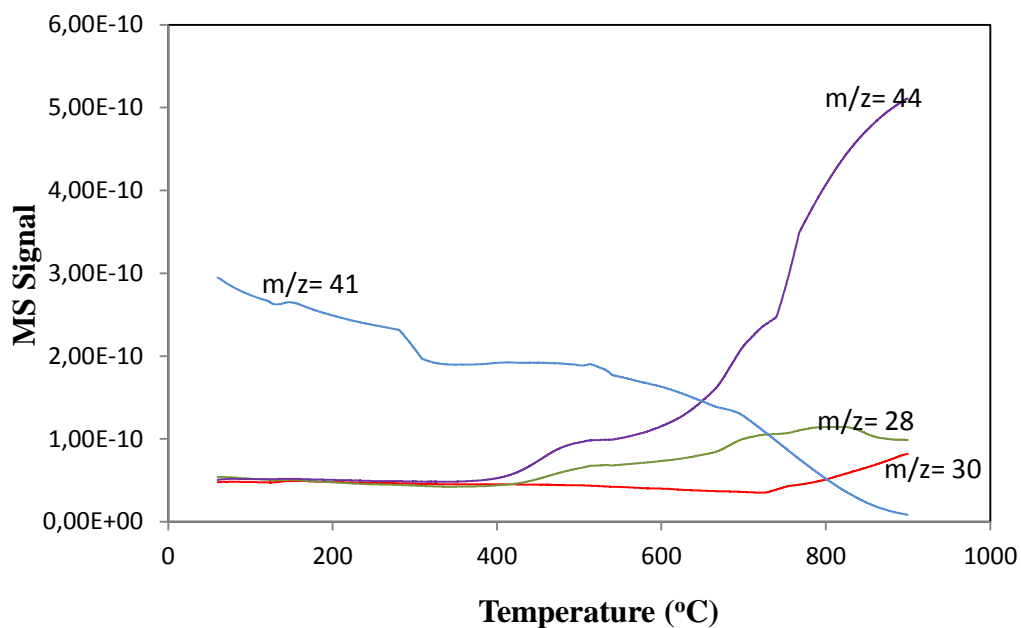
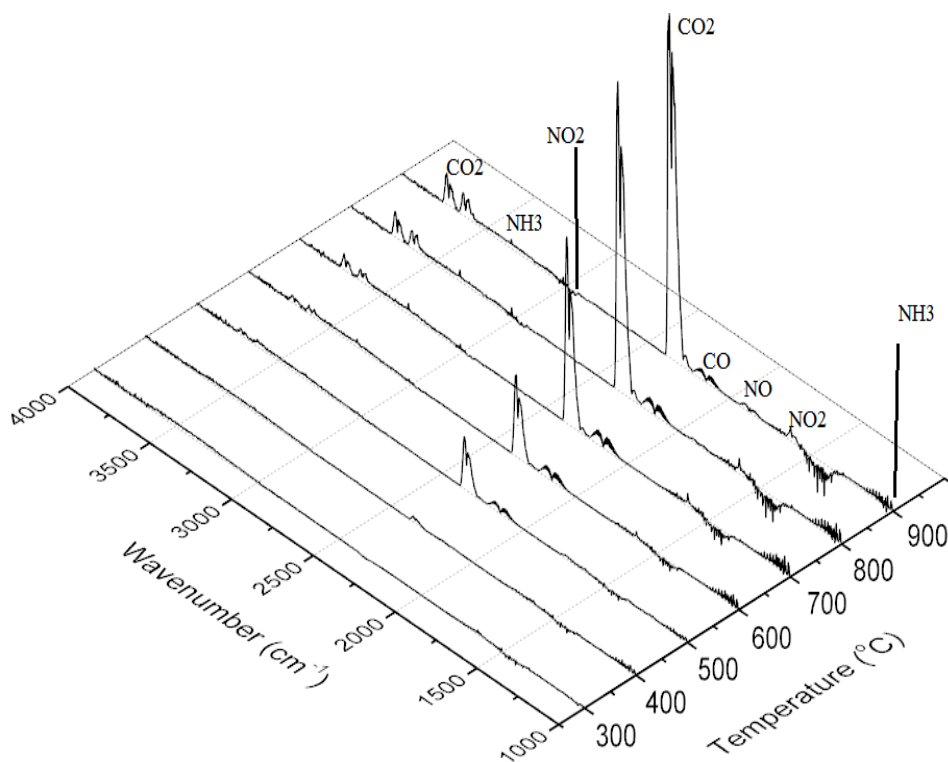**Figure 4. 9:** MS trend of of TPO of acetonitrile over Al_2O_3 support

Figure 4. 10: IR spectra of TPO of acetonitrile over Al_2O_3 support

MS profiles obtained during the TPO experiments over 10 % wt. Cu / Al_2O_3 catalyst is shown in figure 4.11. The reaction starts at 220 ^{o}C which is easily

understood from the increasing m/z=44 signal in the figure 4.11. The rapid increase of m/z=44 signal indicates that the reaction is catalyzed by the presence of Cu. In the FTIR spectra, figure 4.12, ammonia formation can be easily seen after 400 ^{o}C up to 900 ^{o}C but ammonia intensity decreases after 500 ^{o}C. Therefore, it can be stated that acetonitrile oxidation mechanism follows the oxidation step via ammonia formation which is shown in the figure 4.8. The nitrous oxide (N_2O) formation occurs up to 600 ^{o}C, which can be easily seen in the IR range 2150-2300 cm^{-1}. After 600 ^{o}C, NO_2 and NO formation can be seen in the range of 1550-1650 cm^{-1} and 1800-1950 cm^{-1} in the FTIR spectra, respectively. The m/z=28 signal has peak point around 500 ^{o}C then it begins to decrease but it does not come to the baseline up to 900 ^{o}C. The reason of the decrease in the m/z=28 signal, representing nitrogen molecule, after 500 ^{o}C is the shifting of the reaction mechanism to nitric oxide formation mechanism. Despite of the greater intensity of NO2 in the IR spectra, NO is the main product since there is not any change in the m/z=46 signal representing NO2 and the significant increase occurs in the m/z=30 signal representing NO. Therefore, it can be said that, the reaction mainly follows nitrous oxide and nitrogen molecule formation mechanism up to 600 ^{o}C and it mainly follows nitric oxide mechanism after 600 ^{o}C. However, nitrogen molecule still forms as a product since the m/z=28 signal does not come to the baseline up to 900 ^{o}C.
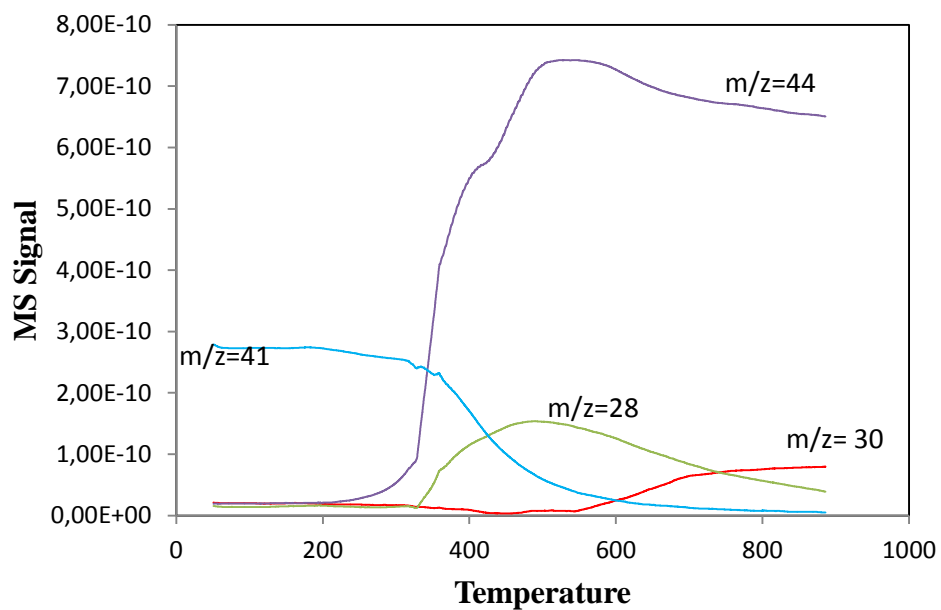
Figure 4. 11: MS trend of TPO of acetonitrile over 10 % wt. Cu / Al$_2$O$_3$ catalyst
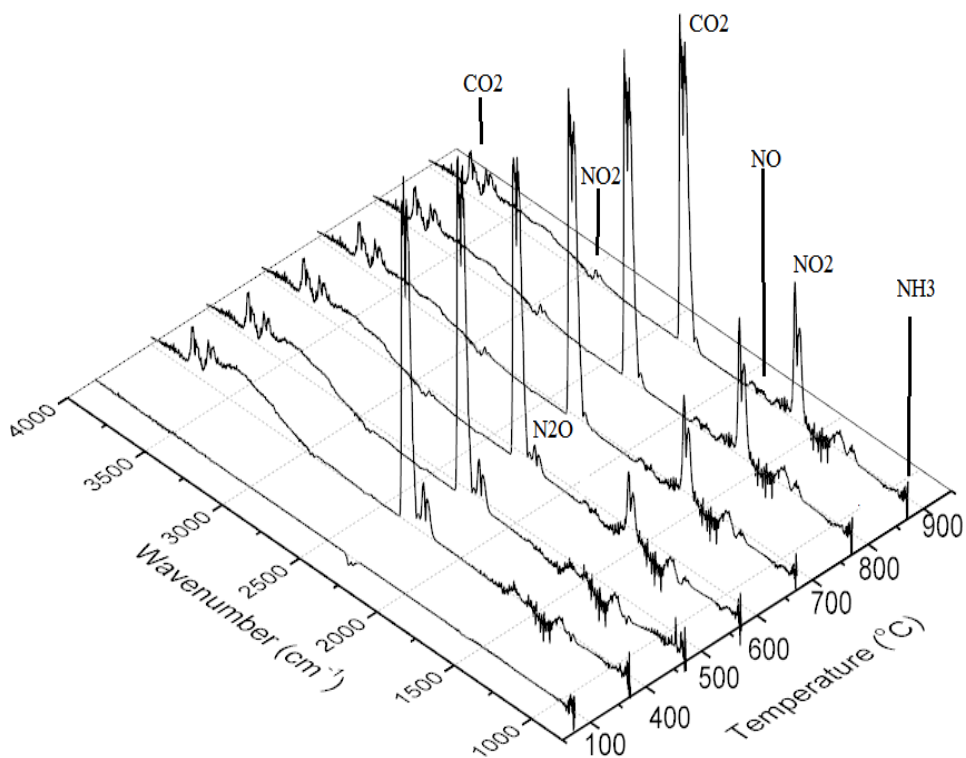

Figure 4. 12: IR Spectra of TPO of acetonitrile over 10 % wt. Cu / Al$_2$O$_3$ catalyst

In the figure 4.13 MS trend of TPO of acetonitrile over 3 % wt. Cu- 7 % wt. Ce / Al_2O_3 catalyst is shown. The increase in the m/z=44 and m/z=28 signals shows the reaction starting point as 300 ^{o}C. The m/z=28 signal increases from 320 ^{o}C up to 600 ^{o}C then it starts to decrease but it does not come to the baseline up to 900 ^{o}C. While the m/z=28 signal starts to decrease after 600 ^{o}C, the m/z=30 signal starts to increase; that is bound nitrogen oxidation mechanism follows the nitric oxide formation mechanism. The decrease in the m/z=28 signal cannot be a result of the carbon monoxide oxidation; since there is not any carbon monoxide intensity in the seen in the IR spectra (figure 4.14) at this temperature. There is an increase in the ammonia formation mechanism up to 600 ^{o}C, which can be seen in the IR spectra range 800-1200 cm^{-1}. Ammonia intensity decreases after 600 ^{o}C and the intensities of the nitric oxide and nitrogen dioxide starts to increase elevated temperatures, but the dominant nitrogen product is the NO due to increasing m/z=30 signal and no change in the m/z=46 in the MS. Therefore, acetonitrile combustion mechanism over 3 % wt. Cu- 7 % wt. Ce / Al_2O_3 catalyst progresses in the the N_2, NO formation mechanism by following ammonia formation path.

As a result of TPO experiments of acetonitrile over 3 % wt. Cu- 7 % wt. Ce / Al_2O_3 catalyst, it can be said that, the combustion reaction mainly follows nitrogen molecule formation mechanism up to 600 ^{o}C, it mainly follows nitric oxide and nitrous oxide formation mechanism after 600 ^{o}C. While the 10 % wt. Cu / Al_2O_3 catalyst follows mainly NO formation mechanism, 3 % wt. Cu- 7 % wt. Ce / Al_2O_3 catalyst follows both N_2O and NO formation mechanism due to bimetallic character of the catalyst; that is, nitrous oxide mechanism on this catalyst is result of ceria addition to alumina supported copper containing catalyst.
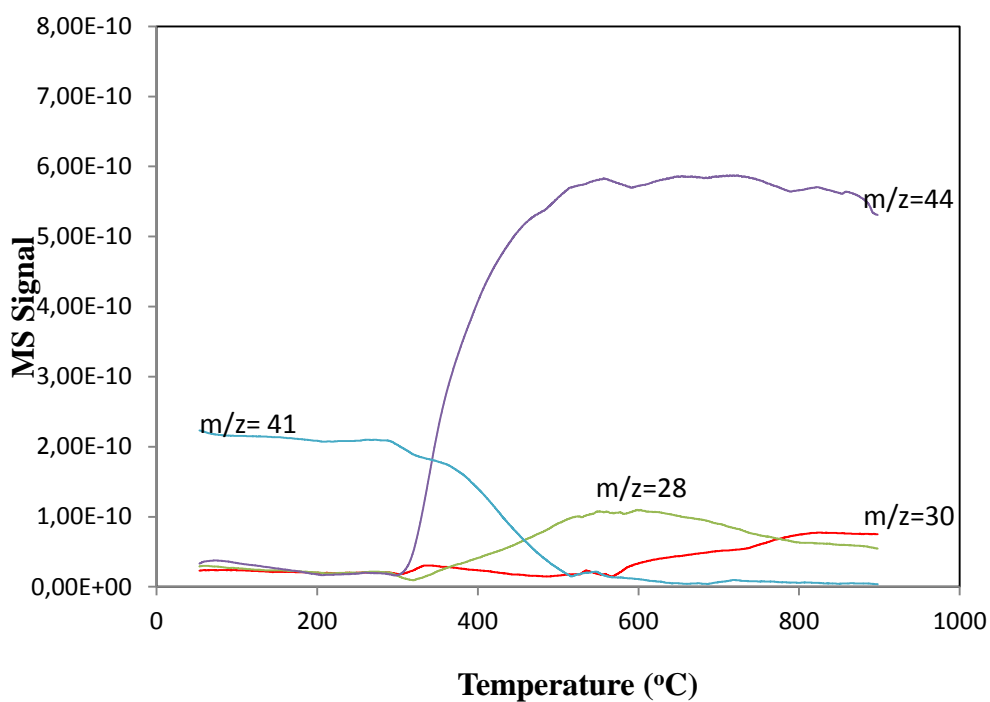
Figure 4. 13: MS trend of TPO of acetonitrile over 3 % wt. Cu- 7 % wt. Ce / Al_2O_3 catalyst

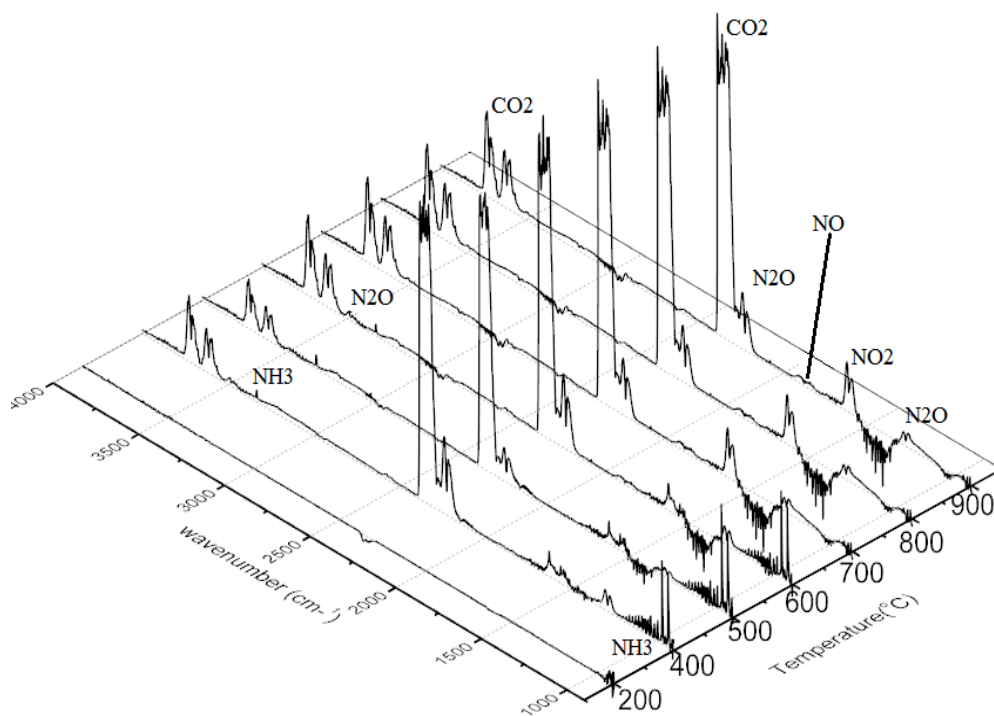**Figure 4. 14:** IR spectra of TPO of acetonitrile over 3 % wt. Cu- 7 % wt. Ce / Al_2O_3 catalyst

MS trend of TPO of acetonitrile over 5 % wt. Fe / Al_2O_3 catalyst is shown in the figure 4.15. The m/z=44 and m/z=28 signals starts to increase around 280 ^{o}C which indicates the reaction starting temperature. The m/z=28 signal has peak around 500, then it starts to decrease which shows the oxidation of carbon monoxide to carbon dioxide and formation of nitrogen oxides instead of nitrogen molecule as it can be seen in figure 4.16. Ammonia formation up to 600 ^{o}C can be easily seen in the figure 4.16 and it starts to decrease after 600 ^{o}C. The oxidation mechanism of the bound nitrogen in the acetonitrile follows the ammonia formation for further oxidation mechanism over 5 % wt. Fe / Al_2O_3 catalyst. The m/z=28 signal comes to baseline value around 720 ^{o}C. Also, it can be seen that, the m/z=30 signal value and nitrogen dioxide and nitric oxide peak in the IR spectra intensity is at steady state in figure 4.15 and 4.16 after 700 ^{o}C. There is no change in the m/z=46 signal in the MS so the main nitrogen product after these temperature is the nitric oxide. Therefore, it can be stated that, complete combustion can be achieved after the temperature 700 ^{o}C as oxidation carbon monoxide to carbon dioxide and bound nitrogen to nitric oxide. As a result of TPO experiments of acetonitrile over 5 % wt. Fe / Al_2O_3 catalyst, it can be said that, the reaction mainly follows nitrogen molecule formation mechanism up to 600 ^{o}C, it mainly follows nitric oxide formation mechanism after 600 ^{o}C by following ammonia formation path and complete oxidation of bound nitrogen to nitric oxide occurs after 700 ^{o}C.
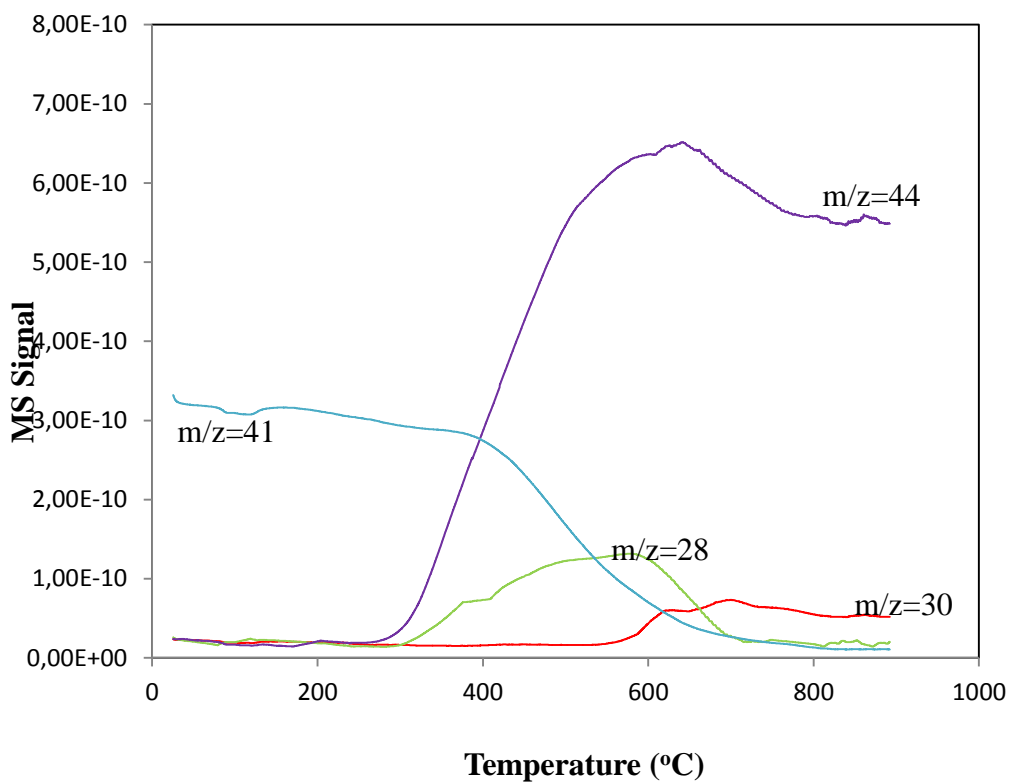
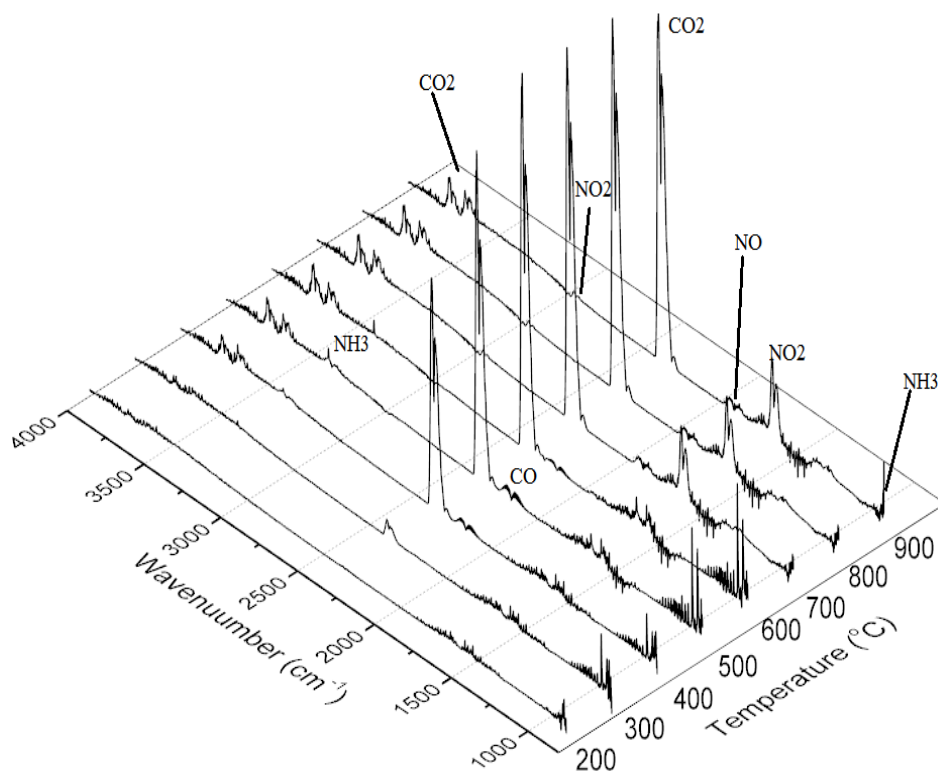**Figure 4. 15:** MS trend of TPO of acetonitrile over 5 % wt. Fe / Al$_2$O$_3$ catalyst

Figure 4.16: IR spectra of TPO of acetonitrile over 5 % wt. Fe / Al$_2$O$_3$ catalyst

According to MS trend of TPO experiments over 1 % wt. Pt / Al_2O_3 catalyst in figure 4.17 , it is understood that the reaction starts around 250 ^{o}C which can be understood from the increase in the signals m/z = 44, m/z = 28 clearly. The m/z=30 signal, which represents major mass spectrum peak of nitric oxide (NO) and fragment of nitrous oxide (N_2O), starts to increase at 300 ^{o}C has the peak point around 420 ^{o}C and then has a slight drop in the trend. Since it is difficult to explain the reason of the increase in m/z=30 signal, which represents major peak of nitric oxide and fragment of nitrous oxide (N_2O), by only investigating MS result. Therefore, the reason of change in this signal is easily explained by the help of IR spectra results which is shown in figure 4.18. N_2O peaks, has two intense peaks at 1285, and 2224 cm^{-1}, shows dramatically decrease of N_2O peak intensities after 400 ^{o}C and it completely dissappers at 800 ^{o}C. While N_2O peak intensities are decreasing, NO and NO_2 peak intensities show an increase prominently. Therefore, the reason of decrease in this signal m/z=30 on the MS results after 400 ^{o}C can be explained as the change in the reaction pathway from N_2O to NO formation mechanism. The signal m/z=28, which represents molecular nitrogen (N_2) and carbon monoxide (CO), starts to increase around 270 ^{o}C, peaks about 400 ^{o}C and is the same with baseline signal between temperatures 700 ^{o}C and 800 ^{o}C. According to IR spectrum in figure 4.18, there is no carbon monoxide, so the signal m/z=28 in the MS represents the nitrogen molecule. In the IR range 1650- 1750 and 1250 – 13000cm^{-1} there are peaks of incomplete combustion products –$CONH_2$ and –NCO. That means, even they are in trace amount, there are still some incomplete combustion products over 1 % wt Pt/Al_2O_3 catalyst at the high temperatures up to 900 ^{o}C. When the reaction temperature exceeds 800 ^{o}C, the reaction pathway again changes to nitrogen molecule formation mechanism instead of nitric oxide mechanism. This means that the temperatures between 700 ^{o}C and 800 ^{o}C can be defined as optimum reaction temperature for the selective oxidation of bound nitrogen of acetonitrile to NO; otherwise, undesirable products for this study, such as N_2O, N_2, are formed.
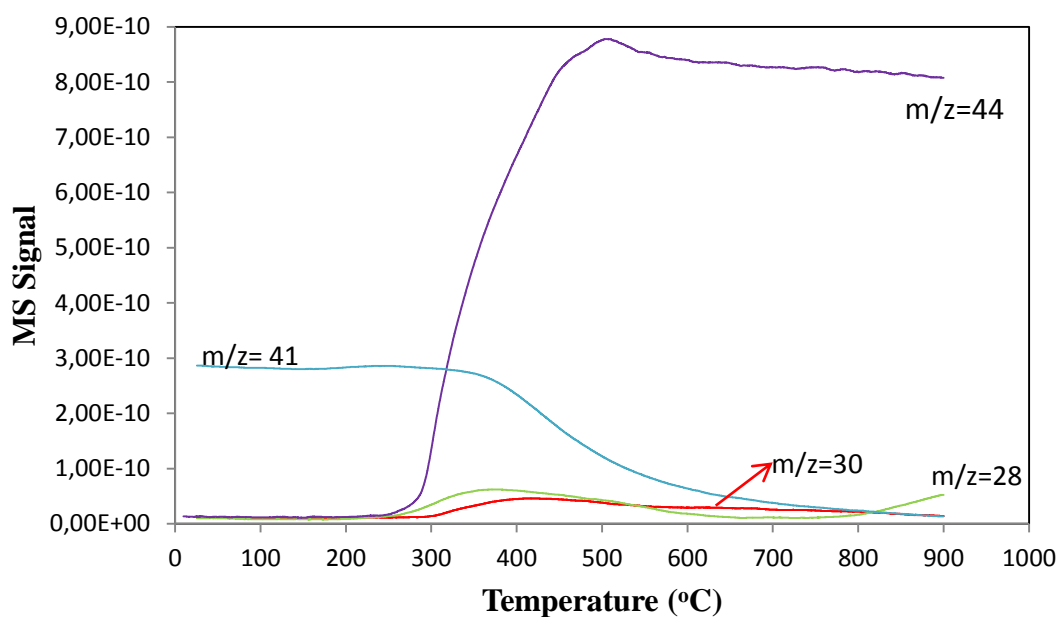
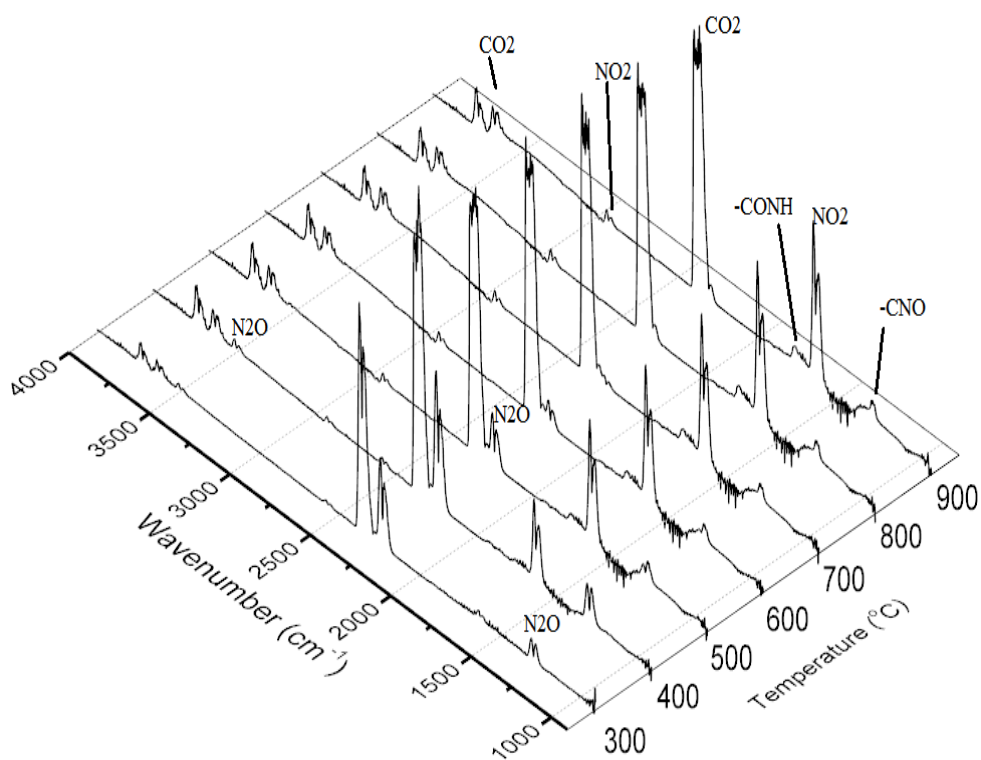**Figure 4. 17:** MS trend of TPO of acetonitrile over 1 % wt. Pt / Al_2O_3 catalyst

Figure 4. 18: IR spectra of TPO of acetonitrile over 1 % wt. Pt / Al_2O_3 catalyst

As a summary the MS and FTIR results of the TPO experiments over Al_2O_3 support and 1 % Pt / Al_2O_3, 10 % Cu / Al_2O_3, 3 % Cu -7 % Ce / Al_2O_3, 5 % Fe /

Al$_2$O$_3$ are shown in the figures 4.9-4.18. There are not any water vapor interference (1700-2000 cm^{-1} and 3400-3800 cm^{-1}) in the FTIR spectrum due to usage of gas conditioning unit at the downstream of the reactor which provides cooling and separation of water in the gas stream. Therefore, nitic oxide and carbon dioxide peaks in this range can be clearly seen in these figures. The catalytic combustion reaction mainly progresses in the direction of N$_2$ formation mechanism over Al$_2$O$_3$ support and 5 % Fe / Al$_2$O$_3$ catalyst up to 600 ^{o}C by following ammonia formation mechanism. The reaction mechanism promotes the N$_2$O and N$_2$ formation by following ammonia formation mechanism up to 600 ^{o}C. For the 1 % Pt / Al$_2$O$_3$ catalyst, the reaction mechanism can be explained as both nitrogen molecule and nitrous oxide formation mechanism up to 600 ^{o}C by following the formation of HCN, CN and NCO intermediates. After 600 ^{o}C, the reactions continues according to nitric oxide formation mechanism over the 1 % Pt / Al$_2$O$_3$ and 5 % Fe / Al$_2$O$_3$ catalysts even by almost achieving complete oxidation at temperatures exceeding 700 ^{o}C. When reaction follows mainly nitrogen molecule mechanisms over the 10 % Cu / Al$_2$O$_3$ catalyst, both nitrogen molecule and nitrous oxide formation can be seen over the 3 % Cu -7 % Ce / Al$_2$O$_3$ catalyst after 600 ^{o}C. As a result, bound nitrogen of the acetonitrile is successfully oxidized to NO at the temperatures between 700-800 ^{o}C over 1 % Pt / Al$_2$O$_3$ and 5 % Fe / Al$_2$O$_3$ catalyst; N$_2$ and N$_2$O are the main nitrogen containing reaction products after 600 ^{o}C over 10 % Cu / Al$_2$O$_3$ and 3 % Cu -7 % Ce / Al$_2$O$_3$ catalysts.

CHAPTER 5

SUMMARY AND CONCLUSIONS

In this study, catalytic activities of four different catalyst samples, 10 % wt Cu/ Al_2O_3, 3% wt Cu- 7 % wt Ce / Al_2O_3, 5 % wt Fe/ Al_2O_3 and 1 % wt Pt/ Al_2O_3, on the complete oxidation of the selected model nitrogen containing compounds were examined. Catalytic activities were investigated by using two different experiment setups. The first experiment setup is HTCO tests to observe the percentage conversion of bound nitrogen in selected model compounds to nitric oxide (NO). The second experiment setup, temperature programmed oxidation (TPO), is to observe reaction mechanism of nitrogen in selected model compound at different temperatures over the catalyst samples and alumina support.

HTCO experiments showed the importance of water as oxidizing agent as oxygen for the oxidation of organic nitrogen to nitric oxide (NO). According to percentage conversion results of the HTCO experiments, 5 % wt Fe/ Al_2O_3 catalyst showed the best catalytic activity for conversion of bound nitrogen in tested model compounds to NO. 1 % wt Pt/ Al_2O_3 catalyst also performed good catalytic activity oxidation of bound nitrogen to nitric oxide except nitrogen of pyridine. 10 % wt Cu/ Al_2O_3 catalyst showed poor conversions of bound nitrogen to NO for compounds, including EDTA, glutamic acid and ammonium sulfate. 3% wt Cu- 7 % wt Ce / Al_2O_3 catalyst also performed poor catalytic activity for the oxidation of bound nitrogen to NO in EDTA, pyridine, ammonium nitrate and glutamic acid. The low percentage conversions were attributed to different reaction mechanism of the bound nitrogen over these catalysts at 700 ^{o}C.

TPO studies showed that complete conversion of bound nitrogen to NO takes place after 700 ^{o}C for the 5 % wt Fe/ Al_2O_3 and 1 % wt Pt/ Al_2O_3 catalysts. According to TPO results of 10 % wt Cu/ Al_2O_3 catalysts N_2 is the dominant reaction product at temperatures up to 900 ^{o}C. TPO results of 3% wt Cu- 7 % wt Ce / Al_2O_3 showed that N_2O and N_2 are the main reaction products at temperatures up to 900 ^{o}C.

As a result, this study shows that 5 % wt Fe/Al_2O_3 catalyst showed the best catalytic activity for conversion of bound nitrogen in the selected model compounds to NO by using HTCO technique. 1 % wt Pt/ Al_2O_3 catalyst, which is generally used in the commercial nitrogen analyzers based on HTCO technique, also performed good catalytic activity oxidation of bound nitrogen to nitric oxide, except pyridine. Therefore, it can be stated for the future works that, alumina supported iron catalysts will be one of the first alternatives in the nitrogen determination by using HTCO technique.

REFERENCES

 [1]: J., Walworth. (2013). Nitrogen in Soil and the Environment. College of Agriculture and Life Science. Retrieved February 20, 2017, from https://extension.arizona.edu/sites/extension.arizona.edu/files/pubs/az1591.pdf.

[2]: "Assessing Nitrogen to Help Reduce Its Environmental Impacts." IES – Institute for Environment and Sustainability – Nitrogen. N.p., n.d. Web. 19 Feb. 2017.

[3]: Galloway, J. N., Townsend, A. R., Erisman, J. W., Bekunda, M., Cai, Z., Freney, J. R., Sutton, M. A., Martinelli, L.A., Seitzinger, S.P. (2008). Transformation of the Nitrogen Cycle: Recent Trends, Questions, and Potential Solutions. Science, 320(5878), 889-892. Doi:10.1126/science.1136674

[4]: Nitrogen Cycle – MicrobeWiki. (n.d.). Retrieved February 20, 2017, from https://microbewiki.kenyon.edu/index.php/Nitrogen_Cycle

[5]: P., Avramidis, A., Nikolaou, & V., Bekiari. (n.d.). Total Organic Carbon and Total Nitrogen in Sediments and Soils: A Comparison of the Wet Oxidation – Titration Method with the Combustion-infrared Method ☆. Retrieved January 04, 2017, from http://www.sciencedirect.com/science/article/pii/S2210784315001114

[6]: Applequist, B. (2012, April 30). A brief introduction to Kjeldahl nitrogen determination. Retrieved January 4, 2017, from http://www.labconco.com/news/a-brief-introduction-to-kjeldahl-nitrogen-determ

[7]: Matejovic, I. (2008). Determination of carbon and nitrogen in samples of various soils by the dry combustion. Communications in Soil Science and Plant Analysis, 28(17-18), 1499–1511. Doi:10.1080/00103629709369892

[8]: Merriam, J., McDowell, W. H., Currie, W. S., & jmerriam, W. H. (1995). A high-temperature catalytic oxidation technique for determining total dissolved nitrogen. Soil Science Society of America Journal, 60(4), 1050–1055. Doi:10.2136/sssaj1996.03615995006000040013x

[9]: Kucharik, C. J., Brye, K. R., Norman, J. M., Foley, J. A., Gower, S. T., & Bundy, L. G. (2001). Measurements and Modeling of Carbon and Nitrogen Cycling in Agroecosystems of Southern Wisconsin: Potential for SOC

Sequestration during the Next 50 Years. Ecosystems, 4(3), 237-258. Doi:10.1007/s10021\n001\n0007-2

[10]: Vitousek, P. (1982). Nutrient Cycling and Nutrient Use Efficiency. The American Naturalist, 119(4), 553-572. Doi:10.1086/283931

[11]: Michopoulos, P., Baloutsos, G., & Economou, A. (2008). Nitrogen cycling in a mature mountainous beech forest. Silva Fennica, 42(1). Doi:10.14214/sf.260

[12]: Vıtousek, P.M. & Farrington, H. Biogeochemistry (1997) 37: 63. Doi:10.1023/A:1005757218475

[13]: Berrier, Kelsey L., "Analysis of Nitrogen and Phosphorus Nutrients in Lake Sediment" (2015). Senior Honors Projects. Paper 70.

[14]: Saha, U. K., Sonon, L., & Kissel, D. E. (2012). Comparison of Conductimetric and Colorimetric Methods with Distillation−Titration Method of Analyzing Ammonium Nitrogen in Total Kjeldahl Digests. Communications in Soil Science and Plant Analysis, 43(18), 2323-2341. Doi:10.1080/00103624.2012.708081

[15]: "Nitrogen Determination by Kjeldahl Method." Panreac AppliChem. N.p., n.d. Web. 06 Mar. 2017. <https://www.applichem.com/>.

[16]: Sáez-Plaza, P., Navas, M. J., Wybraniec, S., Michałowski, T., & Asuero, A. G. (2013). An Overview of the Kjeldahl Method of Nitrogen Determination. Part II. Sample Preparation, Working Scale, Instrumental Finish, and Quality Control. Critical Reviews in Analytical Chemistry, 43(4), 224-272. Doi:10.1080/10408347.2012.751787

[17]: Horneck,D.A.;Miller,R.O.Determination of Total Nitrogen in Plant Tissue.In Handbook of Reference Methods for Plant Analysis;Karla, Y. P.; Ed.; Soil and Plant Science Council; CRC Press: Boca Raton, FL, 1998

[18]: Merriam, J., McDowell, W. H., Currie, W. S., & jmerriam, W. H. (1995). A high-temperature catalytic oxidation technique for determining total dissolved nitrogen. Soil Science Society of America Journal, 60(4), 1050–1055. Doi:10.2136/sssaj1996.03615995006000040013x

[19]: Alavoine, G., & Nicolardot, B. (2001). High-temperature catalytic oxidation method for measuring total dissolved nitrogen in K2SO4 soil extracts. Analytica Chimica Acta,

[20]: A., Mihaljev, S. M., Jakšić, N. B., Prica, Ž N., Ćupić, & Živkov, M. M., Baloš. (2015). Comparison of the Kjeldahl method, Dumas method and NIR method for total nitrogen determination in meat and meat products . Journal of Agroalimentary Processes and Technologies, 21(4), 365-370. Retrieved November 17, 2015.

[21]: Rhee, K. C. Determination of Total Nitrogen. In Current Protocols in Food Analytical Chemistry; Wiley: New York, 2001.

[22]: Saint-Denis, T., & Goupy, J. (2004). Optimization of a nitrogen analyser based on the Dumas method. Analytica Chimica Acta, 515(1), 191-198. Doi:10.1016/j.aca.2003.10.090

[23]: Yeomans, J. C., & Bremner, J. M. (1991). Carbon and nitrogen analysis of soils by automated combustion techniques. Communications in Soil Science and Plant Analysis, 22(9-10), 843-850. Doi:10.1080/00103629109368458

[24]: Tuesday, August 2, 2011 . (n.d.). Achieving Rapid, Accurate, and Reliable Nitrogen Determination in Soils Using Dynamic Flash Combustion. Retrieved March 06, 2017, from http://www.americanlaboratory.com/914-Application-Notes/19521-Achieving-Rapid-Accurate-and-Reliable-Nitrogen-Determination-in-Soils-Using-Dynamic-Flash-Combustion/

[25]: Nitrogen Analysis The Johan Kjeldahl Method. (n.d.). Retrieved March 06, 2017, from http://www.gerhardt.de/

[26]: Walsh, T. W. (1989). Total dissolved nitrogen in seawater: a new-high-temperature combustion method and a comparison with photo-oxidation. Marine Chemistry, 26(4), 295-311. Doi:10.1016/0304-4203(89)90036-4

[27]: Suzuki, Y., Sugimura, Y., & Itoh, T. (1985). A catalytic oxidation method for the determination of total nitrogen dissolved in seawater. Marine Chemistry, 16(1), 83-97. Doi:10.1016/0304-4203(85)90029-5

[28]: Maita, Y., & Yanada, M. (1990). Vertical distribution of total dissolved nitrogen and dissolved organic nitrogen in seawater. Geochemical Journal, 24(4), 245-254. Doi:10.2343/geochemj.24.245

[29]: Hansell, D. A. (1993). Results and observations from the measurement of DOC and DON in seawater using a high-temperature catalytic oxidation technique. Marine Chemistry, 41(1-3), 195-202. Doi:10.1016/0304-

4203(93)90119-9

[30]: Hub, Science. "The Nitrogen Cycle". Science Learning Hub. N.p., 2017. Web. 28 Mar. 2017.

[31]: "BASIN: General Information On Nitrogen". Bcn.boulder.co.us. N.p., 2017. Web. 28 Mar. 2017.

[32]: Vitousek, PM; Aber, J; Howarth, RW; Likens, GE; Matson, PA; Schindler, DW; Schlesinger, WH; Tilman, GD (1997). "Human alteration of the global nitrogen cycle: Sources and consequences". Issues in Ecology. 1 (3): 1–17. Doi:10.1890/1051-0761(1997)007[0737:HAOTGN]2.0.CO;2.

[33]: Perkinelmer. Organic Elemental Analysis of Soils – Understanding the Carbon-Nitrogen Ratio (n.d.): n. pag. Web.

[34]: Bekiari, Vlasoula, and Pavlos Avramidis. "Data Quality in Water Analysis: Validation of Combustion-infrared and Combustion-chemiluminescence Methods for the Simultaneous Determination of Total Organic Carbon (TOC) and Total Nitrogen (TN)." International Journal of Environmental Analytical Chemistry 94.1 (2013): 65-76. Web.

[35]: D., Wall. (2013). Nitrogen in Waters: Forms and Concerns. Minasote: Minesota Pollution Control Agency. Retrieved June, 2013, from https://www.pca.state.mn.us/sites/default/files/wq-s6-26a2.pdf.

[36]: Total Nitrogen. (2013, April 6). Retrieved from https://www.epa.gov/sites/production/files/2015-09/documents/totalnitrogen.pdf

[37]: CHAPTER 2: METHODS OF FOOD ANALYSIS. N.p., n.d. Web. 20 Apr. 2017. <http://www.fao.org/docrep/006/Y5022E/y5022e03.htm>.

[38]: Krotz, Liliana. Nitrogen/Protein Determination in Food and Animal Feed by Combustion Method (Dumas) Using the FlashSmart Elemental Analyzer (n.d.): n. pag. Https://tools.thermofisher.com. Thermofischer. Web. <https://tools.thermofisher.com/content/sfs/brochures/AN-42262-OEA-Nitrogen-Protein-Food-Animal-Feed-FlashSmart-AN42262-EN.pdf>.

[39:] Audeh, C. A., Removal of nitrogen compounds from lubricating oils. Ind. Eng. Chem. Prod. Res. Dev. 22, 276-279 (1983).

[40]: Granchi, Michael P., and Peter Grey. "Total Nitrogen in Petroleum Products and Inorganic Materials by an Automated Micro-Dumas Nitrogen Analyzer."

Microchemical Journal 35.2 (1987): 244-53. Web.

[41]: Pavlova, Antoaneta I., Dimitar S. Dobrev, and Pavlina G. Ivanova. "Determination of Total Nitrogen Content by Different Approaches in Petroleum Matrices." Fuel 88.1 (2009): 27-30. Web.

[42]: Svoboda, K., Baxter, D., & Martinec, J. (2006). Nitrous oxide emissions from waste incineration. Chemical Papers, 60(1). Doi:10.2478/s11696-006-0016-x

[43]: Svoboda, K., Cermak, J., & Hartman, M. (2000). ChemInform Abstract: Chemistry and Emissions of Nitrogen Oxides (NO, NO2, N2O) in Combustion of Solid Fuels. Part 2. Heterogeneous Reactions N2O. ChemInform, 31(38). Doi:10.1002/chin.200038264

[44]: Nitrogen Oxide (Nox) Pollution. (n.d.). Retrieved July 06, 2017, from http://www.icopal-noxite.co.uk/nox-problem/nox-pollution.aspx

[45]: Grappin, R.; Horwitz, W. Determination of Nitrogen-Content in Milk by the Kjeldahl Method UsingCopper Sulfate: Interlaboratory Study. J. Assoc. Off. Anal. Chem. 1988, 71 (5), 893–898.

[46]: Hambræus, L., Forsum, E., Abrahamsson, L., & Lönnerdal, B. (1976). Automatic total nitrogen analysis in nutritional evaluations using a block digestor. *Analytical Biochemistry,72*(1-2), 78-85. Doi:10.1016/0003-2697(76)90508-x

[47]: Kane, P. (1987). Comparison of HgO andCuSO4/TiO2 as Catalysts in Manual Kjeldahl Digestion for Determination of Crude Protein in Animal Feed: Collaborative Study. *Association of Official Analytical Chemists,* 70 (5) ,907-911. Retrieved from https://www.ncbi.nlm.nih.gov/pubmed/3680131.

[48]: A Guide To Kjeldahl Nitrogen Determination Methods and Apparatus. (n.d.). Retrieved July 07, 2017, from http://www.expotechusa.com/

[49]: Klopper, W. J. (2013, April 09). USE OF TITANIUM DIOXIDE AS A CATALYST IN THE KJELDAHL DETERMINATION OF THE TOTAL NITROGEN CONTENT OF BARLEY, MALT AND BEER. Retrieved July 07, 2017, from http://onlinelibrary.wiley.com/doi/10.1002/j.2050-0416.1975.tb06963.x/pdf

[50]: (n.d.). Retrieved July 07, 2017, from

http://www.brooklyn.cuny.edu/bc/ahp/SDKC/Chem/SD_KjeldahlMethod.html

[51]: Ryba, S. A., & Burgess, R. M. (2002). Effects of sample preparation on the measurement of organic carbon, hydrogen, nitrogen, sulfur, and oxygen concentrations in marine sediments. Chemosphere, 48(1), 139-147. Doi:10.1016/s0045-6535(02)00027-9

[52]: Muñoz-Huerta, R., Guevara-Gonzalez, R., Contreras-Medina, L., Torres-Pacheco, I., Prado-Olivarez, J., & Ocampo-Velazquez, R. (2013). A Review of Methods for Sensing the Nitrogen Status in Plants: Advantages, Disadvantages and Recent Advances. Sensors, 13(8), 10823-10843. Doi:10.3390/s130810823

[53]: Kowalenko, C. G. (2001). Assessment of Leco CNS-2000 analyzer for simultaneously measuring total carbon, nitrogen, and 82ehydra in soil. Communications in Soil Science and Plant Analysis, 32(13-14), 2065-2078. Doi:10.1081/css-120000269

[54]: Rogora, M., Minella, M., Orr[Ugrave], A., & Tartari, G. A. (2006). A comparison between high-temperature catalytic oxidation and persulfate oxidation for the determination of total nitrogen in freshwater. International Journal of Environmental Analytical Chemistry, 86(14), 1065-1078. Doi:10.1080/03067310600739632

[55]: ASTM International, Designation: WK50658. New Test Method for Total Nitrogen in Water by High Temperature Catalytic Combustion using Electrochemical Detection (2015).

[56]: ASTM International, Designation: D5176–08. Standard Test Method for the Total Chemically Bound Nitrogen in Water by Pyrolysis and Chemiluminescence Detection (2008).

[57]: Sharp, J., Beauregard, A., Burdige, D., Cauwet, G., Curless, S., Lauck, R., . . . Styles, R. (2004). A direct instrument comparison for measurement of total dissolved nitrogen in seawater. Marine Chemistry, 84(3-4), 181-193. Doi:10.1016/j.marchem.2003.07.003

[58]: Ammann, A. (2000). Simultaneous determination of TOC and TNb in surface and wastewater by 82ehydrate high temperature catalytic combustion. Water Research, 34(14), 3573-3579. Doi:10.1016/s0043-1354(00)00108-1

[59]: Álvarez-Salgado, X. A., & Miller, A. E. (1998). Simultaneous

determination of dissolved organic carbon and total dissolved nitrogen in seawater by high temperature catalytic oxidation: conditions for precise shipboard measurements. Marine Chemistry, 62(3-4), 325-333. Doi:10.1016/s0304-4203(98)00037-1

[60] : Badr, E. A., Achterberg, E. P., Tappin, A. D., Hill, S. J., & Braungardt, C. B. (2003). Determination of dissolved organic nitrogen in natural waters using high-temperature catalytic oxidation. TrAC Trends in Analytical Chemistry, 22(11), 819-827. Doi:10.1016/s0165-9936(03)01202-0

[61]: Haber, J., Janas, J., Kryściak-Czerwenka, J., Machej, T., Sadowska, H., & Helldén, S. (2002). Total oxidation of nitrogen-containing organic compounds to N2, CO2 and H2O. Applied Catalysis A: General, 229(1-2), 23-34. Doi:10.1016/s0926-860x(02)00013-3

[62]: R. Prasad, L.A. Kennedy, E. Ruckenstein. Catal. Rev.-Sci. Eng., 26, 1 (1984).

[63]: Haynes, B. S. (1977). Production of nitrogen compounds from molecular nitrogen in fuel-rich hydrocarbon-air flames. Fuel, 56(2), 199-203. Doi:10.1016/0016-2361(77)90146-6

[64]: Watanabe, K., Badr, E., Pan, X., & Achterberg, E. P. (2007). Conversion efficiency of the high-temperature combustion technique for dissolved organic carbon and total dissolved nitrogen analysis. International Journal of Environmental Analytical Chemistry, 87(6), 387-399. Doi:10.1080/03067310701237023

[65]: J.E. Bauer, M.L. Occelli, P.M. Williams, P.C. McCaslin. Mar. Chem., 42, 95 (1993).

[66]: Pan, X., Sanders, R., Tappin, A. D., Worsfold, P. J., & Achterberg, E. P. (2005). Simultaneous Determination of Dissolved Organic Carbon and Total Dissolved Nitrogen on a Coupled High-Temperature Combustion Total Organic Carbon-Nitrogen Chemiluminescence Detection (HTC TOC-NCD) System. Journal of Automated Methods and Management in Chemistry, 2005(4), 240-246. Doi:10.1155/jammc.2005.240

[67]: Tuesday, February 17, 2015 Tweet Email Print. (n.d.). Total Nitrogen in Water by High-Temperature Catalytic Combustion and Chemiluminescence

Detection. Retrieved July 16, 2017, from http://www.americanlaboratory.com/913-Technical-Articles/171561-Total-Nitrogen-in-Water-by-High-Temperature-Catalytic-Combustion-and-Chemiluminescence-Detection/

[68]: G. Cauwet. In Methods of Seawater Analysis, 3rd Edn, K. Grasshoff, K. Kremling, M. Ehrhardt (Eds),

pp. 407–420, Wiley-VCH, Weinheim (1999).

[69]: W. A. Daniel and J. T . Wentworth , Paper 486B, presented at March Meeting of The Society of Automotive Engineers, 1962.

[70]: Menon, P., Zwinkels, M., & Järs, S. (1998). Catalytic combustion for pollution abatement and cleaner thermal power generation. Recent Advances In Basic and Applied Aspects of Industrial Catalysis, Proceedings of 13th National Symposium and Silver Jubilee Symposium of Catalysis of India Studies in Surface Science and Catalysis, 97-109. Doi:10.1016/s0167-2991(98)80278-4

[71]: Kjeldahl method. (2017, July 10). Retrieved July 16, 2017, from https://en.wikipedia.org/wiki/Kjeldahl_method

[72]: Wartelle, C., & Bedioui, F. (2004). Novel biocompatible hydrogel-based amperometric sensor for nitric oxide gas detection: towards a non-invasive device. Chemical Communications, (11), 1302. Doi:10.1039/b402735c

[74]: N.N. Sazonova, A.V. Simakov, T.A. Nikoro, G.B. Barannik, V.F. Lyakhova, V.I.Zheivot, Z.R. Ismagilov, H. Veringa, Catalysis Letters 57 (1996) 71–79.

[75]: Águila, G., Gracia, F., & Araya, P. (n.d.). CuO and CeO2 catalysts supported on Al2O3, ZrO2, and

[76]: Miki, T., & Tai, Y. (2011). Catalytic Oxidation of Toluene over Fe2O3/Al2O3 Catalyst. Materials Science Forum MSF, 695, 101-104.

[77]: (n.d.). Retrieved July 21, 2017, from http://www.cambustion.com/products/cld500/cld-principles

[78]: Cava, S. et al. "Structural Characterization Of Phase Transition Of Al2o3 Nanopowders Obtained By Polymeric Precursor Method". Materials Chemistry and Physics 103.2-3 (2007): 394-399. Web.

[79]: Gulshan, F. , & Okada, K. (2013). Preparation of Alumina-Iron Oxide

Compounds by Coprecipitation Method and Its Characterization. American Journal of Materials Science and Engineering, 1(1), 6-11.

[80]: Bauer, J. Chris et al. "Converting Nanocrystalline Metals Into Alloys And Intermetallic Compounds For Applications In Catalysis". J. Mater. Chem. 18.3 (2008): 275-282. Web. 4 June 2017.

[81]: Wonpark, J., Hyeokjeong, J., Yoon, W., Kim, C., Lee, D., Park, Y., & Rhee, Y. (2005). Selective oxidation of CO in hydrogen-rich stream over Cu?Ce catalyst promoted with transition metals. International Journal of Hydrogen Energy, 30(2), 209-220. Doi:10.1016/j.ijhydene.2004.04.016

[82]: Prakash, A., Shivakumara, C., & Hegde, M. (2007). Single step preparation of $CeO_2/CeAlO_3/\gamma-Al_2O_3$ by solution combustion method: Phase evolution, thermal stability and surface modification. Materials Science and Engineering: B, 139(1), 55-61. Doi:10.1016/j.mseb.2007.01.034

[83]: Guo, R., Zhou, Y., Pan, W., Hong, J., Zhen, W., Jin, Q., . . . Guo, S. (2013). Effect of preparation methods on the performance of CeO_2/Al_2O_3 catalysts for selective catalytic reduction of NO with NH_3. Journal of Industrial and Engineering Chemistry, 19(6), 2022-2025. Doi:10.1016/j.jiec.2013.03.010

[84]: Radwan, N., Fagal, G., & El-Shobaky, G. (2001). Effects of CeO_2-doping on surface and catalytic properties of CuO/Al_2O_3 solids. Colloids and Surfaces A: Physicochemical and Engineering Aspects, 178(1-3), 277-286. Doi:10.1016/s0927-7757(00)00709-3

[85]: Zhang, R., Shi, D., Liu, N., Cao, Y., & Chen, B. (2014). Mesoporous SBA-15 promoted by 3d-transition and noble metals for catalytic combustion of acetonitrile. Applied Catalysis B: Environmental, 146, 79-93. Doi:10.1016/j.apcatb.2013.03.028

[86]: Di, L., Xu, W., Zhan, Z., & Zhang, X. (2015). Synthesis of alumina supported Pd–Cu alloy nanoparticles for CO oxidation via a fast and facile method. RSC Adv., 5(88), 71854-71858. Doi:10.1039/c5ra13813b

[87]: Tao, T., Glushenkov, A. M., Chen, Q., Hu, H., Zhou, D., Zhang, H., . . . Chen, Y. (2011). Porous TiO_2 with a controllable bimodal pore size distribution from natural ilmenite. CrystEngComm, 13(5), 1322-1327. Doi:10.1039/c0ce00533a

[88]: Meessen, J. H.; Petersen, H. (2005), "Urea", *Ullmann's Encyclopedia of Industrial Chemistry*, Weinheim: Wiley-VCH, *doi*:*10.1002/14356007.a27_333*

[89]:Here's Why the Carbon-Nitrogen Ratio Matters. (2016, March 19). Retrieved August 17, 2017, from http://www.agriculture.com/crops/cover-crops/heres-why-carbonnitrogen-ratio-matters_568-ar48014

[90]: Gil, S. (2012). Fuel-N Conversion to NO, N2O and N2 During Coal Combustion. Fossil Fuel and the Environment. Doi:10.5772/38176

[91]: Alavoine, G., & Nicolardot, B. (2000). Comparison of various methods for the determination of total N in liquid effluents. Analusis, 28(1), 88-92. Doi:10.1051/analusis:2000102

ORIGINLAB SOFTWARE INTEGRATED AREA CALCULATIONS

A.1 The m/z =30 Signal as a Function of Time and Integrated Area of the Signal Collected in HTCO Experiments of 4 Different Amount of $(NH_4)_2SO_4$ over 1 % wt Pt / Al_2O_3 Catalyst Sample at 700 ^{o}C for Calibration

The m/z=30 signals as a function of time and integration of areas under the m/z=30 signal curve of HTCO experiments of 10, 20, 40 and 60 mg of $(NH_4)_2SO_4$ over 1 % wt Pt / Al_2O_3 catalyst sample for calibration are shown in the figures A-1 to A-10, respectively.
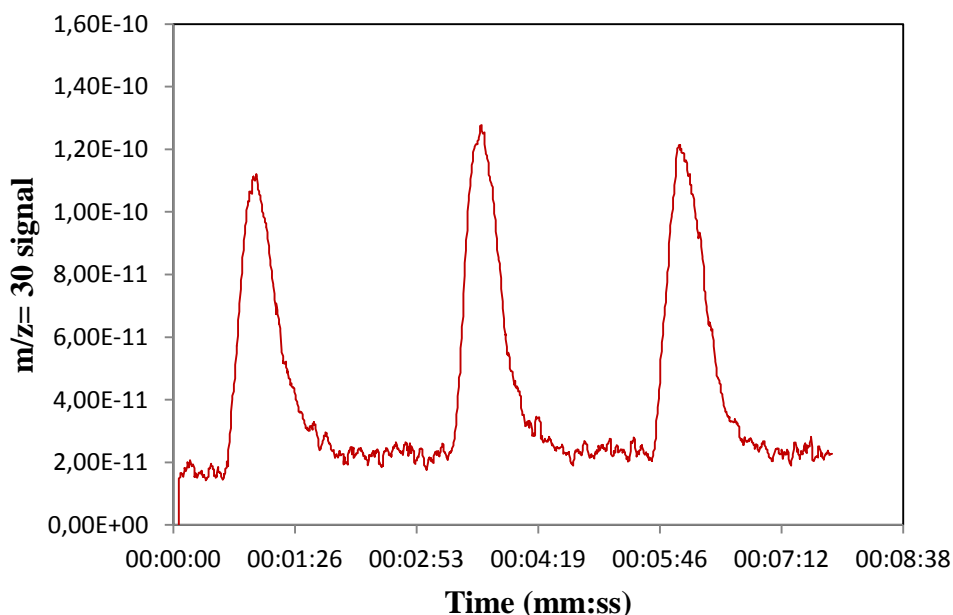
Figure A. 1: The m/z = 30 signal as a function of time of three repetitive HTCO analysis of 10 mg $(NH_4)_2SO_4$ over 1 % wt Pt / Al_2O_3 Catalyst Sample at 700 ^{o}C in the presence of 500 sccm air flow
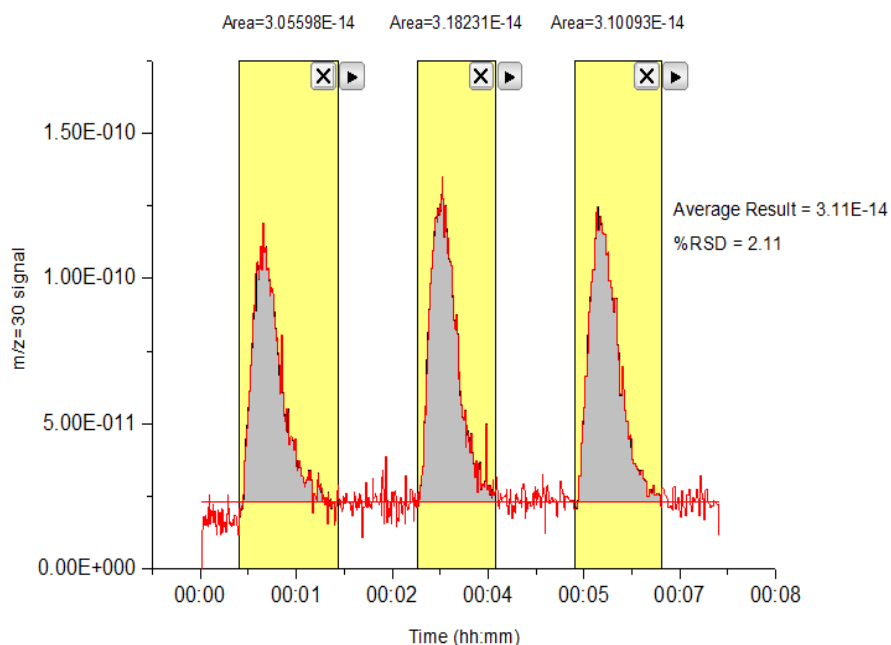
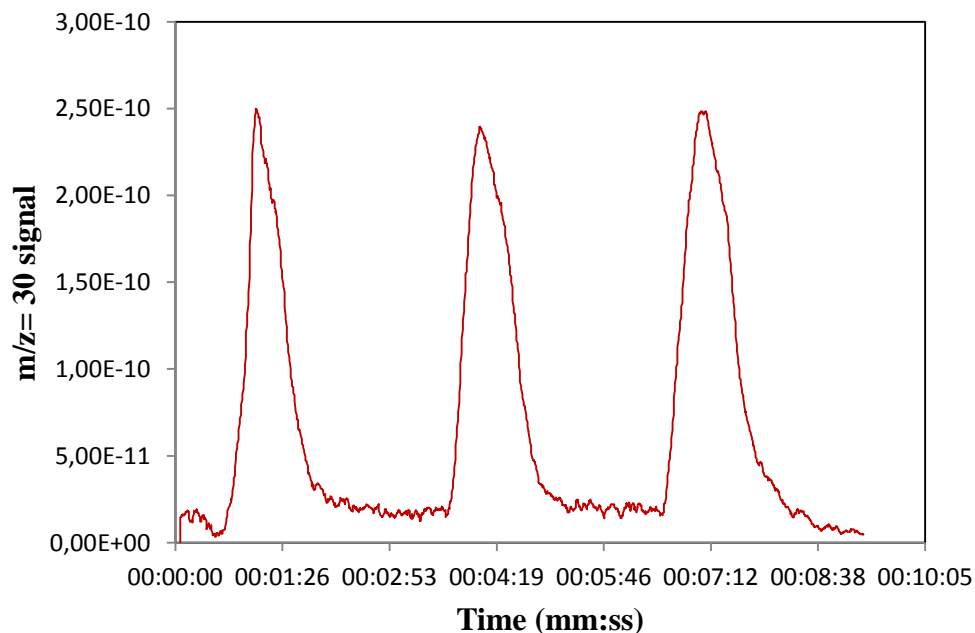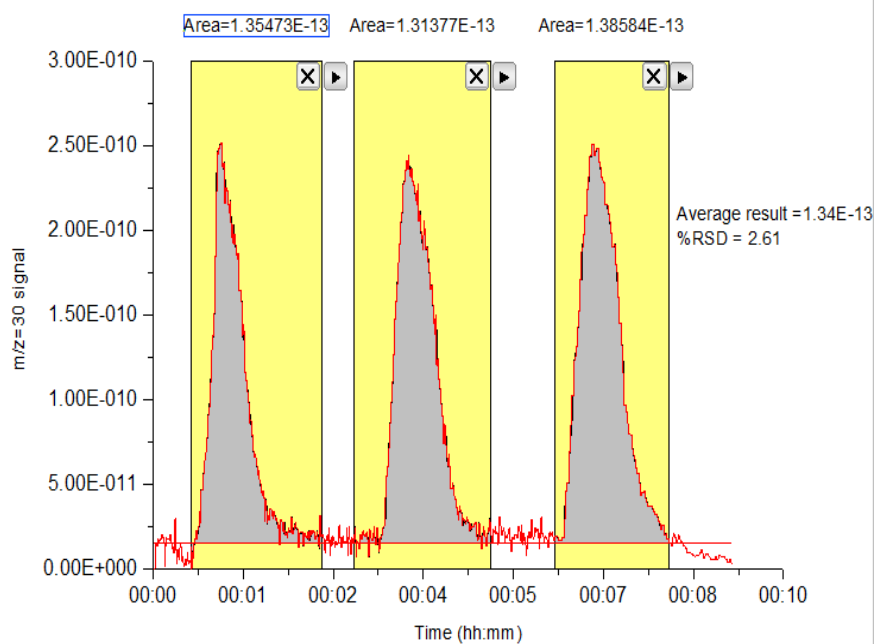**Figure A. 2:** Integrated area of the m/z = 30 signal curve of three repetitive HTCO analysis of 10 mg $(NH_4)_2SO_4$ over 1 % wt Pt / Al_2O_3 Catalyst Sample at 700 ^{o}C in the presence of 500 sccm air flow
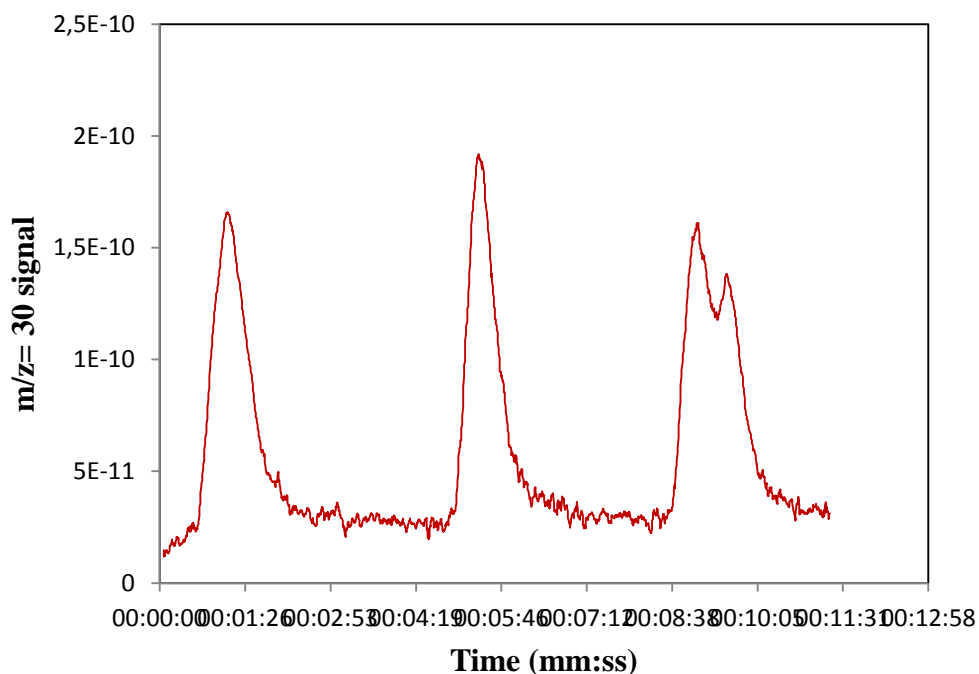
Figure A. 3: The m/z = 30 signal as a function of time of three repetitive HTCO analysis of 20 mg $(NH_4)_2SO_4$ over 1 % wt Pt / Al_2O_3 Catalyst Sample at 700 ^{o}C in the presence of 500 sccm air flow
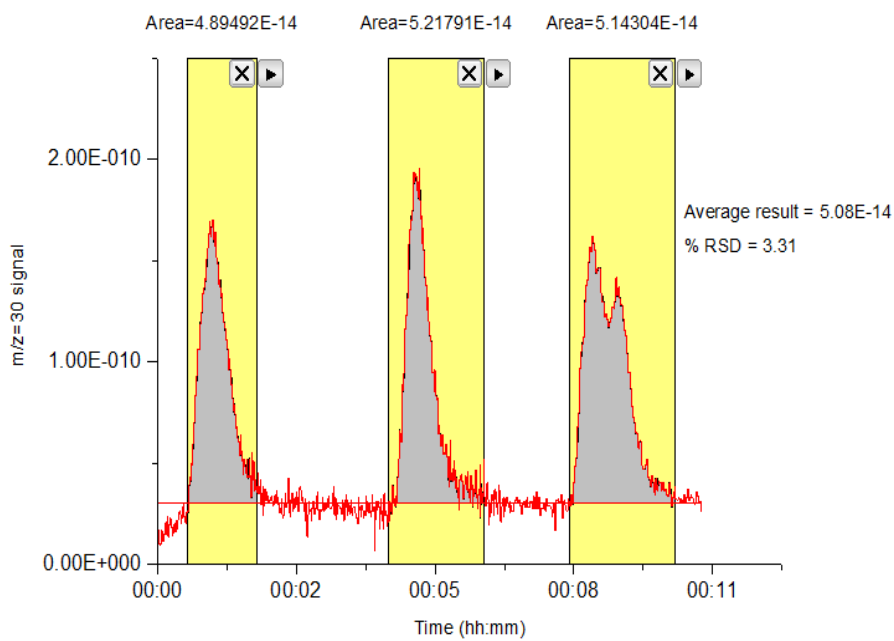
Figure A. 4: Integrated area of the m/z = 30 signal curve of three repetitive HTCO analyses of 20 mg $(NH_4)_2SO_4$ over 1 % wt Pt / Al_2O_3 Catalyst Sample at 700 ^oC in the presence of 500 sccm air flow
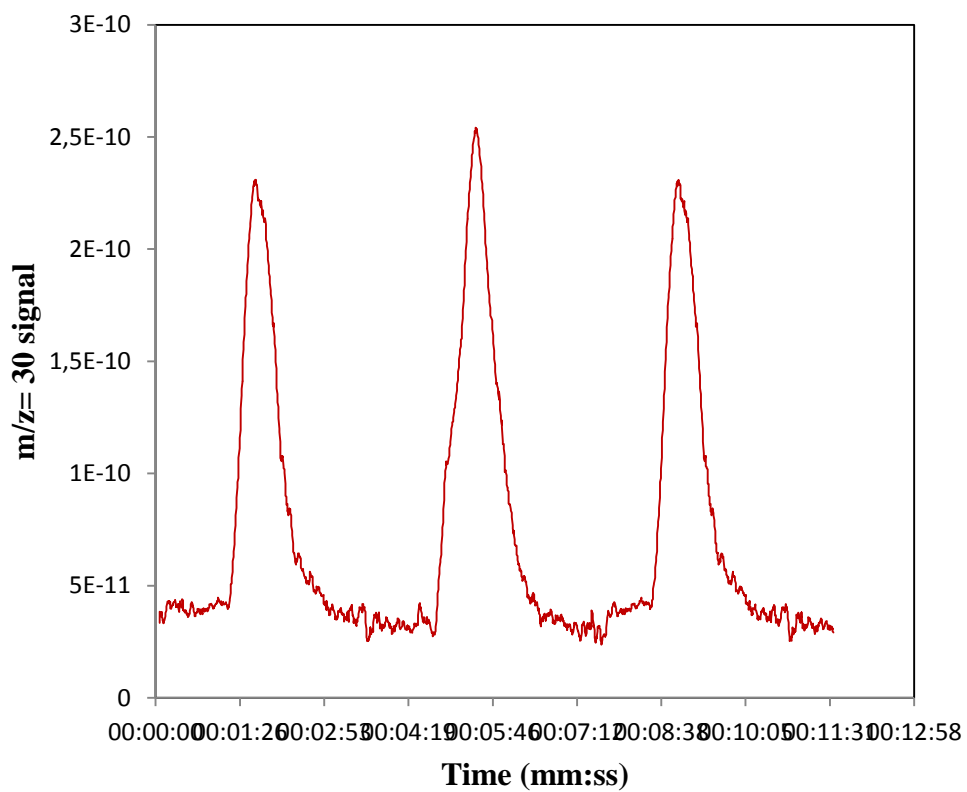
Figure A. 5: The m/z = 30 signal as a function of time of three repetitive HTCO analysis of 40 mg $(NH_4)_2SO_4$ over 1 % wt Pt / Al_2O_3 Catalyst Sample at 700 ^{o}C in the presence of 500 sccm air flow
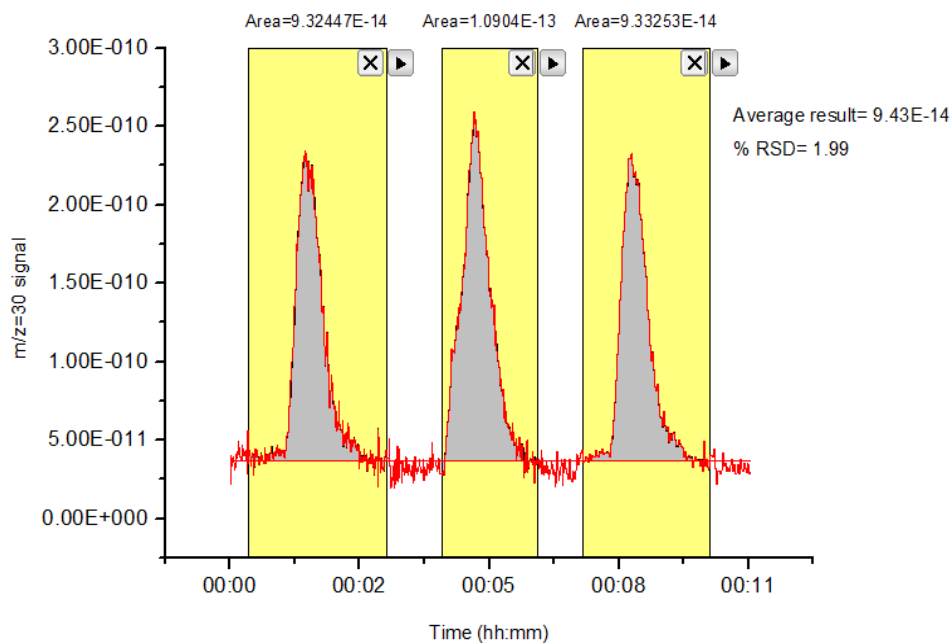
Figure A. 6: Integrated area of the m/z = 30 signal curve of three repetitive HTCO analysis of 40 mg $(NH_4)_2SO_4$ over 1 % wt Pt / Al_2O_3 Catalyst Sample at 700 ^{o}C in the presence of 500 sccm air flow

Figure A. 7: The m/z = 30 signal as a function of time of three repetitive HTCO analysis of 60 mg $(NH_4)_2SO_4$ over 1 % wt Pt / Al_2O_3 Catalyst Sample at 700 ^{o}C in the presence of 500 sccm air flow

91

Figure A. 8: Integrated area of the m/z = 30 signal curve of three repetitive HTCO analysis of 60 mg $(NH_4)_2SO_4$ over 1 % wt Pt / Al_2O_3 Catalyst Sample at 700 ^{o}C in the presence of 500 sccm air flow

A.2 Integrated Area Calculations of the m/z=30 Signal Collected in HTCO Experiments of Model Compounds over 10 % Cu / Al$_2$O$_3$ Catalyst Sample

Areas under the m/z=30 signal curve of HTCO experiments of model compounds over 10 % Cu / Al$_2$O$_3$ catalyst sample were done by using Originlab software. The results are shown on the figures A-11 to A-16.
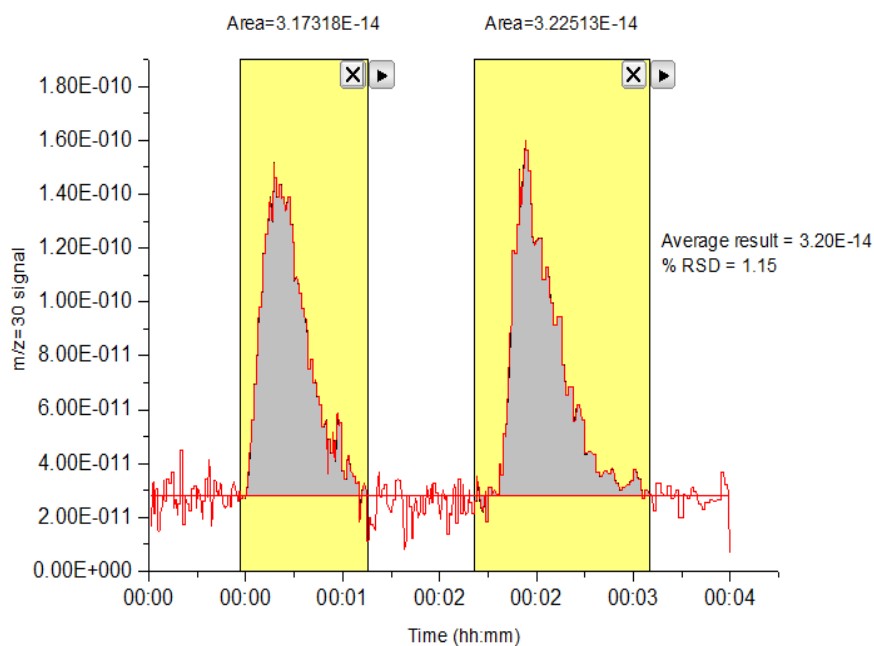
Figure A. 9: Integrated area of the m/z = 30 signal curve of HTCO analysis of 5 mg urea over 10 % Cu / Al$_2$O$_3$ catalyst sample at 700 ^{o}C in the presence of 500 sccm air flow
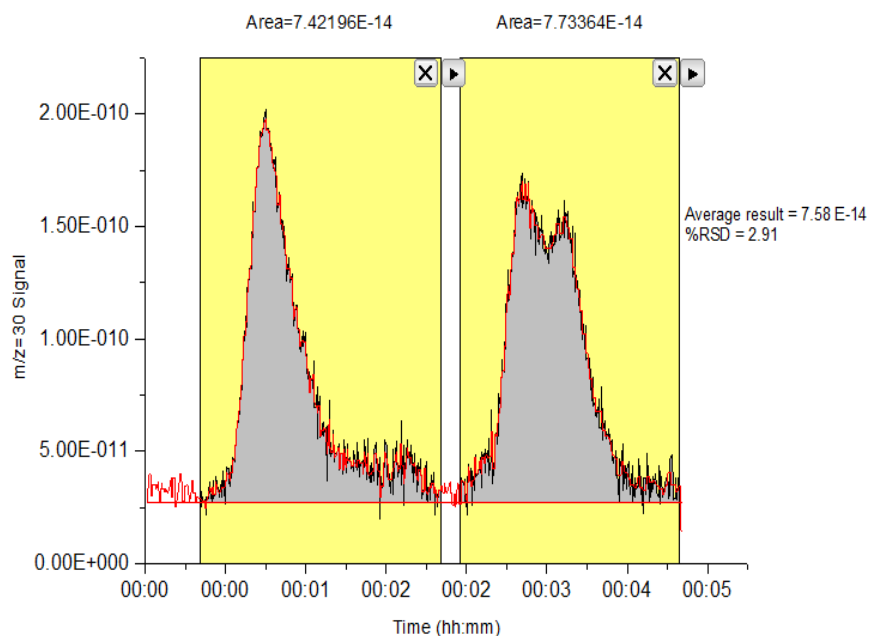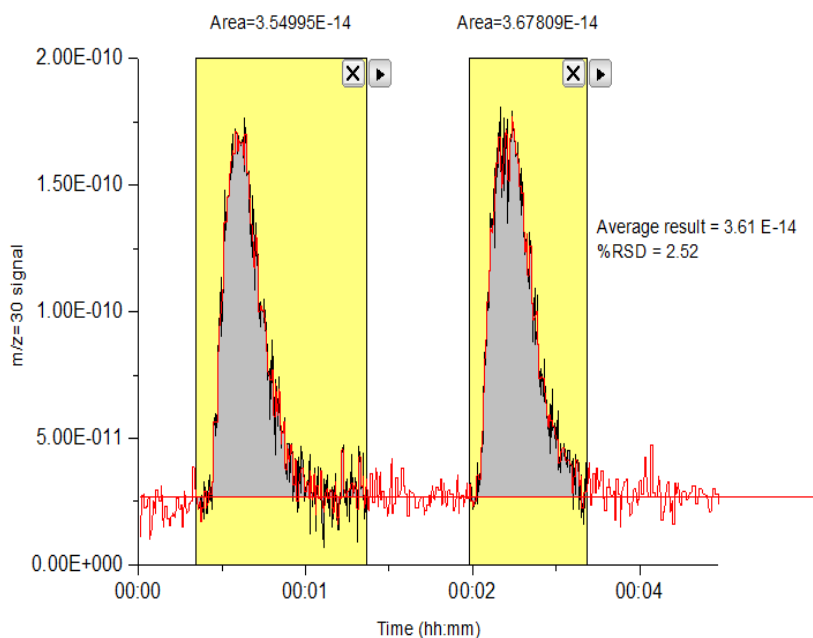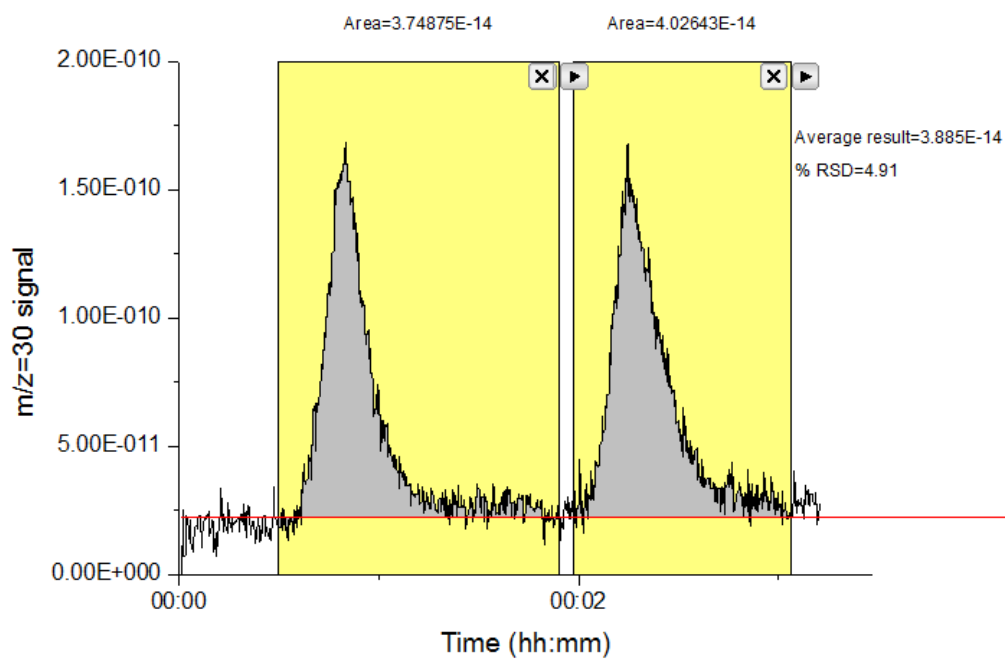
Figure A. 10: Integrated area of the m/z = 30 signal curve of HTCO analysis of 20 mg ammonium nitrate over 10 % Cu / Al_2O_3 catalyst sample at 700 ^{o}C in the presence of 500 sccm air flow
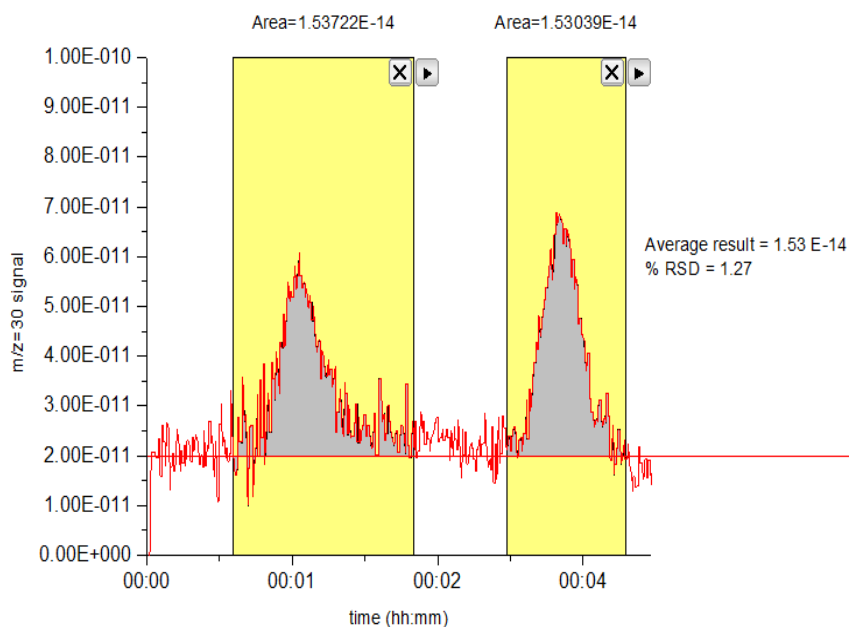
Figure A. 11: Integrated area of the m/z = 30 signal curve of HTCO analysis of 20 mg Edta disodium salt 94ehydrate over 10 % Cu / Al_2O_3 catalyst sample at 700 ^{o}C in the presence of 500 sccm air flow
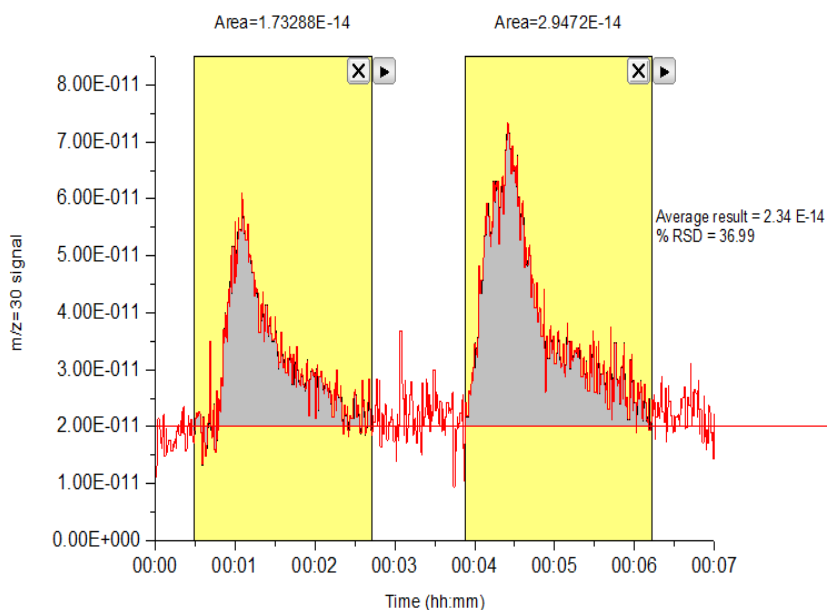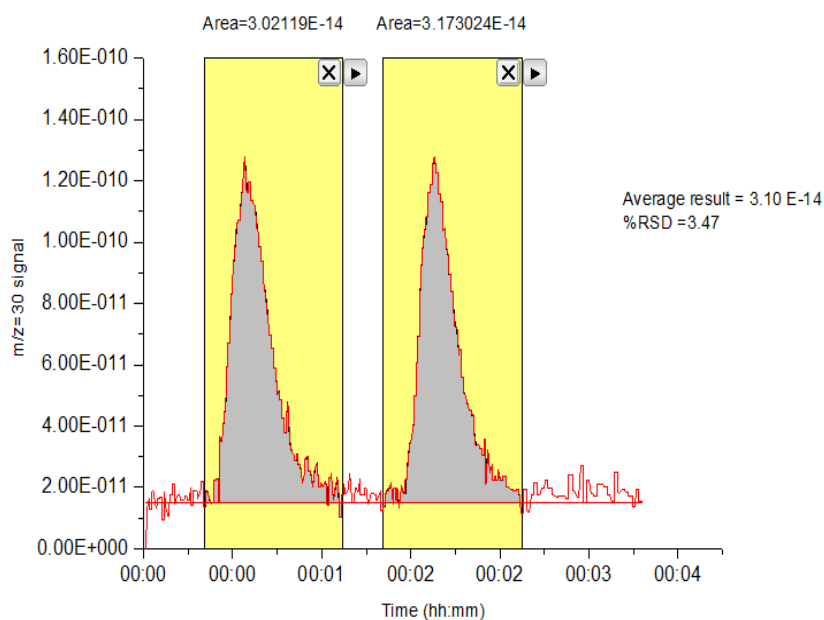
Figure A. 12: Integrated area of the m/z = 30 signal curve of HTCO analysis of 40 mg glutamic acid over 10 % Cu / Al$_2$O$_3$ catalyst sample at 700 $^{\circ}$C in the presence of 500 sccm air flow

Figure A. 13: Integrated area of the m/z = 30 signal curve of HTCO analysis of 600 μl of 2.5 % by volume pyridine solution over 10 % Cu / Al$_2$O$_3$ catalyst sample at 700 $^{\circ}$C in the presence of 500 sccm air flow
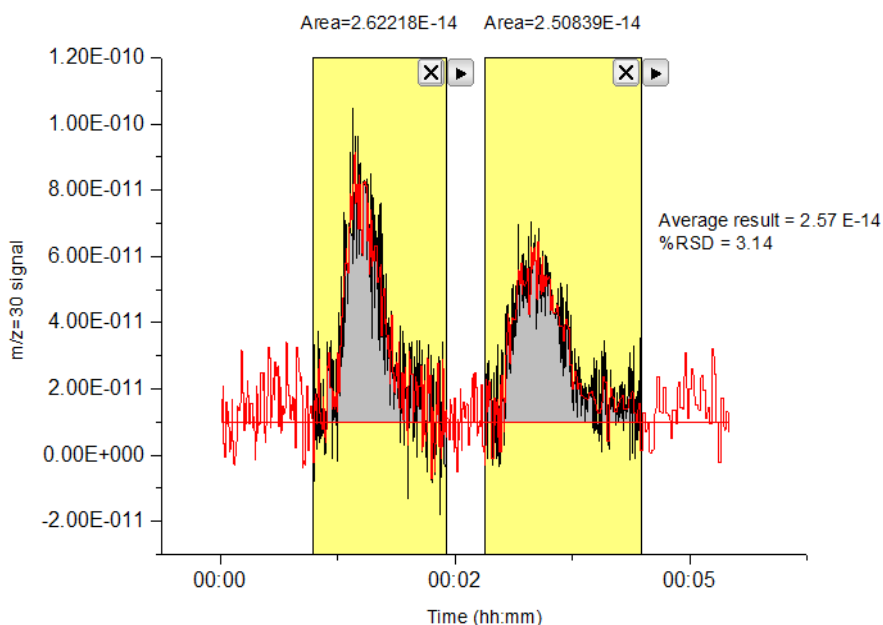
Figure A. 14: Integrated area of the m/z = 30 signal curve of HTCO analysis of 20 mg ammonium sulfate over 10 % Cu / Al$_2$O$_3$ catalyst sample at 700 ^{o}C in the presence of 500 sccm air flow

A.3 Integrated Area Calculations the m/z=30 signal Collected in HTCO Experiments of Model Compounds over 3 % wt Cu- 7 % wt Ce / Al$_2$O$_3$ Catalyst Sample

Areas under the m/z=30 signal curve of HTCO experiments of model compounds over 3 % wt Cu - % 7 wt Ce / Al$_2$O$_3$catalyst sample were done by using Originlab software. The results are shown on the figures A-18 to A-23.

Figure A. 15: Integrated area of the m/z = 30 signal curve of HTCO analysis of 5 mg urea over 3 % Cu-7% Ce / Al$_2$O$_3$ catalyst sample at 700 ^{o}C in the presence of 500 sccm air flow

Figure A. 16: Integrated area of the m/z = 30 signal curve of HTCO analysis of 20 mg ammonium nitrate over 3 % Cu-7% Ce / Al_2O_3 catalyst sample at 700 ^{o}C in the presence of 500 sccm air flow
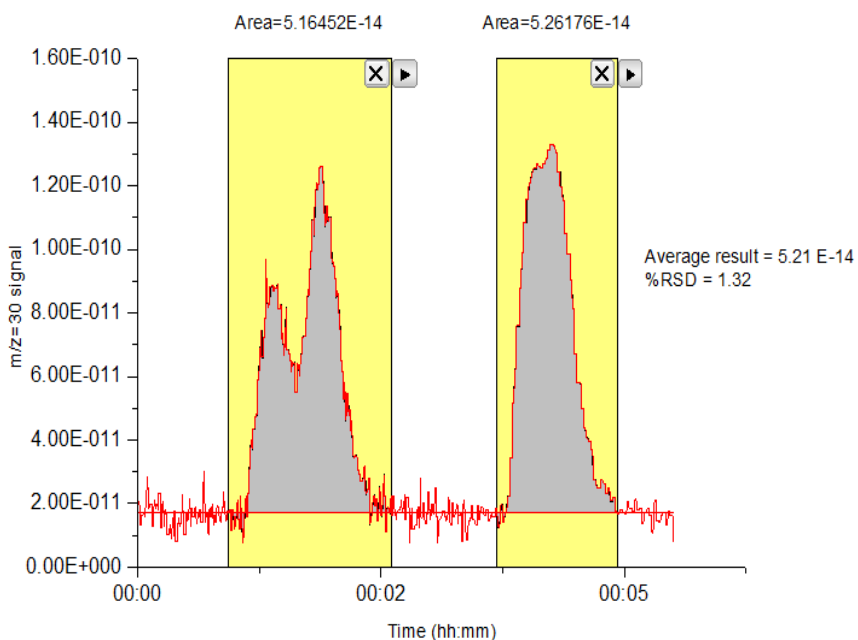

Figure A. 17: Integrated area of the m/z = 30 signal curve of HTCO analysis of 20 mg ammonium sulfate over 3 % Cu-7% Ce / Al_2O_3 catalyst sample at 700 ^{o}C in the presence of 500 sccm air flow
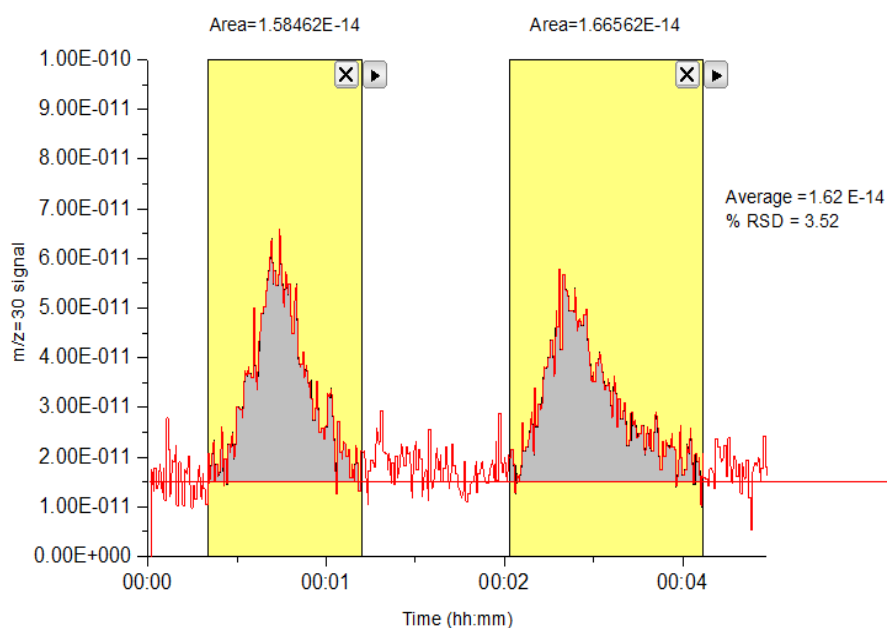
Figure A. 18: Integrated area of the m/z = 30 signal curve of HTCO analysis of 20 mg edta disodium salt 99ehydrate over 3 % Cu-7% Ce / Al_2O_3 catalyst sample at 700 ^{o}C in the presence of 500 sccm air flow
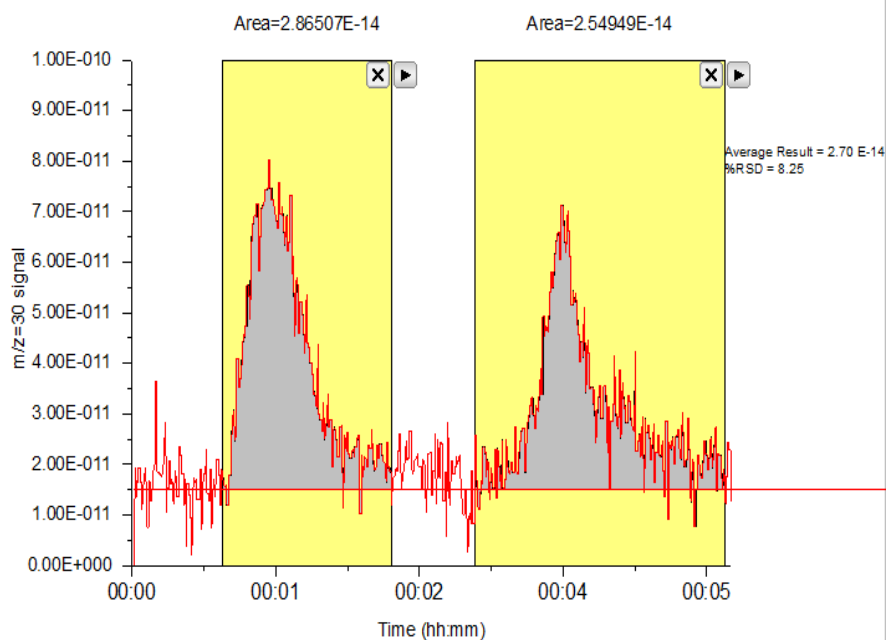

Figure A. 19: Integrated area of the m/z = 30 signal curve of HTCO analysis of 40 mg glutamic acid over 3 % Cu-7% Ce / Al_2O_3 catalyst sample at 700 ^{o}C in the presence of 500 sccm air flow
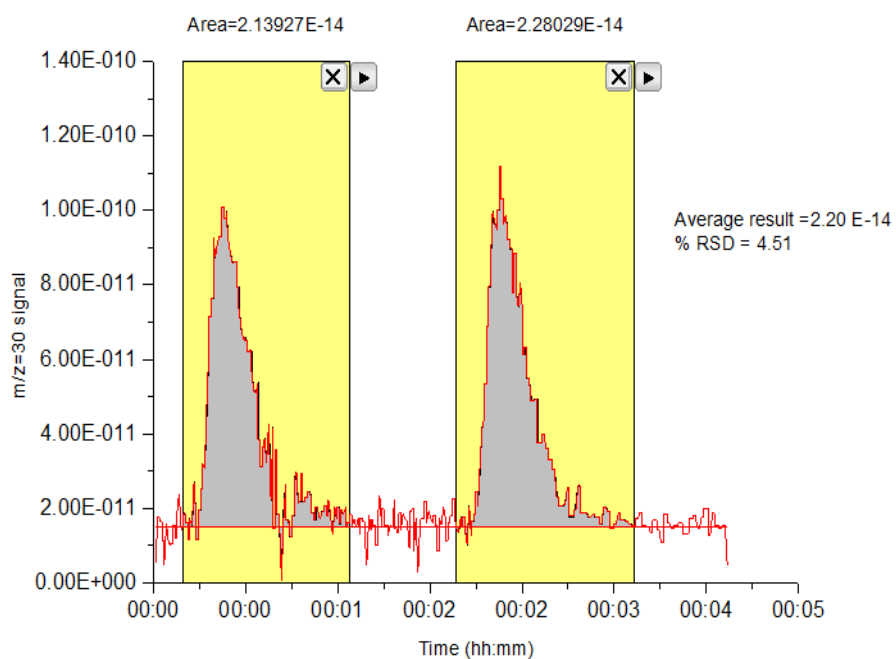
Figure A. 20: Integrated area of the m/z = 30 signal curve of HTCO analysis of 600 µl of 2.5 % by volume pyridine solution over 3 % Cu-7% Ce / Al$_2$O$_3$ catalyst sample at 700 ^{o}C in the presence of 500 sccm air flow

A.4 Integrated Area Calculations the m/z=30 signal Collected in HTCO Experiments of Model Compounds over 5 % wt Fe / Al$_2$O$_3$ Catalyst Sample

Areas under the m/z=30 signal curve of HTCO experiments of model compounds over 5 % wt Fe/Al$_2$O$_3$catalyst sample were done by using Originlab™ software. The results are shown on the figures A-24 to A-29.
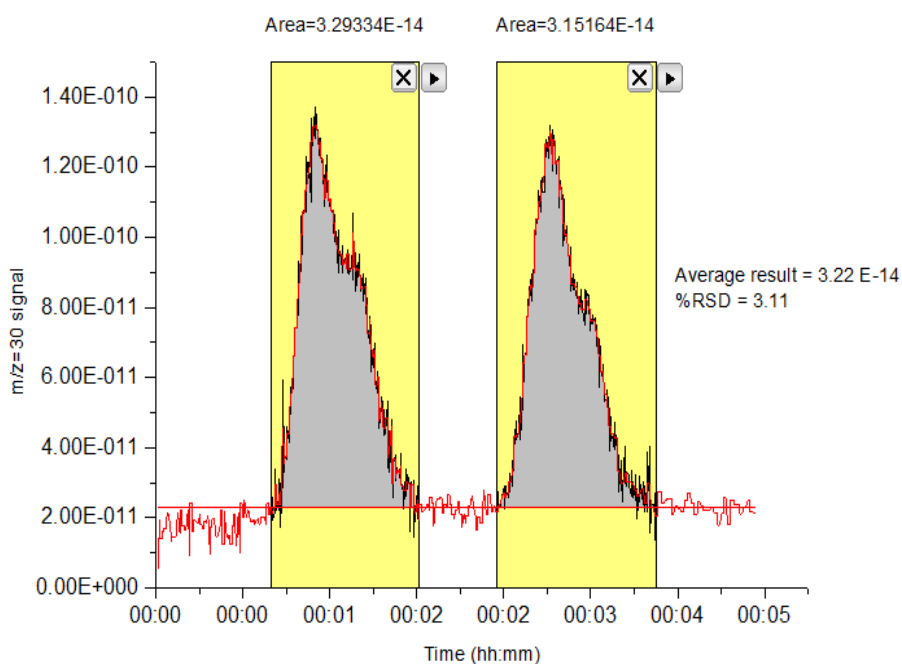

Figure A. 21: Integrated area of the m/z = 30 signal curve of HTCO analysis of 5 mg urea over 5 % wt Fe / Al$_2$O$_3$ catalyst sample at 700 ^{o}C in the presence of 500 sccm air flow
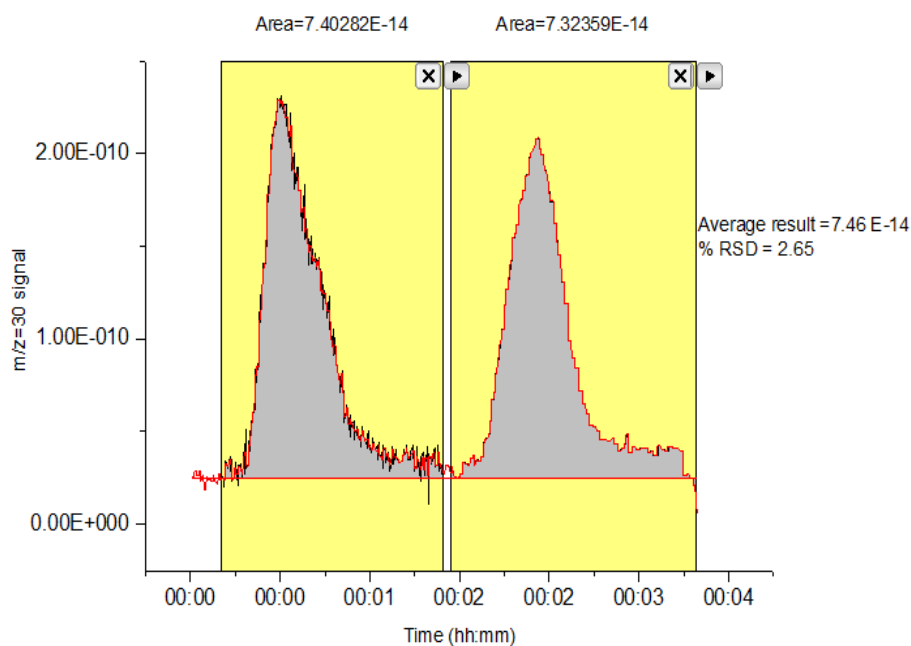
Figure A. 22: Integrated area of the m/z = 30 signal curve of HTCO analysis of 20 mg ammonium nitrate over 5 % wt Fe / Al$_2$O$_3$ catalyst sample at 700 ^{o}C in the presence of 500 sccm air flow
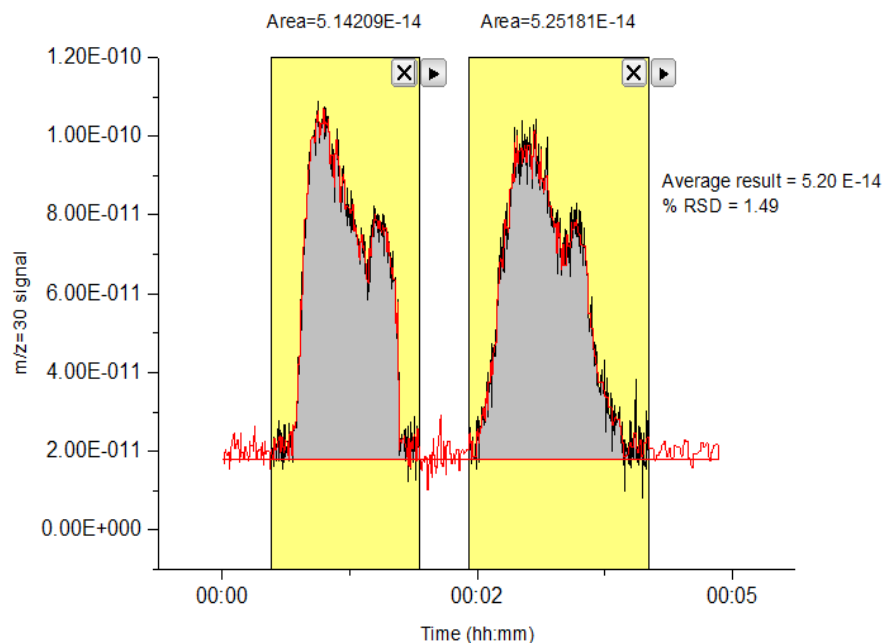

Figure A. 23: Integrated area of the m/z = 30 signal curve of HTCO analysis of 20 mg ammonium sulfate over 5 % wt Fe / Al$_2$O$_3$ catalyst sample at 700 ^{o}C in the presence of 500 sccm air flow
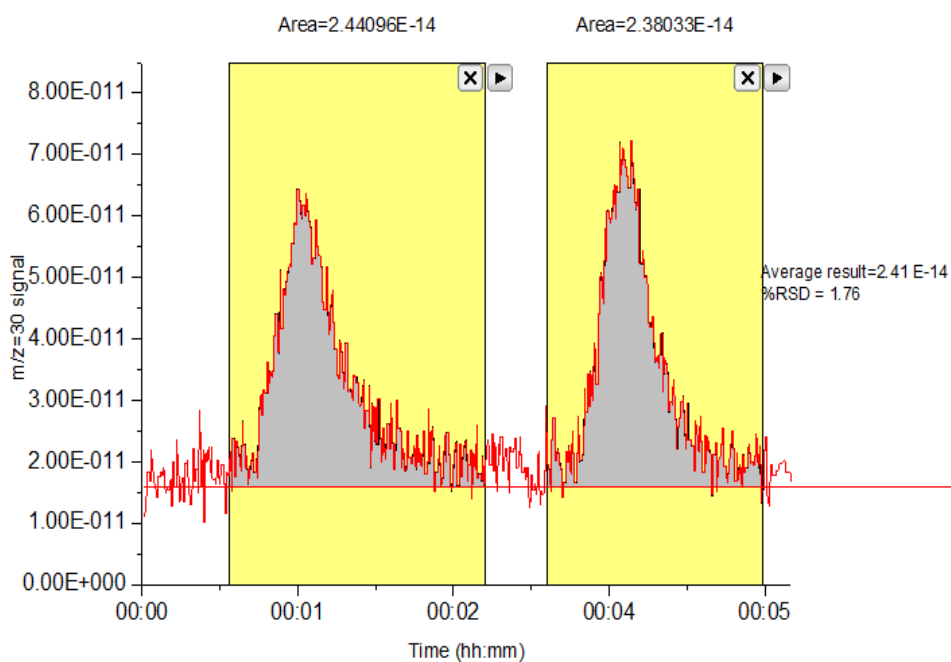
Figure A. 24: Integrated area of the m/z = 30 signal curve of HTCO analysis of 20 mg edta disodium salt dihydrate over 5 % wt Fe / Al_2O_3 catalyst sample at 700 $^{\circ}$C in the presence of 500 sccm air flow
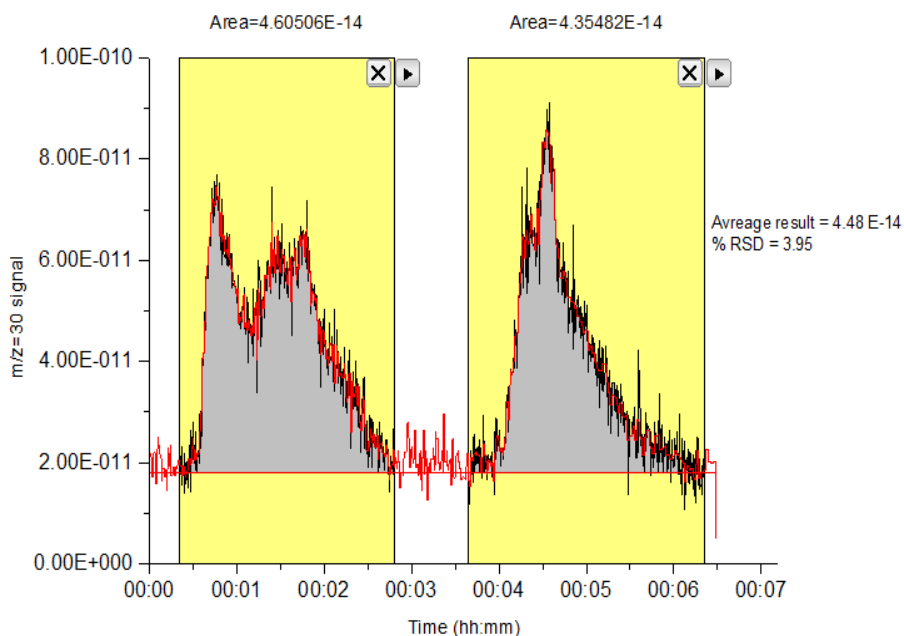

Figure A. 25: Integrated area of the m/z = 30 signal curve of HTCO analysis of 40 mg glutamic acid over 5 % wt Fe / Al_2O_3 catalyst sample at 700 $^{\circ}$C in the presence of 500 sccm air flow
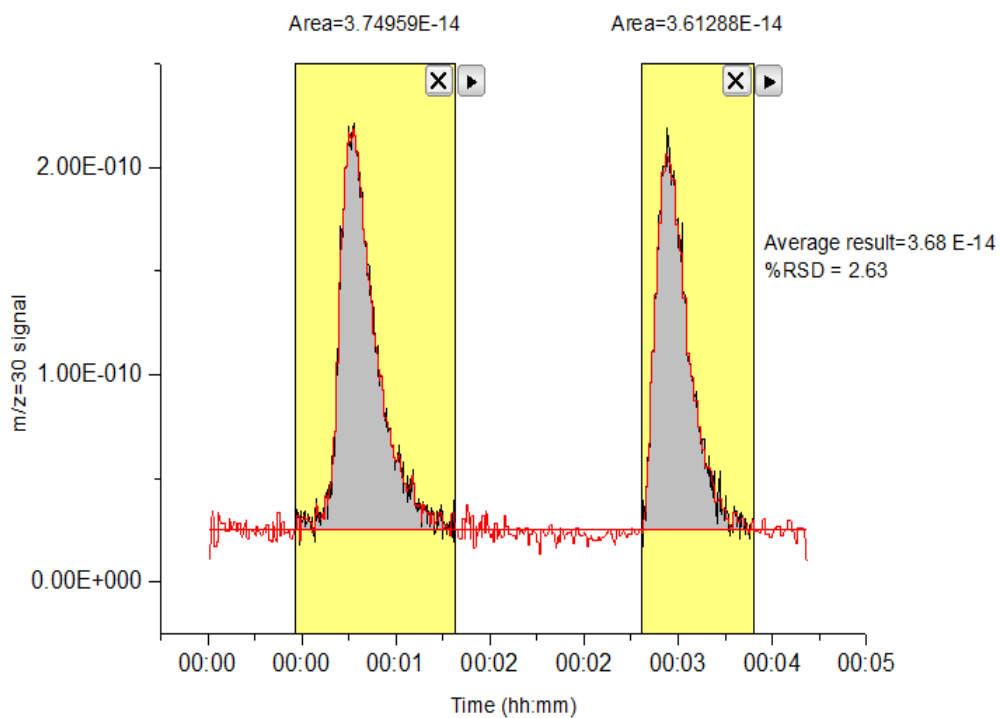
Figure A. 26: Integrated area of the m/z = 30 signal curve of HTCO analysis of 600 µl of 2.5 % by volume pyridine solution over 5 % wt Fe / Al_2O_3 catalyst sample at 700 ^{o}C in the presence of 500 sccm air flow

A.5 Integrated Area Calculations the m/z=30 signal Collected in HTCO Experiments of Model Compounds over 1 % wt Pt / Al$_2$O$_3$ Catalyst Sample

Areas under the m/z=30 signal curve of HTCO experiments of model compounds over 1 % wt Pt / Al$_2$O$_3$catalyst sample were done by using Originlab software. The results are shown on the figures A-30 to A-34.
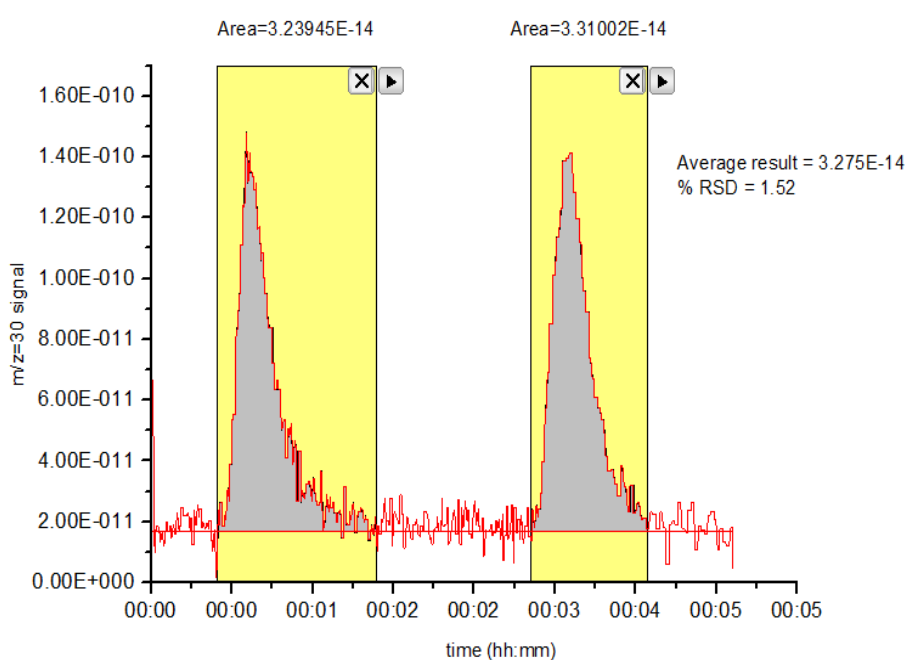

Figure A. 27: Integrated area of the m/z = 30 signal curve of HTCO analysis of 5 mg urea over 1 % wt Pt / Al$_2$O$_3$ catalyst sample at 700 ^{o}C in the presence of 500 sccm air flow

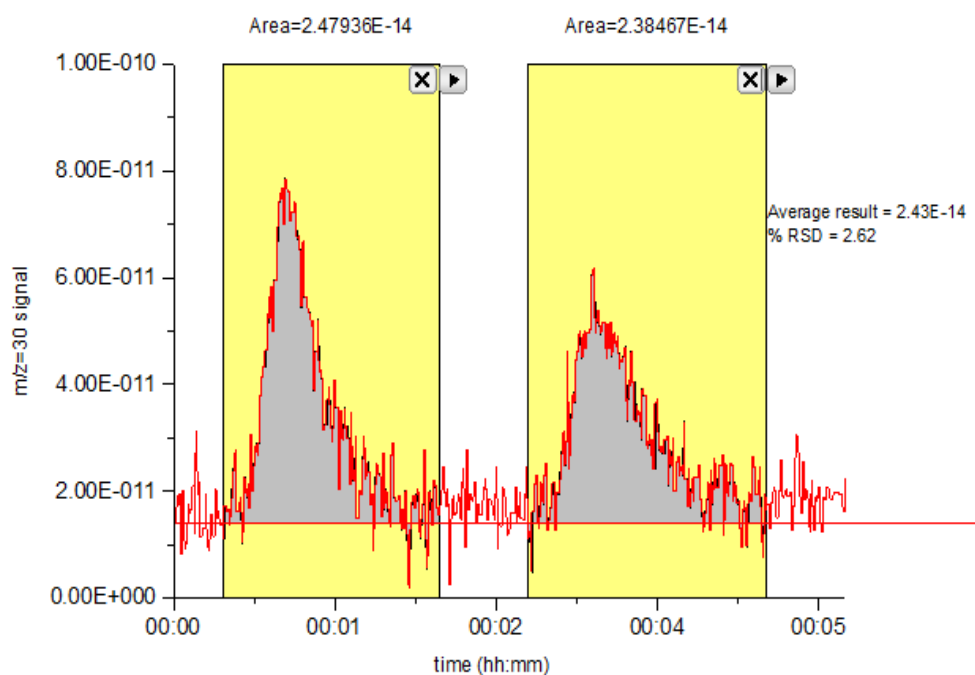**Figure A. 28:** Integrated area of the m/z = 30 signal curve of HTCO analysis of 20 mg edta disodium salt dihydrate over 1 % wt Pt / Al_2O_3 catalyst sample at 700 ^{o}C in the presence of 500 sccm air flow
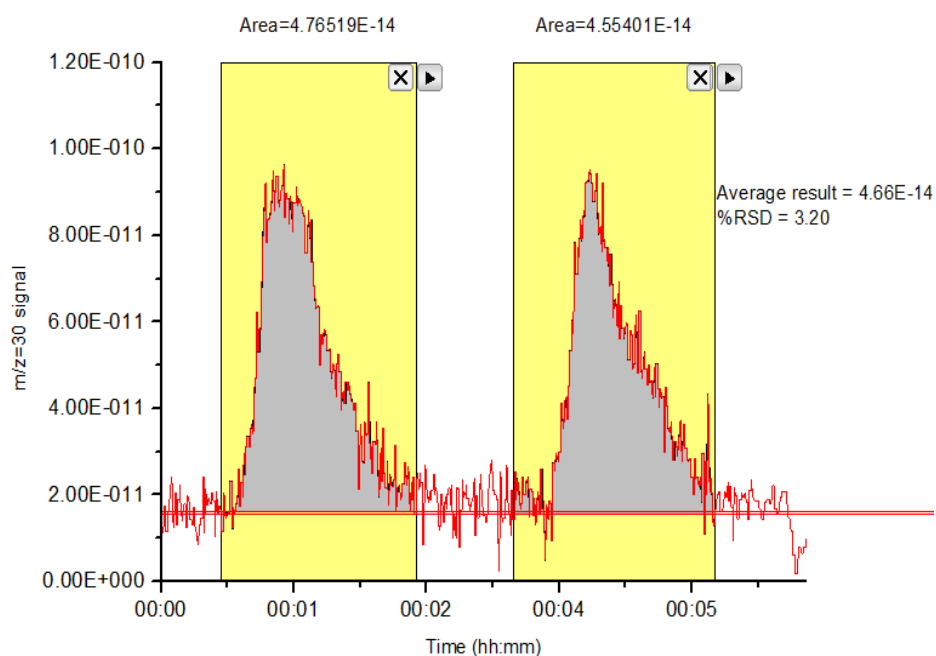
Figure A. 29: Integrated area of the m/z = 30 signal curve of HTCO analysis of 40 mg glutamic acid over 1 % wt Pt / Al_2O_3 catalyst sample at 700 ^{o}C in the presence of 500 sccm air flow

Figure A. 30: Integrated area of the m/z = 30 signal curve of HTCO analysis of 600 µl of 2.5 % by volume pyridine solution over 1 % wt Pt / Al$_2$O$_3$ catalyst sample at 700 ^{o}C in the presence of 500 sccm air flow

Figure A. 31: Integrated area of the m/z = 30 signal curve of HTCO analysis of 20 mg ammonium nitrate over 1 % wt Pt / Al$_2$O$_3$ catalyst sample at 700 ^{o}C in the presence of 500 sccm air flow
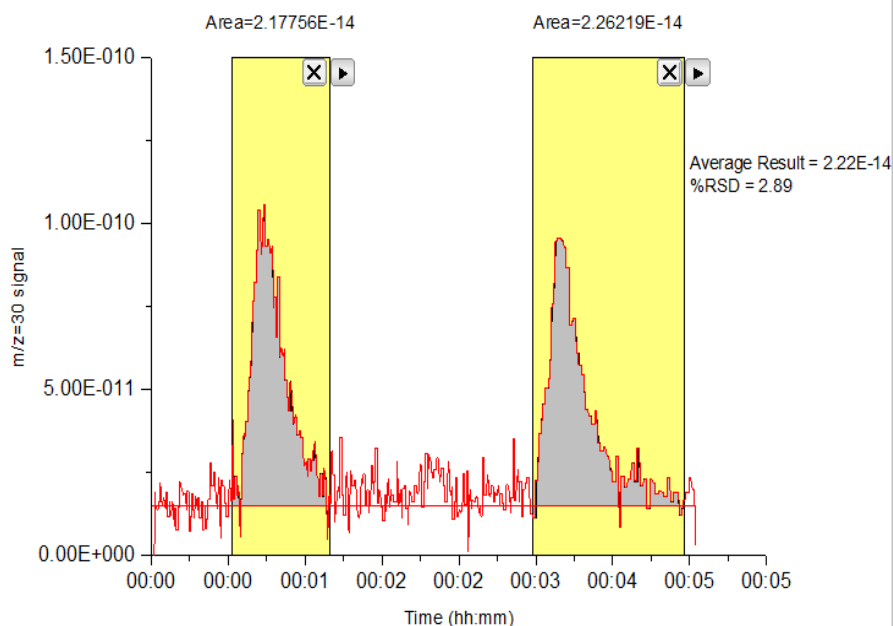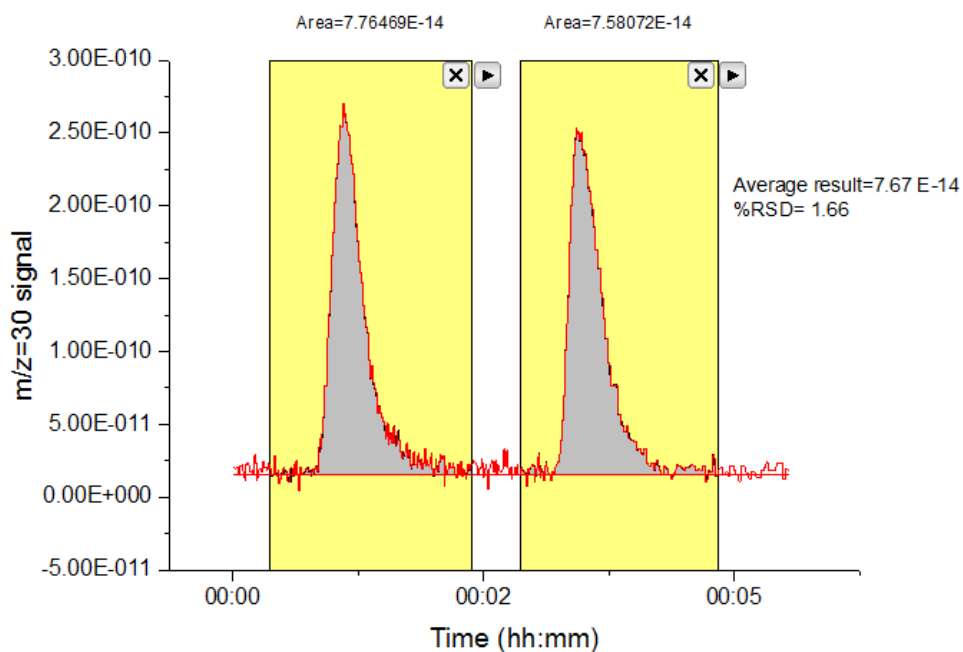
APPENDIX B

SAMPLE CALCULATIONS

B.1 Calculations for Creating Calibration Line

5, 10, 20, 40, 60 mg of ammonium sulfate, which contain 1.06, 2.12, 4.24, 8.48 and 12.72 mg of nitrogen, respectively, were used to create a calibration as integrated area vs nitrogen content. The nitrogen contents of the ammonium sulfate were calculated as the following;

$MW_{(NH4)2SO4}$= 132,14 g/mol

Nitrogen percentage is calculated according to equation B.1 and nitrogen content of a compound is calculated according to equation B.2.

$$\% \text{ N in a model compound}=\frac{Mass\ of\ nitrogen\ in\ 1\ mole\ of\ \text{compound}}{Mass\ of\ 1\ mole\ of\ \text{compound}} \qquad \text{(B.1)}$$

$$\text{N amount in a compound} = mg\ of\ compound \times \%N\ percentage \qquad \text{(B.2)}$$

$$\text{N percentage in } (NH_4)_2SO_4 = \frac{28\ g}{132.14\ g} \times 100 = 21.20\ \%$$

$$\text{N content in an amount of} (NH_4)_2SO_4 = mg\ of\ (NH4)2SO4 \times \frac{21.20}{100}$$

$$\text{N content in 5 mg } (NH_4)_2SO_4 = 5\ mg \times \frac{21.20}{100} = 1.06\ mg$$

N content of 10, 20, 40 and 60 mg $(NH_4)_2SO_4$ were also calculated as in the equation B.1and B.2 and tabulated in table B.1.

Integration areas of the three repetitive analysis of 5, 10, 20, 40, 60 mg of $(NH_4)_2SO_4$were calculated by using Originlab shown in Appendix A and the % RSD (relative standard deviation) values of the repeats were calculated as:

$$\% \text{ RSD} = \frac{s}{\bar{x}} \times 100 \qquad \text{(B.3)}$$

$$s = \sqrt{\frac{1}{N-1}\sum_{i=1}^{N}(x_i - \bar{x})^2} \qquad \text{(B.4)}$$

where

s = sample standard deviation

$\bar{x}$= mean value of sample data set

$x_i, \ldots, x_N$= the sample data set

N = size of the sample data set

For HTCO experiments of 5 mg $(NH_4)_2SO_4$:

$$\bar{x} = \frac{(2.052 + 2.064 + 1.943) \times 10^{-14}}{3} = 2.019 \times 10^{-14}$$

$$s = \sqrt{\frac{1}{3-1}\sum_{i=1}^{3}(x_i - 2.019 \times 10^{-14})^2} = 6.67 \times 10^{-16}$$

$$\%RSD = \frac{6.67 \times 10^{-16}}{2.019 \times 10^{-14}} \times 100 = 3.30\ \%$$

Percentage RSD calculations of integrated area of HTCO experiment results of 10, 20, 40 and 60 mg $(NH_4)_2SO_4$ were also calculated by using equations B.3 and B.4 and represented in table B.1.

Table B. 1:Integrated area of HTCO experiment results of 5 different amounts of ammonium sulfate over 1 % Pt / Al_2O_3 catalyst

Sample	Repeat Number	Nitrogen Content (mg)	Integrated area of m/z=30 signal	% RSD of repetitive HTCO analyses
5 mg $(NH_4)_2SO_4$	3	1.06	2.02E-14	3.30
10 mg $((NH_4)_2SO_4$	3	2.12	3.11E-14	2.11
20 mg $(NH_4)_2SO_4$	3	4.24	5.08E-14	3.31
40 mg $(NH_4)_2SO_4$	3	8.48	9.43E-14	1.99
60 mg $(NH_4)_2SO_4$	3	12.72	1.34E-13	2.61

According to nitrogen content and integrated area of the m/z=30 signal in the table B.1, calibration curve was created by using Excel and the curve is shown in the figure B.1.

B.2 HTCO Experiments Percentage Conversion Calculations

B.2.1 Calculations of Nitrogen Content in the Model Compounds

Nitrogen percentage and nitrogen amount of used model compounds were calculated by using the equation B.1 and B.2.

$$\text{Nitrogen content in 20 mg } (NH_4)_2SO_4 = 20 \ mg \times \frac{21.20}{100} = 4.24 \ mg \ N$$

Calculations of amount of nitrogen in 5 mg urea, 20 mg Edta disodium salt dehydrate, 20 mg ammonium nitrate, 40 mg glutamic acid, and 600 μl of 2.5% by volume pyridine solution were done according to equations B.1 and B.2 and the results are represented in table B.2.

Table B. 2: Molecular weights, percentage nitrogen amount and nitrogen content of the selected nitrogen containing compounds

	Molecular weight (g/mol)	% wt Nitrogen amount	Total Bound Nitrogen Content (mg)
5 mg Urea (CH_4N_2O	60.06	46.62	2.33
20 mg Edta disodium salt lihydrate ($C_{10}H_{14}N_2Na_2O_8 \cdot$ 2H_2O)	372.24	7.52	1.50
40 mg Glutamic acid ($C_5H_9NO_4$)	147.13	9.52	3.81
20 mg Ammonium sulfate ($NH_4)_2SO_4$	132.14	21.19	4.24
20 mg Ammonium nitrate ($NH_4)(NO_3$)	80.04	34.98	7.00
600 ul of 2.5 % by volume pyridine solution	79.10	0.435 (in solution)	2.61

B.2.2 Calculations of Percentage Conversions of Nitrogen in the Model Compounds to Nitric Oxide

$$\text{Percentage Conversion} = \frac{\text{Calculated nitrogen amount in sample}}{\text{True amount of nitrogen in sample}} \times 100 \qquad \text{(B.5)}$$

where "calculated nitrogen amount in sample" refers to nitrogen amount that is calculated according to calibration equation in figure D.1 which is

$$y = 9.80 \times 10^{-15}x + 9.96 \times 10^{-15} \qquad \text{(B.6)}$$

where x is the nitrogen amount in terms of milligrams and y is representing the integrated area, which are shown in the tables B.3, B.4, B.5 and B.6.

Nitrogen conversion to nitric oxide in the 5 mg urea sample over 1 % wt Pt/Al_2O_3 catalyst sample can be calculated as follows:

Equation B.6 is used to find calculated amount of nitrogen in the 5 mg urea sample;

$$3.20 \times 10^{-14} = 9.80 \times 10^{-15}x + 9.96 \times 10^{-15}$$
$$x = 2.25 \; mg \; N$$

Then, percentage conversion can be calculated by using equation B.5 as follow;

$$\%conversion = \frac{2.25}{2.33} \times 100 = 99.79 \; \%$$

The percentage conversions of bound nitrogen in the model compounds to NO were calculated by using equations B.5, B.6 and table B.3 as above and are shown in the table B.4.

Table B. 3: Average integrated area of the m/z=30 signal, % RSD values and percentage conversions of bound nitrogen to NO of HTCO experiments of model compounds over 10 % wt Cu/Al_2O_3 catalyst samples

Sample	Average Integrated area of m/z=30 signal	% RSD of repetitive HTCO analyses	% Conversion of bound nitrogen to nitric oxide
5 mg Urea	3.20 E-14	1.15	96.50
20 mg EDTA	1.53 E-14	1.27	36.29
40 mg Glutamic acid	2.34 E-14	36.99	36.08
600 ul 2.5 % by volume pyridine solution	3.61 E-14	2.52	98.41
20 mg ammonium nitrate	7.58 E-14	2.91	94.80
20 mg ammonium sulfate	3.88 E-14	4.91	69.40

Table B. 4 : Average integrated area of the m/z=30 signal, % RSD values and percentage conversions of bound nitrogen to NO of HTCO experiments of model compounds over 3 % wt Cu – 7 % Ce/Al_2O_3 catalyst samples

Sample	Average Integrated area of m/z=30 signal	% RSD of repetitive HTCO analyses	% Conversion of bound nitrogen to nitric oxide
5 mg Urea	3.10 E-14	3.47	91.99
20 mg EDTA	1.62 E-14	3.52	42.42
40 mg Glutamic acid	2.70 E-14	8.25	45.74
600 ul 2.5 % by volume pyridine solution	2.20 E-14	4.21	47.05
20 mg ammonium nitrate	2.57 E-14	3.14	22.94
20 mg ammonium sulfate	5.21 E-14	1.32	101.40

Table B. 5 : Average integrated area of the m/z=30 signal, % RSD values and percentage conversions of bound nitrogen to NO of HTCO experiments of model compounds over 5 % Fe/Al_2O_3 catalyst samples

Sample	Average Integrated area of m/z=30 signal	% RSD of repetitive HTCO analyses	% Conversion of bound nitrogen to nitric oxide
5 mg Urea	3.22 E-14	3.11	97.38
20 mg EDTA	2.41 E-14	1.76	100.92
40 mg Glutamic acid	4.48 E-14	3.95	102.14
600 ul 2.5 % by volume pyridine solution	3.68 E-14	2.63	104.91
20 mg ammonium nitrate	7.46 E-14	2.65	94.22
20 mg ammonium sulfate	5.20 E-14	1.49	101.26

Table B. 6 : Average integrated area of the m/z=30 signal, % RSD values and percentage conversions of bound nitrogen to NO of HTCO experiments of model compounds over 1 % Pt/Al$_2$O$_3$ catalyst samples

Sample	Average Integrated area of m/z=30 signal	% RSD of repetitive HTCO analyses	% Conversion of bound nitrogen to nitric oxide
5 mg Urea	3.28 E-14	1.52	99.79
20 mg EDTA	2.43 E-14	2.62	97.52
40 mg Glutamic acid	4.66 E-14	3.2	98.19
600 ul 2.5 % by volume pyridine solution	2.22 E-14	2.89	47.83
20 mg ammonium nitrate	7.67 E-14	1.66	97.28
20 mg ammonium sulfate	3.28 E-14	1.52	98.27

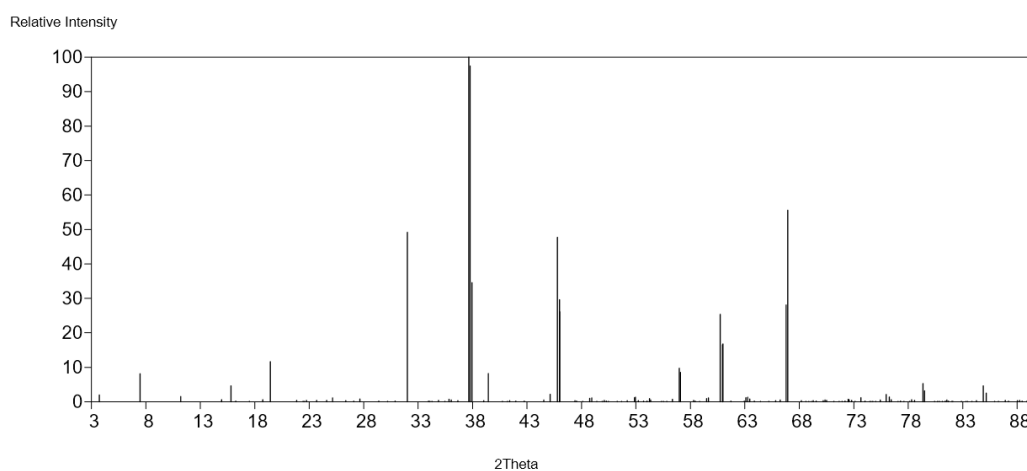**REFERENCE XRD PATTERNS OF THE CATALYST SAMPLES AND Al$_2$O$_3$ SUPPORT**

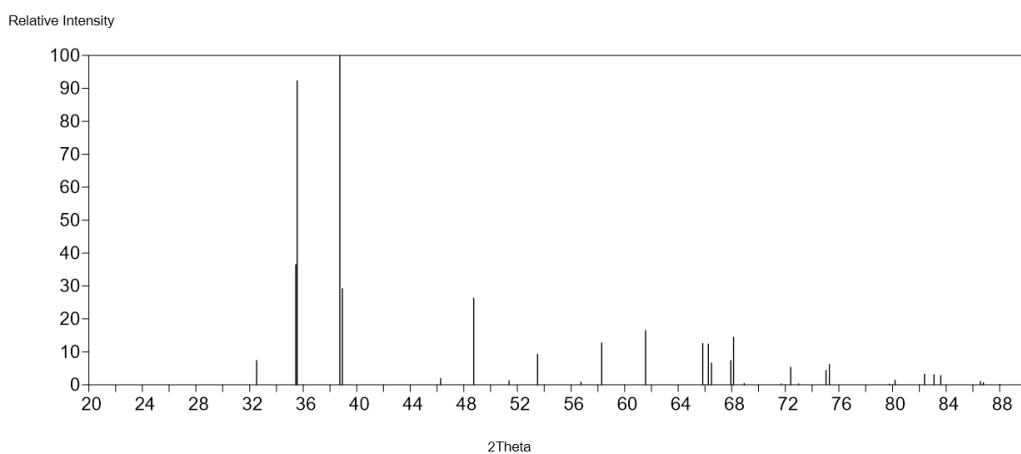**Figure C. 1:** Reference XRD pattern of Al$_2$O$_3$ structure obtained from ICDS PDF Card No.: 01-088-1609

Figure C. 2: Reference XRD pattern of CuO structure obtained from ICDS PDF Card No.: 01-089-5897
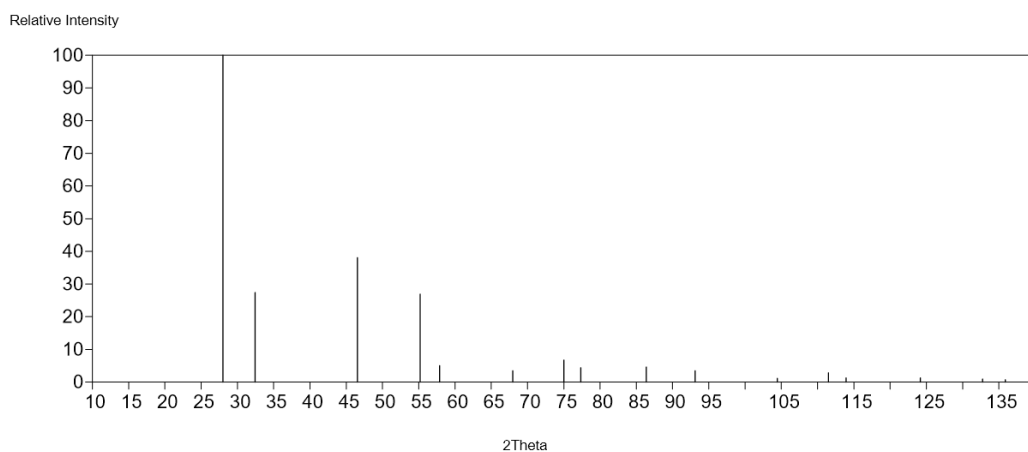
Relative Intensity

Figure C. 3: Reference XRD pattern of CeO_2 structure obtained from ICDS
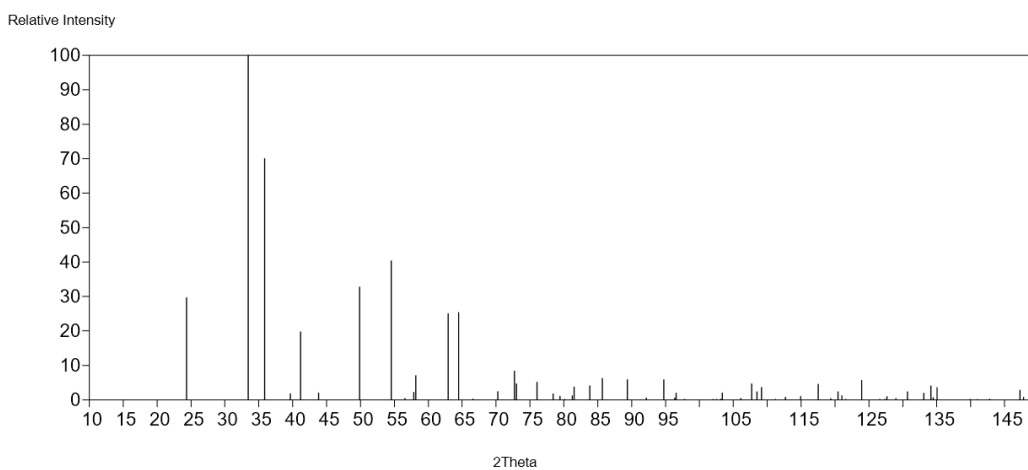
PDF Card No.: 01-073-7747

Relative Intensity

Figure C. 4: Reference XRD pattern of CeO_2 structure obtained from ICDS
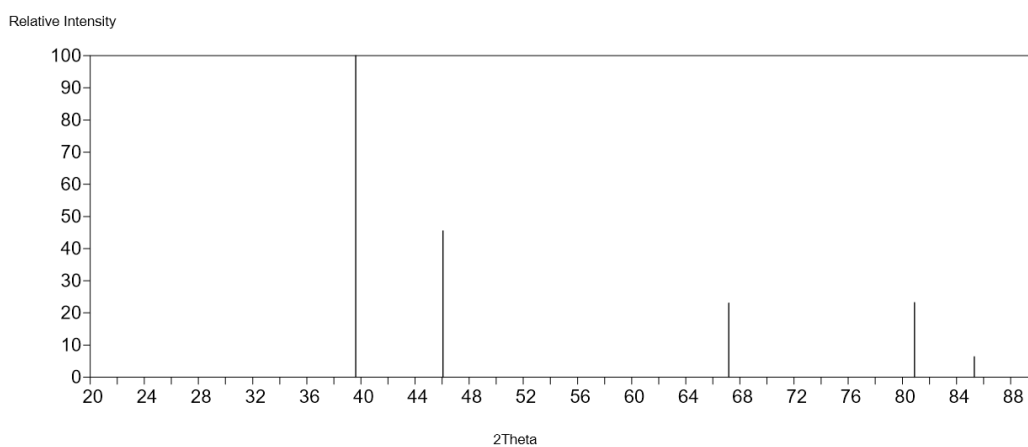
PDF Card No.: 01-084-0311

Figure C. 5: Reference XRD pattern of CeO_2 structure obtained from ICDS
PDF Card No.: 01-087-0642